

# **The Role of the Lysine-Specific Demethylase 1 in the Development of Hepatocellular Carcinoma**

Inaugural Dissertation

zur

Erlangung des Doktorgrades  
Dr. nat. med.

der Medizinischen Fakultät  
und  
der Mathematisch-Naturwissenschaftlichen Fakultät  
der Universität zu Köln

vorgelegt von

**Jie Wang**

aus Hebei, China

(Hundt Druck GmbH)

Köln, 2022

Betreuerin: Prof. Dr. Margarete Odenthal

Referent\*innen: Prof. Dr. Dr. Michal-Ruth Schweiger  
PD Dr. Thomas Wunderlich

Datum der mündlichen Prüfung: 17.08.2022

## Summary

Hepatocellular carcinoma (HCC) has a low survival rate and is currently the third leading cause of cancer-related deaths worldwide. Most HCC develops on the basis of chronic liver diseases, such as HBV and HCV hepatitis, alcoholic liver disease, or non-alcoholic fatty liver disease.

Epigenetic alterations, including an altered pattern in histone modification, are crucial for cancer progression. However, the epigenetic aberrations involved in the development of HCC are not well understood. The lysine-specific demethylase 1 (LSD1) is involved in chromatin remodeling by demethylating lysine 4 and lysine 9 histone 3 (H3K4 and H3K9), causing transcriptional repression or activation, respectively. Strikingly, overexpression of LSD1 contributes to the malignancy of several cancers. Therefore, my research focused on the mechanistic links affected by LSD1 in liver cancer cells. To investigate this, I used three different hepatoma cells (Huh7, HepG2, and Hep3B), in which LSD1 was inhibited pharmacologically or by anti-LSD1 siRNA species. For conditional LSD1 inhibition, stable Tet-On hepatoma cell lines were generated in which expression of short-hairpin anti-LSD1 RNA was inducible after doxycycline exposure. The effect of LSD1 on cell viability was measured by the MTT test. Gene expression was studied at the transcript level by ultra-deep RNA sequencing and qPCR and at the protein level by immunoblotting. Moreover, I analyzed the histone H3K4 methylation patterns and the interaction of LSD1 with promoter sites by chromatin immunoprecipitation (ChIP) followed by whole-genome sequencing or qPCR.

These studies showed that LSD1 inhibition in the different hepatoma cell types leads to cell growth arrest and downregulation of PLK1. ChIP analysis revealed that PLK1 is a direct target of LSD1 regulation in hepatoma cells. In addition, gene expression profiling by RNA sequencing followed by metabolic pathway analysis revealed striking dysregulation of genes involved in metabolic dysregulation after LSD1 was inhibited. In particular, genes of the citrate cycle and lipid metabolism were affected by LSD1 which was validated by qPCR. Noteworthy, ChIP assays showed alteration of histone methylation and LSD1 binding at promoter sites of many metabolic genes, downregulated after LSD1 inhibition. In particular, the gene FABP5, which is involved in fat metabolism, was found to be a novel direct target of LSD1. To

demonstrate the effects of LSD1 on the regulation of metabolic genes, an in vivo mouse model for non-alcoholic fatty liver disease was used with respect to its high metabolic imbalance and LSD1 was pharmacologically inhibited in the early progression phase of the disease where fat accumulation occurs (steatosis). Importantly, LSD1 inhibition resulted in weight loss, lower serum AST liver enzymes, and no signs of fat accumulation, while control mice had all the features of steatosis.

In conclusion, my study emphasizes that LSD1 which is an important mediator in cell cycle control affects HCC progression not only by cell cycle interruption but also by metabolism and lipid dysregulation.

## Zusammenfassung

Das hepatozelluläre Karzinom (HCC) hat eine niedrige Überlebensrate und ist derzeit weltweit die dritthäufigste Ursache für krebserkrankte Todesfälle. Die meisten hepatozellulären Karzinome entwickeln sich auf der Grundlage chronischer Lebererkrankungen, wie HBV- und HCV-Hepatitis, einer alkoholischen Lebererkrankung oder einer nichtalkoholischen Fettlebererkrankung.

Epigenetische Veränderungen, einschließlich Veränderungen in der Histonmodifikation spielen in der Karzinogenese eine entscheidende Rolle. Dabei sind aber epigenetische Aberrationen, welche bei der Entstehung von HCC wichtig sind, noch nicht ausreichend erforscht. Die lysinspezifische Demethylase 1 (LSD1) zum Beispiel ist an der Restrukturierung des Chromatins beteiligt, indem sie Lysin 4 und Lysin 9 von Histon 3 (H3K4, H3K9) demethyliert und so die Transkription unterdrückt bzw. aktiviert. Besonders auffällig ist dabei, dass gerade die Überexpression von LSD1 zur Bösartigkeit verschiedener Krebsarten beiträgt. Meine Doktorarbeit konzentrierte sich daher auf die mechanistischen Zusammenhänge, die LSD1 in Leberkrebszellen bewirken. Zu diesem Zweck verwendete ich drei verschiedene Hepatomzellen (Huh7, HepG2 und Hep3B), in denen LSD1 pharmakologisch oder durch anti-LSD1-siRNA gehemmt wurde. Für die konditionale LSD1-Inhibierung wurden stabile Tet-On-Hepatomzelllinien erzeugt, in denen die Expression von short-hairpin-anti-LSD1-RNA nach Doxycyclin-Exposition induzierbar war. Der Einfluss von LSD1 auf die Lebensfähigkeit der Zellen wurde mithilfe eines MTT-Testes gemessen. Die Genexpression wurde auf der Transkriptionsebene durch ultra-tiefe-RNA-Sequenzierung und qPCR und auf der Proteinebene durch Immunoblotting untersucht. Darüber hinaus analysierte ich die Histon-H3K4-Methylierungsmuster und die Interaktion von LSD1 mit Promotorstellen durch Chromatin-Immunpräzipitation (ChIP), gefolgt von Sequenzierung des gesamten Genoms oder qPCR.

Diese Studien zeigten, dass die Hemmung von LSD1 in den verschiedenen Hepatomzelltypen zu einem Stillstand des Zellwachstums und einer Herunterregulierung von PLK1 führen. Die ChIP-Analyse offenbarte, dass PLK1 in Hepatomzellen ein direktes Ziel der LSD1-

Regulierung ist. Darüber hinaus ergab die Erstellung von Genexpressionsprofilen mittels RNA-Sequenzierung und anschließender Analyse von metabolischen Signalwegen eine auffällige Dysregulation von Genen, die an der Dysregulation des Stoffwechsels beteiligt sind, nachdem LSD1 gehemmt wurde. Insbesondere Gene des Zitratzyklus und des Lipidstoffwechsels waren von der LSD1 Hemmung betroffen, was durch qPCR bestätigt wurde. In Übereinstimmung zu diesen Ergebnissen zeigten die CHIP-Assays eine Veränderung der Histon-Methylierung und LSD1-Bindung an den Promotorstellen vieler Stoffwechselgene. Insbesondere das Gen FABP5, das am Fettstoffwechsel beteiligt ist, erwies sich als neues, direktes Ziel von LSD1. Um die Auswirkungen von LSD1 auf die Regulierung von Stoffwechselgenen nachzuweisen, wurde ein in-vivo Mausmodell für nicht-alkoholische Lebererkrankungen eingesetzt und LSD1 in der frühen Phase der Erkrankung, wo die Fettansammlung stattfindet (Steatose), pharmakologisch gehemmt. Die Hemmung von LSD1 führte zu einer Gewichtsabnahme, und zu niedrigeren AST-Leberenzymen im Serum. Die typischen Anzeichen einer Steatose, wie Fettansammlungen in Hepatozyten, konnten nach LSD1 Inhibierung nicht festgestellt werden, während die Kontrollmäuse alle Merkmale einer Steatose aufwiesen.

Zusammenfassend unterstreicht meine Arbeit, dass LSD1 wichtig in der Zellzykluskontrolle ist, aber zudem auch Gene des Metabolismus insbesondere der Lipogenese beeinflusst.

## Table of Contents

1. Introduction .....	8
1.1 Hepatocellular carcinoma .....	8
1.1.1 Causes of hepatocellular carcinoma development.....	8
1.1.1.1 Chronic virus .....	8
1.1.1.2 Alcohol abuse.....	9
1.1.1.3 Nitrosamines .....	9
1.1.2 Non-alcoholic fatty liver disease and HCC .....	10
1.1.3 Pathophysiology of NAFLD .....	11
1.1.3.1 Cellular mediators and inflammation .....	12
1.1.3.2 Metabolic dysregulation in NAFLD .....	13
1.1.3.3 Mitochondrial dysfunction and ER stress in NAFLD .....	14
1.2 Epigenetic impact on chronic liver diseases and HCC .....	14
1.3 Epigenetic modifier lysine-specific demethylase 1 .....	15
1.3.1 LSD1 impact on cancer.....	16
1.3.2 LSD1 in cell cycle and proliferation .....	17
1.3.3 Novel aspects of LSD1 function .....	17
1.3.4 Pharmacological inhibition of LSD1 .....	18
1.4 Aim .....	18
2. Material and methods.....	20
2.1 Materials.....	20
2.1.1 List of devices .....	20
2.1.2 List of kits .....	20
2.1.3 List of software .....	21
2.1.4 Plastic material .....	22
2.1.5 Reagents for cell culture .....	22
2.1.6 Reagents for molecular experiment .....	23
2.1.7 Solutions.....	24
2.1.7.1 Solutions for immunoblotting .....	24
2.1.7.2 Solutions for agarose gel electrophoresis.....	26
2.1.7.3 Solutions for plasmid cloning.....	26
2.1.8 Enzymes.....	26
2.1.9 Antibodies .....	27
2.1.10 Primers .....	27
2.1.11 Sequences of siRNAs .....	28
2.1.12 Cell lines .....	29
2.2 Methods .....	29
2.2.1 Cell culture.....	29
2.2.1.1 Thawing and freezing of cells .....	29
2.2.1.2 Determination of cell number .....	30

---

2.2.1.3 Mycoplasma test.....	30
2.2.2 Cells treated with compounds.....	30
2.2.2.1 Treatment of cells with LSD1 inhibitors.....	30
2.2.2.2 Transfection of cells with small interfering RNA (siRNA).....	30
2.2.2.3 Conditional shLSD1 knockdown plasmids.....	31
2.2.2.4 Transfection of cells with plasmids.....	32
2.2.3 Lentiviral transduction.....	32
2.2.3.1 Preparation of lentiviruses.....	32
2.2.3.2 Treatment of lentivirus to hepatoma cells.....	32
2.2.4 In vitro analysis of cell viability and proliferation.....	33
2.2.4.1 Determination of cell viability using the MTT test.....	33
2.2.4.2 Incucyte live-cell imaging and analysis.....	33
2.2.5 Analysis of gene expression.....	33
2.2.5.1 RNA isolation.....	34
2.2.5.2 Reverse transcription of RNA.....	34
2.2.5.3 Real-time PCR.....	35
2.2.5.4 Pathway analysis using transcriptome data.....	36
2.2.6 Analysis of protein expression.....	36
2.2.6.1 Cell lysis.....	36
2.2.6.2 Determination of protein concentration.....	36
2.2.6.3 Western blot analysis.....	37
2.2.6.4 Dot slot immunoblotting.....	37
2.2.7 Chromatin immunoprecipitation.....	38
2.2.8 Induction of NAFLD in mice and inhibition of LSD1 by HCI-2509 treatment.....	39
2.2.8.1 Experimental design of drug-mediated inhibition of LSD1 in vivo.....	39
2.2.8.2 Application of LSD1 inhibitor HCI-2509.....	40
2.2.8.3 Determination of serum ALT and AST values.....	41
2.2.8.4 Sacrificing of mice and isolation of organs.....	41
3. Results.....	42
3.1 LSD1 regulates the level of di-methylation at H3K4.....	42
3.1.1 Enhancement of H3K4me2 by LSD1 pharmacological inhibition.....	42
3.1.2 Enhancement of H3K4me2 by LSD1 siRNA.....	43
3.1.3 Enhancement of H3K4me2 by LSD1 knockdown construct.....	46
3.2 LSD1 inhibition decreases cell viability.....	47
3.2.1 Cell viability is reduced by LSD1 pharmacological inhibition.....	47
3.2.2 Cell viability is reduced by LSD1 siRNA/shRNA.....	51
3.3 LSD1 inhibition results in an alteration of gene expression.....	53
3.3.1 The expression of liver disease-related genes was altered upon LSD1 inhibition.....	57
3.3.2 Cell cycle pathway enrichment upon LSD1 inhibition.....	58
3.3.3 LSD1 inhibition represses pathways in cell cycle progression.....	59
3.3.4 LSD1 inhibition results in the alteration of metabolic genes.....	61
3.4 Promoter interactions of LSD1 in liver cancer cells.....	64

---

3.4.1 LSD1 regulates PLK1 by binding its promoter.....	64
3.4.2 Enrichment of H3K4me2 to promoters of metabolic genes .....	65
3.4.3 LSD1 mediates lipid metabolic reprogramming by directly regulating the metabolic genes .....	67
3.4.4 LSD1 regulates FABP5 by binding its promoter .....	68
3.4.5 Overexpression of FABP5 contributes to HCC.....	69
3.4.6 LSD1 inhibition downregulates FABP5 expression.....	70
3.5 LSD1 inhibition with HCI-2509 using rodent NAFLD model .....	71
3.5.1 Effect of LSD1 inhibition on mice body weight .....	71
3.5.2 Effect of LSD1 inhibition on serum AST and ALT .....	73
3.5.3 Effect of LSD1 inhibition on fat accumulation .....	73
4. Discussion .....	75
4.1 LSD1-mediated H3K4me2 demethylation regulates cell cycle .....	75
4.2 LSD1 inhibition by pharmacological inhibitors.....	77
4.3 LSD1 involvements in lipid metabolic reprogramming.....	79
4.4 LSD1 inhibition reduced fat accumulation in NAFLD in vivo .....	82
5. References .....	85
6. Abbreviations .....	94
7. Supplementary information .....	98
Acknowledgments.....	99
Erklärung .....	100
Curriculum Vitae .....	101

## **1. Introduction**

### **1.1 Hepatocellular carcinoma**

Cancer is a leading cause of death in both developed and developing countries. Hepatocellular carcinoma (HCC) which accounts for 75% of liver cancer cases is currently the third leading cause of cancer-related deaths globally and is the most common primary liver malignancy [1]. HCC has an extremely high mortality rate and the morbidity of this cancer is almost equal to the mortality rate. The incidence of individual cancers in developing countries is upwards of 80% and HCC is more common in men than in women, with a worldwide distribution ratio of 2.4 [2]. The average age of patients diagnosed with HCC is usually between 30 and 50 years [3]. The difficulties of early diagnosis, the rapid progression of HCC and the lack of targeted therapeutic drugs result in an extremely low survival rate of liver cancer.

#### **1.1.1 Causes of hepatocellular carcinoma development**

Most HCC develops on the basis of chronic liver diseases, including viral hepatitis such as chronic hepatitis B virus (HBV) and hepatitis C virus (HCV) infection, long-lasting alcohol abuse, chemicals and others. In addition, non-alcoholic fatty liver disease (NAFLD), which has a high and increasing prevalence even among young people, is a major factor in the development of HCC[4].

##### **1.1.1.1 Chronic virus**

HBV is considered to be the most common cause of HCC globally, accounting for an estimated 54% of all liver cancers [5, 6]. HBV is a hepatotropic virus transmitted via contaminated blood transfusions, intravenous injections, and sexual contact that can establish a persistent and chronic infection in humans through immune anergy. HBV induces hepatocellular carcinogenesis by integrating itself into the pivotal location in the cellular genome [7]. Chronic HBV infection increases the relative risk of HCC by 15-20 fold. The mortality rate is approximately 30-50% in all cases of chronic HBV infection [8].

HCV is the second most important risk factor for HCC, with 10-25% of all HCC cases

worldwide being considered to be based on HCV infection [9]. However, in contrast to HBV, which can integrate into the host genome leading to potential direct carcinogenic activity, there is limited integration of the genetic material of HCV into the host genome. About 80% of patients with HCV can further develop into chronic hepatitis, of which about 20% develop cirrhosis [10]. When compared to uninfected individuals, chronic HCV infection is associated with a 20–30 fold increased risk of developing HCC. Approximately 2.5% of patients with chronic HCV infection develop HCC [11].

#### **1.1.1.2 Alcohol abuse**

Long-term alcohol abuse is also an important factor to increase the risk of developing liver cancer. Alcohol is a small polar organic molecule that can diffuse through cell membranes and distribute into all tissues via the bloodstream. Acetaldehyde and various ROS, the metabolites of ethanol in the presence of alcohol dehydrogenase and cytochrome P450 2E1 (CYP2E1), are pronounced to contribute to the development of cirrhosis and malignancy by inducing chronic oxidative stress and chronic inflammation [12, 13]. Excess ROS are produced in chronic liver injury by alcohol exposure, thereby disrupting the interactions of DNA, RNA, lipids, and proteins, which leads to genomic instability and insufficient repair pathways eventually [12]. Genetic variations in these enzymes are closely related to differences in susceptibility to HCC [14].

#### **1.1.1.3 Nitrosamines**

Nitrosamines are found in many products such as meat [15], tobacco smoke [16], and food coloring additives [17] and are a large group of very common chemical carcinogens. Studies have shown that DEN and DMN induce cancer by depending on cytochrome P450 enzymes, especially CYP2E1, to produce alkylated metabolites, which causes DNA adduct formation [18, 19]. It has been demonstrated that excessive consumption of nitrosamines leads to an increased risk of gastrointestinal tract cancer and hepatocellular carcinoma [20]. Furthermore, increasing evidence showed that inflammation promotes the progress of DEN-induced hepatocarcinogenesis. DEN is not only a genotoxin, it is also hepatotoxic and can lead to cell necrosis. This damage triggers an inflammatory response, such as interleukin-6, which causes

an increase in mitogen expression and promotes compensatory proliferation of viable hepatocytes [21]. In humans, patients with liver cancer that progresses from advanced liver fibrosis or cirrhosis account for 80-90% of all HCC patients. Noteworthy, long-term exposure to nitrosamines can induce liver fibrosis, cirrhosis, and hepatocellular carcinoma [22].

The DEN-induced rodent liver cancer model has been widely used in *in vivo* experiments to better understand the pathological evolution of liver cancer. Studies have shown that long-term oral or parenteral application of high doses of DEN in mice can be effective in inducing liver tumors [23]. The livers of infant mice are the most sensitive to carcinogenesis, and the enzymatic competence (i.e. DEN-dealkylating activity) increases progressively with age, in the late stages, the metabolic activity of the enzyme decreases with age. During the period between days 7 and 15, the enzyme activity reaches its peak activity and is approximately the same in males and females [24].

### **1.1.2 Non-alcoholic fatty liver disease and HCC**

Non-alcoholic fatty liver disease (NAFLD) is a leading cause of chronic liver disease worldwide. NAFLD) is a multifaceted metabolic disorder and has a broad spectrum that covers histological and pathophysiological developments ranging from simple steatosis to non-alcoholic steatohepatitis (NASH) and liver fibrosis, potentially evolving into cirrhosis, eventually developing into hepatocellular carcinoma and liver failure (Figure 1) [25]. For terminology, NAFLD in general includes non-alcoholic fatty liver (NAFL) and non-alcoholic steatohepatitis (NASH) [26]. The main feature of NAFL is steatosis of the liver, comprising more than 5% of the liver parenchyma, without hepatocyte injury [27]. By comparison, NASH is a necroinflammatory process in which the liver cells are also being injured in the context of hepatic steatosis. Although the natural history of NAFLD is not well elucidated, the increased risk of progression to cirrhosis and HCC is already known in the previous study [28].

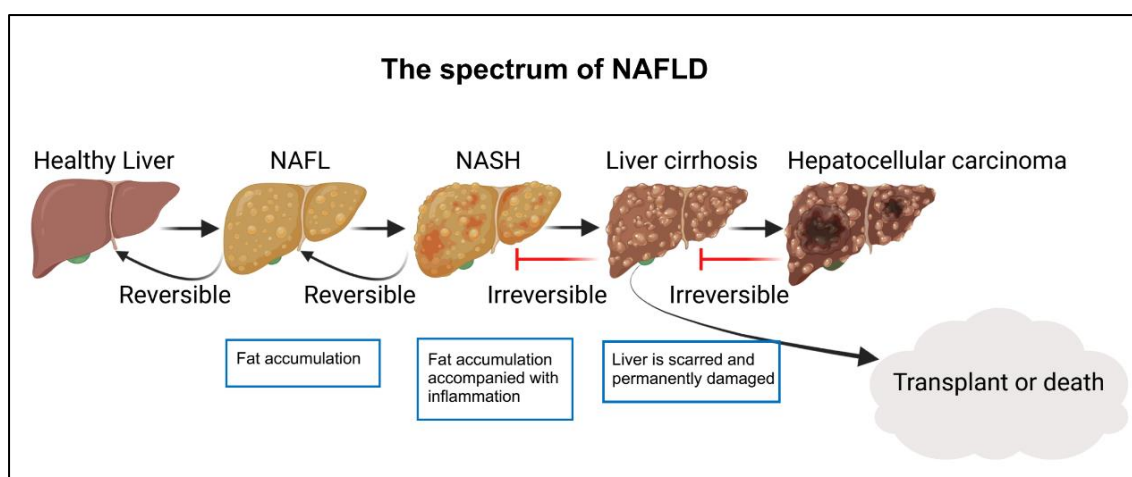


**Figure 1. The spectrum of NAFLD progression.**

There can be four stages in the development of NAFLD: simple steatosis (or NAFL), NASH, liver cirrhosis and HCC [29]. Western HFHSDs, obesity, T2DM (especially associated IR) and other metabolic diseases can lead to simple steatosis. Inflammation and hepatocyte apoptosis are the main contributors to the development of NASH. Liver fibrosis is a transitional phase of NASH that leads to the development of liver cirrhosis. Modified from KV Rao et al. [24]. *Created in BioRender.com*

### 1.1.3 Pathophysiology of NAFLD

The underlying mechanism for the development and progression of NAFLD is complex and multifactorial (Figure 2). The NAFLD can be triggered by dietary habits, environmental and genetic factors [30]. Insulin resistance is a critical factor in the development of steatosis and NASH, leading to increased hepatic *de novo* lipogenesis (DNL) and reduced inhibition of adipose tissue lipogenesis. This results in an increased fatty acid influx into the liver [31] as well as alterations of adipokines and inflammatory cytokines production and secretion [32]. In the conditions of obesity, excess free fatty acids can contribute to an increase in lipid synthesis and gluconeogenesis [33]. Fat accumulation, free cholesterol and other lipid metabolite synthesis can promote triglycerides (TG) synthesis and accumulation, leading to mitochondrial dysfunction, oxidative stress and ROS production and endoplasmic reticulum (ER) stress, all of which can lead to hepatic inflammation [34].

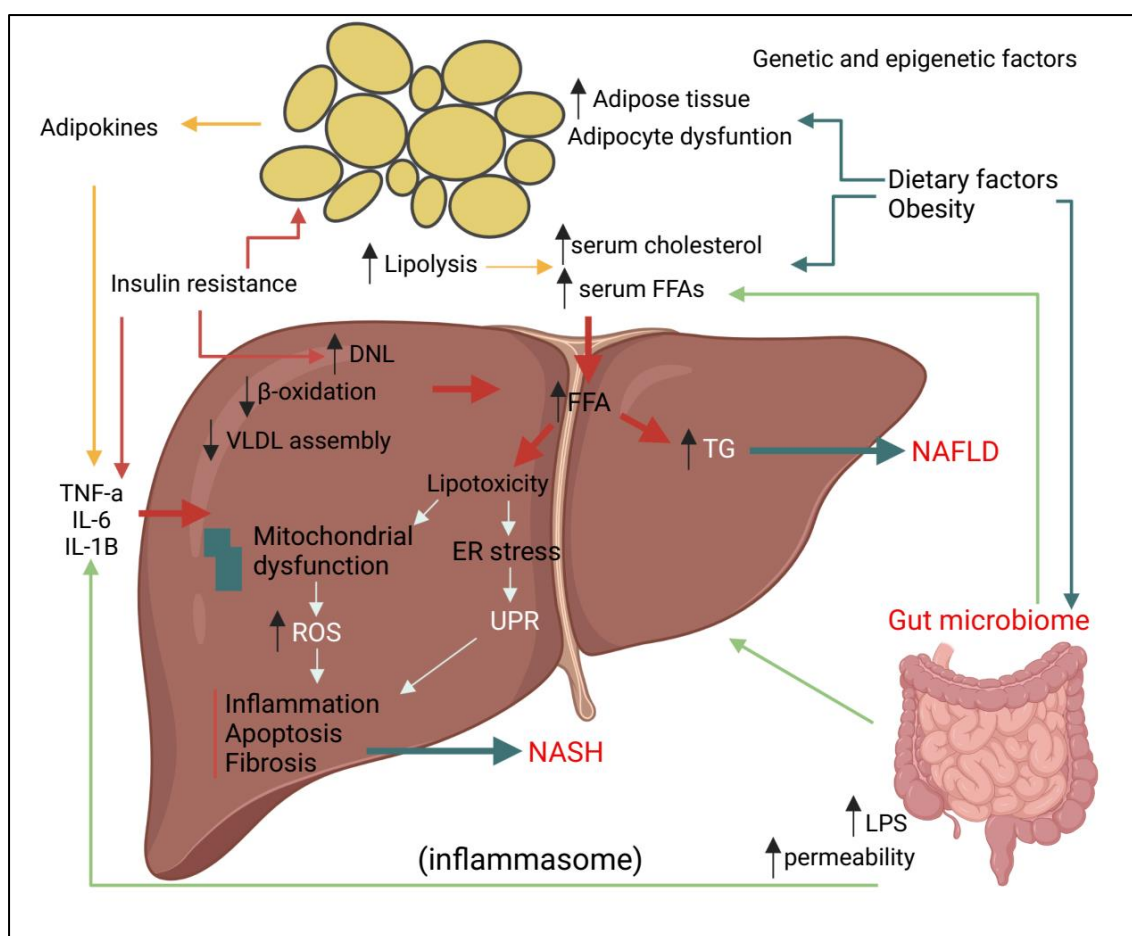


**Figure 2. Multiple hit hypothesis for the development of NAFLD.**

Abbreviations: CH, cholesterol; DNL, *de novo* lipogenesis; ER, endoplasmic reticulum; FFAs, free fatty acids; IL-6, interleukin 6; LPS, lipopolysaccharide; NAFLD, non-alcoholic fatty liver disease; NASH, non-alcoholic steatohepatitis; ROS, reactive oxygen species; TG, triglycerides; TNF- $\alpha$ , tumor necrosis factor-alpha; UPR, unfolded protein response; VLDL, very-low-density lipoproteins. Modified from E Buzzetti et al. [30]. Created in BioRender.com

### 1.1.3.1 Cellular mediators and inflammation

Similar to other liver diseases, various inflammatory and immunological mechanisms play an important role in the progression of NASH and NAFLD. These include innate immunity represented by NK cells, NK T cells, neutrophils and macrophages, adaptive immunity represented by T and B cells, inflammasome activation as well as the gut-liver axis [35]. Resident hepatic macrophages, known as Kupffer cells (KCs) have been reported to contribute to hepatic steatosis [36]. KCs and recruited hepatic macrophages can activate the M1 phenotype of macrophages to produce various cytokines, such as IL-1 $\beta$ , IL-12, and TNF-

$\alpha$  [37, 38], thus leading to inflammation, fibrosis, and cell death in NASH [39, 40]. In addition, The activation of KCs, specifically the M1 phenotype, recruits hepatic stellate cells (HSCs) by secreting the cytokines CCL2 and CCL5. Activation of HSCs to myofibroblasts is a key event in liver fibrosis and is an important player in liver cirrhosis and liver cancer [41].

### **1.1.3.2 Metabolic dysregulation in NAFLD**

Not only NAFLD, but the dysregulation of metabolic factors caused by NAFLD can also increase the risk of developing HCC, such as obesity and diabetes, especially type 2 diabetes mellitus (T2DM). A prospective study followed up for 16 years in the US has shown that obesity is associated with an increased risk of many cancers. In addition, T2DM is also considered to be an independent risk factor for HCC [42]. In an age-, sex- and weight-matched background, patients with T2DM have 80% higher liver fat content than non-diabetic patients. As a result, patients with T2DM are more likely to develop NASH as well as a two to four-fold increased risk of fatty liver-associated complications [43].

Recent studies have reported that saturated fatty acids and other lipid metabolites, including lysophosphatidylcholine (LPC), ceramides and free cholesterol serve as potential contributors to hepatocyte lipotoxicity in NAFLD/NASH [44]. Palmitic acid is the most abundant long-chain saturated fatty acid in vivo. Studies have shown that palmitic acid can trigger oxidative stress and ER/lysosomal/mitochondrial stress, leading to cell death related to lipotoxicity [45]. Besides, LPC and ceramides which are generated from palmitic acid have also been reported to affect hepatocyte lipotoxicity. In particular, LPC has been reported to activate the G-protein-coupled receptor Galpha(i)-JNK pathway [46] or the CCAAT/enhancer-binding homologous protein (CHOP)/JNK pathway [47] to induce the mitochondria-dependent apoptosis. Ceramides contribute to hepatocyte death by impairing the mitochondrial respiratory chain and increasing the permeability of the mitochondrial membrane [48]. Other lipid metabolites, such as free cholesterol, can also induce hepatocyte necrosis, pyroptosis and apoptosis through mitochondrial glutathione consumption and cholesterol crystals production within lipid droplets [49]. All of the above as mentioned have contributed to the development and progress of NASH.

### **1.1.3.3 Mitochondrial dysfunction and ER stress in NAFLD**

The accumulation of excessive lipids in the liver causes lipotoxicity in hepatocytes by triggering endoplasmic reticulum (ER) stress and the dysregulation of mitochondrial can lead to hepatocyte death [50]. Abnormal mitochondrial function promotes toxic lipid metabolite production and excessive ROS [51]. In combination with oxidized LDL particles, ROS could lead to inflammation and fibrosis by activating Kupffer and hepatic stellate cells [52]. Furthermore, obesity, insulin resistance and TNF-alpha levels are closely related to mitochondrial dysfunction [53].

ER stress has been associated with the development and progression of NAFLD [54]. The unfolded protein response (UPR) is a cellular stress response related to ER stress and is important for maintaining ER homeostasis. However, long-term and excessive lipotoxic ER stress suppresses the ability of the UPR and induces hepatocyte death by mediating both mitochondria-dependent intrinsic pathways and death receptor-mediated extrinsic pathways [55]. Furthermore, continuous ER stress causes the overproduction of ROS and activates the NF- $\kappa$ B or JNK pathway, leading to hepatic inflammation [54]. In addition, continuous ER stress [50] activates *de novo* fatty acid synthesis in a manner that relies on ER stress-sensing pathways, resulting in hepatic lipid accumulation [56], suggesting that this adverse cycle between ER stress and hepatic steatosis may contribute to the development and progression of NAFLD/NASH.

## **1.2 Epigenetic impact on chronic liver diseases and HCC**

Like most other cancers, hepatocarcinogenesis is a multistep process. Various molecular pathways are implicated in the HCC pathogenesis including activation of WNT/ $\beta$ -catenin, HGF/MET, EGF/EGFR, or IGF2/IGFR signaling et al [57], ultimately leading to the malignant transformation of hepatocytes [58]. Oncogenic cellular signaling is due to dysregulation of gene expression caused by genetic and epigenetic alterations. Epigenetic abnormalities, regulating gene expression [59], including aberrations in DNA methylation and histone modifications are important features in carcinogenesis. Dysregulation of DNA methylation, for

example, hypermethylated genes TM6SF1, TLX3, EMILIN2 and WNK2 have been shown to contribute to the development of HBV-related HCC [60]. Abnormal expression patterns of miRNAs also have been reported to drive the progression of HCC, such as miR-122 and miR-21 [61, 62]. Importantly, an altered pattern in histone modification has been shown to be crucial for cancer progression and drug resistance in response to molecular targeted therapy [63]. Notwithstanding LSD1 has been reported to overexpress in many cancer types and has oncogenic properties. But the function of LSD1 in liver cancer is not well understood.

### **1.3 Epigenetic modifier lysine-specific demethylase 1**

Lysine-specific demethylase 1 (LSD1) (also named KDM1A; BHC110; AOF2) is the first reported histone demethylase. According to sequence analysis, LSD1 is defined as a homolog of flavin-dependent monoamine oxidase (MAO), and LSD1 catalyzes demethylation via the cofactor flavin adenine dinucleotide (FAD). FAD is commonly associated with transcriptional repressor complexes in the regulation of gene transcription and is an indispensable cofactor for the catalytic activity of LSD1 [64]. LSD1 can specifically demethylate histone 3, lysines 4 and 9 (H3K4 and H3K9) to regulate gene expression (Figure 3). LSD1 commonly interacts with transcriptional repressor complexes such as HDAC1/2, CoREST and BHC80, contributing to gene silence [64]. In addition, LSD1 is associated with nuclear hormone receptors, for example, LSD1 can interact with androgen receptors and stimulates androgen-receptor-dependent transcription [65]. LSD1 can target and identify cancer-related genes in cancer cells, suggesting that it may promote the progression of cancers.

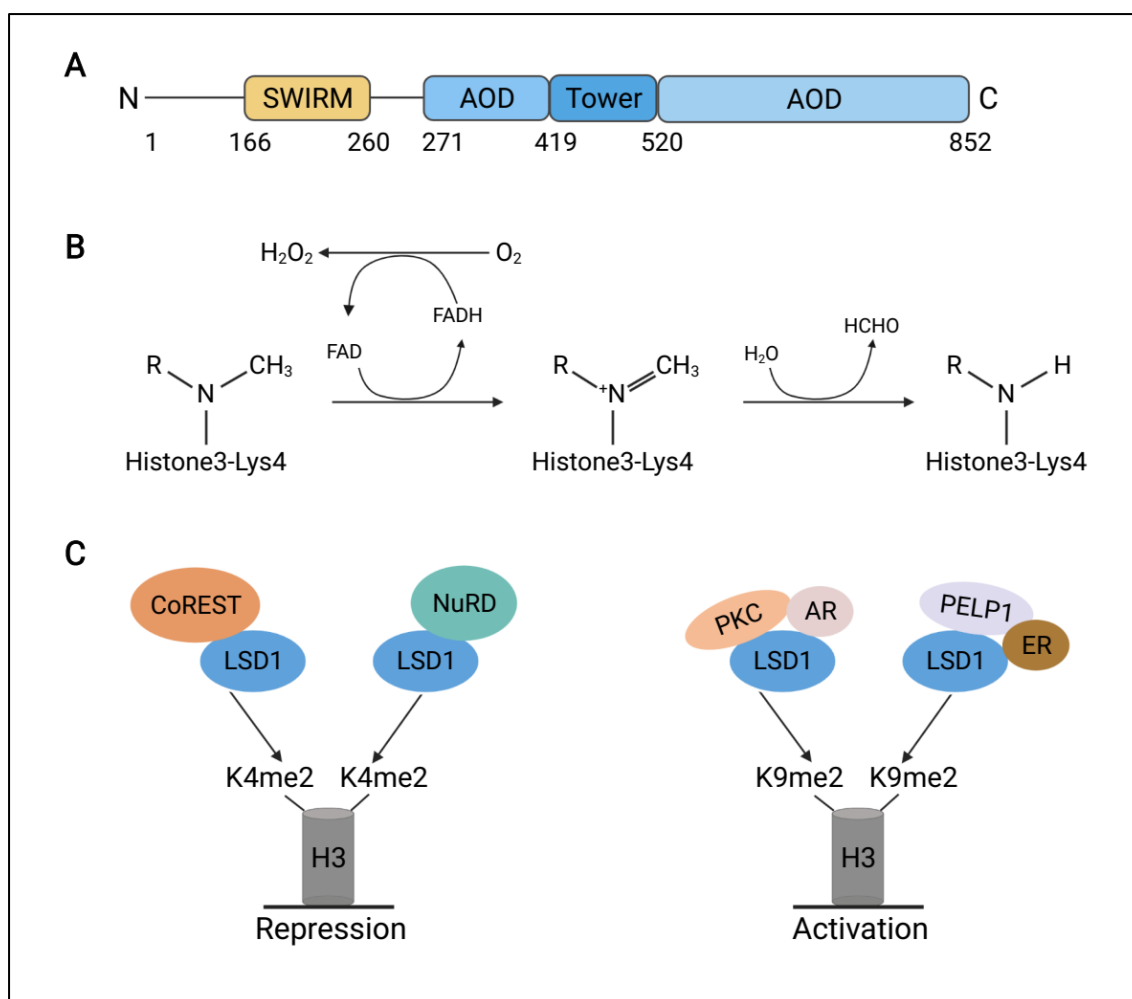


**Figure 3.** (A) Schematic representation of the LSD1 protein. (B) The FAD-dependent catalytic activity of LSD1. (C) LSD1-associated complexes and their demethylation targets. Modified from S Amente et al. [66]. Created in BioRender.com

### 1.3.1 LSD1 impact on cancer

Transcriptional regulation by LSD1 affects several pathways related to cell proliferation, development, and cell cycle control, such as the transforming growth factor  $\beta$ - (TGF- $\beta$ -) related pathway, important for cell survival and epithelial-mesenchymal transition (EMT). LSD1 has been shown to be overexpressed in many various cancer types, such as prostate cancer, bladder cancer, neuroblastomas and lung cancer as well as hepatocarcinoma [67]. Furthermore, High expression levels of LSD1 are associated with a poor prognosis of cancer. In these tumors, inhibition of LSD1 inhibition has been shown to reduce or block cell growth whereas overexpression of LSD1 can promote human carcinogenesis by modifying chromatin.

Because of the similar structure of the LSD1 catalytic domain to conventional amine oxidases, the monoamine oxidase (MAO) inhibitors can inhibit LSD1 activity by covalently binding FAD.

### **1.3.2 LSD1 in cell cycle and proliferation**

LSD1 exhibits diverse transcriptional activities, demethylation of H3K4 represses gene expression while demethylation of H3K9 activates gene expression. The cell cycle is accompanied by methylation and demethylation dynamics of histone and non-histone proteins. It is reported that LSD1 plays a role in chromosomal segregation during mitosis [68]. It appears that multiple KDMs play important roles in regulating cell cycle progression transcriptionally and through demethylation of specific targets, such as retinoblastoma (Rb). LSD1 regulates cell cycle progression through Lys 442 demethylation of myosin phosphatase target subunit 1 (MYPT1). MYPT1 is a protein phosphatase that can remove Ser 807/811 phosphorylation to activate the growth inhibitory [69]. LSD1 induces transcriptional activation of E2F target genes, leading to cell cycle progression [70]. In addition, it has also been shown that LSD1 deficiency causes partial cell cycle arrest and makes cells sensitive to growth inhibition [71]. Interaction of LSD1 with chromatin leads to the short-time-scale gene expression alteration during cell cycle progression. Furthermore, LSD1 is known to colocalize with centrosomes during mitosis [68].

### **1.3.3 Novel aspects of LSD1 function**

LSD1 has been reported to be overexpressed in various types of cancer and is associated with low overall survival in patients [72, 73]. Furthermore, recent reports have shown that LSD1 is involved in inflammatory and immune response mechanisms [74] as well as in metabolic changes and mitochondrial dysfunction [75]. LSD1 is a positive modulator of HIF-1 $\alpha$  stability and transcriptional activity through the demethylation of HIF-1 $\alpha$ . [76]. Sakamoto et al. proposed that the histone demethylation portion of LSD1 is involved in the metabolic reprogramming of cancer cells [77]. Many studies have confirmed the LSD1-mediated promotion of the EMT in various types of cancer [78]. Furthermore, LSD1 is a key epigenetic regulator in inflammatory disease. As a positive regulator, LSD1 increases the expression of inflammatory response genes in inflammatory diseases [79]. Conversely, as a negative

regulator, LSD1 decreased the expression of cytokine genes in cancer cells, smooth muscle cells (SMCs) as well as hematopoietic stem cells (HSCs) [80-82]. In summary, the regulation of gene expression by LSD1 in metabolic and inflammatory processes is critical in the pathogenesis of the disease.

### **1.3.4 Pharmacological inhibition of LSD1**

Previous studies have shown that LSD1 is overexpressed in many different human cancers, such as acute myeloid leukemia (AML), small cell lung carcinoma (SCLC) and colon cancer, inhibition of LSD1 may inhibit tumor growth and metastasis [83, 84]. Consequently, many LSD1 inhibitors have been developed for clinical use in the treatment of AML and SCLC, such as GSK2879552 [85]. Since LSD1 is chemically a monoamine oxidase, some MAO-A/B inactivators were firstly applied and tested as LSD1 inhibitors, such as pargyline, tranylcypromine (2-PCPA) and phenelzine. The 2-PCPA can inhibit LSD1 activity by developing a covalent adduct through a flavin loop after one-electron oxidation and cyclopropyl loop opening. However, These series of compounds cannot be used as specific LSD1 inhibitors because of their potency and selectivity limitations [86]. Promisingly, a number of LSD1 inhibitors, such as ORY1001 and GSK2879552, are in pre-clinical development for the treatment of cancer. HCI-2509, also known as SP2509, is a potent, reversible and selective LSD1 inhibitor that has been shown to have preclinical efficacy in Ewing's sarcoma [87], acute myeloid leukemia [88] and endometrial cancer [89]. HCI-2509 is not yet used in clinical studies but the derivative is used in some scientific work [90]. Inactivation or downregulation of LSD1 inhibits the development of cancer cells, therefore, LSD1-targeted inhibitors might represent a new insight into the discovery of anti-cancer drugs.

## **1.4 Aim**

Due to the pronounced upregulation of LSD1 in hepatocellular carcinoma cells, I hypothesize that LSD1 also triggers HCC progression, as previously shown for other cancer types. Furthermore, primary signaling analysis of our team and recent reports, argue for additional mechanistic links of LSD1 to fat metabolism and inflammatory pathways, which are assumed

to promote liver disease progression.

My study will focus on the function of LSD1 in the development of hepatocellular carcinoma. Firstly, I will address the question of if LSD1 inhibition affects cellular signaling, that retards hepatocellular initiation and progression. Since HCC develops most frequently on the basis of chronic liver disease with inflammatory and metabolic dysregulation processes, the question arises if LSD1 is also involved in HCC prelesions, promoting cellular transformation and cancer initiation. By means of using a mouse model, mimicking human HCC development based on non-alcoholic fatty liver disease, the potential role of LSD1 in fat accumulation and inflammation will be additionally considered in my study.

## 2. Material and methods

### 2.1 Materials

#### 2.1.1 List of devices

Listed below are the devices used during the study

Name	Manufacturer
Olympus Fluoview FV 1000 (Confocal microscope)	Olympus, Hamburg, GER
Water bath	Dr. Hirtz & Co, Cologne, GER
Countess II FL Automated Cell Counter	Thermo Fisher Scientific, Waltham, GER
Eppendorf centrifuge Type 5417R	Eppendorf, Hamburg, GER
Nanodrop 1000 Spectrophotometer	Peqlab, Erlangen, GER
Qubit® 2.0 Fluorometer	Invitrogen, Waltham, Massachusetts, USA
BioRad CFX96 Real-time PCR Cycler	Bio-Rad, Munich, GER
Roche Lightcycler 480	Roche, Mannheim, GER
My Cycler™ (thermal cycler)	Biorad, Hercules, USA
Promega Maxwell® 16	Promega, Mannheim, GER
Mini-PROTEAN® Tetra Cell Systems	Biorad, Hercules, USA
Bio-Dot SF Assembly	Biorad, Hercules, USA
ChemiDoc™ Imaging System	Biorad, Hercules, USA
Elisa-Reader	BMG-LABTECH GmbH, Ortenberg, GER
ImageXpress Micro 4 High-Content Imaging System	CACED, Cologne, GER
Reflotron® System	Roche, Basel, Switzerland

#### 2.1.2 List of kits

Listed below are the kits used during the study

Name	Manufacturer
Venor®GeM one step	Minerva Biolabs, Berlin, GER
CellTiter 96® AQueous One Solution Cell Proliferation Assay	Promega, Madison, USA

TaqMan reverse transcription Kit	Applied Biosystems, Darmstadt, GER
GoTaq® qPCR Master Mix Kit	Promega, Mannheim GER
Pierce™ BCA protein assay Kit	Thermo Fisher Scientific, Waltham, GER
Pierce™ ECL western blotting substrate	Thermo Fisher Scientific, Waltham, GER
SimpleChIP® enzymatic chromatin IP Kit	Cell Signalling, Frankfurt, GER
Maxwell® LEV simplyRNA tissue kit AS1280	Promega, Madison, USA
PicoGreen® dsDNA kit	Invitrogen, Waltham, Massachusetts, USA

### 2.1.3 List of software

Listed below are the softwares used during the study

Application	Name	Developer
<b>Data analysis</b>	Chromas	Technelysium Pty. Ltd.
	CLC Sequence Viewer 8.0	QIAGEN
	Ensembl	Open source
	Excel 2010	Microsoft, Redmont, USA
	Expression Console	Affymetrix, Santa Clara, USA
	GraphPad Prism 8	GraphPad Software, Inc., La Jolla, USA
	Galaxy	Galaxy Team, Penn State University & John Hopkins University, USA
	GSEA	UC San Diego and Broad Institute
	Reactome	Open source
	Transcriptome Analysis Console (TAC)	Affymetrix, Santa Clara, USA
<b>Real-time PCR data analysis</b>	BioRad IQ5	BioRad, München, GER
	Lightcycler®480 SW 1.5	Roche, Mannheim, GER
	Stratagene MxPro 3000P V4.00	Stratagene, La Jolla, USA
<b>Western blot analysis</b>	Image Lab	BioRad, München, GER

<b>ChIP-seq analysis</b>	bamCompare	Open source
	Integrated Genome Browser (IGB)	Open source
<b>Imaging</b>	CellP	Olympus Soft Imaging Solutions, Münster, GER
	Photoshop CS2	Adobe, Dublin, Ireland
	Redasoft Plasmid 1.1	Redasoft, Toronto, Canada

### 2.1.4 Plastic material

All the plastic ware and multi-well plates are sterile. The pipette tips were autoclaved for 20 min at 121°C and 1.2 bar pressure conditions before being used. Dry heat for sterilizing by baking them in an oven at 180°C for 8 hours.

<b>Name</b>	<b>Standard</b>	<b>Manufacturer</b>
Plastic-ware	6 cm, 10 cm, 15 cm	Sarstedt, Nümbrecht, GER
Multi-well plates	6-well, 12-well, 24-well, 96-well	TPP, Hörstel, GER or Nunc, Wiesbaden, GER
Falcon tubes	15 ml, 50 ml	Greiner Bio-One
Eppendorf tubes	0.5 ml, 1.5 ml, 2 ml, 5 ml	Biozym, Oldendorf, GER
Pipette tips	10 µl, 200 µl, 1 ml	Biozym, Oldendorf, GER
Cryo-vials	2 ml	Sigma-Aldrich, Taufkirchen, GER

### 2.1.5 Reagents for cell culture

<b>Reagent</b>	<b>Manufacturer</b>
DMEM (Dulbecco's Modified Eagle Medium)	GibcoBRL, Karlsruhe, GER
DMSO	Sigma-Aldrich, Taufkirchen, GER
Doxycycline	Sigma-Aldrich, Taufkirchen, GER
Fetal Bovine Serum (FBS)	Pan Biotech, Aidenbach, GER
GSK2879552	Xcessbio, San diego, USA
HCI-2509 (C12)	Xcessbio, San diego, USA
HCI-2577 (SP-2577)	Salarius Pharmaceuticals, Houston, USA

OptiMEM	GibcoBRL, Karlsruhe, GER
Phosphate buffered saline (PBS)	GibcoBRL, Karlsruhe, GER
Poly-L/D-Lysine	Sigma-Aldrich, Taufkirchen, GER
Puromycin	Sigma-Aldrich, Taufkirchen, GER
Trypsin-EDTA (0.05%)	GibcoBRL, Karlsruhe, GER
Lipofectamine 2000	Thermo Scientific, Waltham, USA

### 2.1.6 Reagents for molecular experiment

Reagent	Manufacturer
Acetic acid	Sigma-Aldrich, Taufkirchen, GER
Acrylamide/bis-acrylamide, 30%	Sigma-Aldrich, Taufkirchen, GER
Agarose	Biozym, Oldendorf, GER
Ammonium peroxodisulfate (APS)	Carl Roth, Karlsruhe, GER
$\beta$ -Mercaptoethanol	Carl Roth, Karlsruhe, GER
Chloroform (99%)	Sigma-Aldrich, Taufkirchen, GER
Dipotassium hydrogenphosphate (K <sub>2</sub> HPO <sub>4</sub> )	Carl Roth, Karlsruhe, GER
Disodium hydrogenphosphate (Na <sub>2</sub> HPO <sub>4</sub> )	Carl Roth, Karlsruhe, GER
Ethylenediaminetetraacetic acid (EDTA)	Carl Roth, Karlsruhe, GER
Ethanol (99%)	Carl Roth, Karlsruhe, GER
Fish Gelatin	Sigma-Aldrich, Taufkirchen, GER
Formaldehyde (4%)	Carl Roth, Karlsruhe, GER
Glycine	Sigma-Aldrich, Taufkirchen, GER
Glycogen Blue	Thermo Scientific, Waltham, USA
Isopropanol (99%)	Carl Roth, Karlsruhe, GER
Laemmli buffer 2x & 4x	Biorad, Hercules, USA
Magnesium chloride (MgCl <sub>2</sub> )	Carl Roth, Karlsruhe, GER
Methanol (99%)	Carl Roth, Karlsruhe, GER
Milk powder	Carl Roth, Karlsruhe, GER
NEB cell lysis buffer 10x	New England Biolabs, Frankfurt, GER
NP-40	Sigma-Aldrich, Taufkirchen, GER

Phenylmethanesulfonyl fluoride (PMSF)	Sigma-Aldrich, Taufkirchen, GER
Potassium chloride (KCl)	Carl Roth, Karlsruhe, GER
Potassium dihydrophosphate (KH <sub>2</sub> PO <sub>4</sub> )	Carl Roth, Karlsruhe, GER
Prestained protein standard (11–245 kDa)	New England Biolabs, Frankfurt, GER
Protease inhibitor tablets	Roche, Grenzach-Wyhlen, GER
RIPA buffer	Thermo Scientific, Waltham, USA
Silencer Select SiRNA against LSD1 (s619)	Thermo Scientific, Waltham, USA
Sodium dodecyl sulphate (SDS)	Carl Roth, Karlsruhe, GER
Sodium chloride (NaCl)	Carl Roth, Karlsruhe, GER
Sodium acetate (NaCH <sub>3</sub> COOH)	Carl Roth, Karlsruhe, GER
Sodium hydroxide (NaOH)	Carl Roth, Karlsruhe, GER
Tetramethylethylenediamine (TEMED)	Thermo Scientific, Waltham, USA
TRIS-HCl	Carl Roth, Karlsruhe, GER
Trizol	Thermo Scientific, Waltham, USA
Tween-20	Sigma-Aldrich, Taufkirchen, GER
Random primer	Thermo Scientific, Waltham, USA
dNTPs	Thermo Scientific, Waltham, USA

## 2.1.7 Solutions

Lists below are the solutions that were made using standard recipes in the laboratory required for biochemical assays. Purified water was used from the completely desalted Millipore machine (Millipore-Q Plus, Millipore, Molsheim, GER) for all the solutions.

### 2.1.7.1 Solutions for immunoblotting

#### Running buffer 10X

Reagent	Amount
Tris	30.3 g (250 mM)
Glycin	187.7 (2.5 M)
10% SDS	1%
ddH <sub>2</sub> O	Add up to 1000 ml

**Transfer buffer 12.5X**

Reagent	Amount
Tris	75 g (312.5mM)
Glycin	356 g (2.4M)
Methanol	20%
ddH <sub>2</sub> O	Add up to 2000 ml

**PBS 5X**

Reagent	Amount
Na <sub>2</sub> HPO <sub>4</sub>	36 g (0.05M)
NaCl	200 g (0.68M)
KH <sub>2</sub> PO <sub>4</sub>	6 g (8.8 mM)
KCl	5 g (0.013M)
ddH <sub>2</sub> O	QS to 5 L

Adjust solution to desired pH (typically pH ≈ 7.4)

**PBST 1X**

PBST was made with 0.05% (v/v) solution of Tween-20 in PBS.

**TBS 10X**

Reagent	Amount
Tris	12.114 g (0.2 M)
NaCl	43.83 g (1.5 M)
ddH <sub>2</sub> O	QS to 500 ml

Adjust solution to desired pH 7.2-7.4

**TBST 1X**

TBST was made by 0.05% (v/v) solution of Tween-20 in PBS.

**SDS Stacking gel (2X)**

Reagent	Amount (%V/mass)
0.5M TRIS pH 6.8	1.26 ml
10% APS	50 µl
10% SDS	50 µl

Acrylamide (30%)	830 µl
TEMED	5 µl
ddH <sub>2</sub> O	2.74 ml

### 2.1.7.2 Solutions for agarose gel electrophoresis

#### TAE buffer 10X

Reagent	Amount
EDTA (pH 8.0)	1 mM
Sodium acetate (CH <sub>3</sub> COONa)	5 mM
Tris-acetate (pH 7.8)	40 mM

### 2.1.7.3 Solutions for plasmid cloning

#### LB medium

Reagent	Amount
Tryptone	10 g
NaCl	10 g
Yeast extract	5 g
ddH <sub>2</sub> O	Up to 1 L

Adjust the pH to 7.0 by using sodium hydroxide (NaOH) solution (1 N)

### 2.1.8 Enzymes

Enzyme	Manufacturer
Dnase	Macherey & Nagel, Düren, GER
GoTaq® G2 DNA Polymerase	Promega, Mannheim GER
GoTaq® QPCR Master Mix	Promega, Mannheim GER
RNase A	Macherey & Nagel, Düren, GER
SYBR Green	Promega, Mannheim, GER

### 2.1.9 Antibodies

Primary antibody	Host species	Dilution	Manufacturer
LSD1	Rabbit	WB: 1:1000 ChIP: 3 µg for 10 µg chromatin	Abcam, Cambridge, UK
FABP5	Rabbit	WB: 1:1000	Cell Signalling Technology, Massachusetts, USA
H3K4me2	Rabbit	WB: 1:2000 ChIP: 2 µg for 10 µg chromatin	Abcam, Cambridge, UK
PLK1	Mouse	WB: 1:500	Thermo Scientific, Waltham, USA
β-actin	Mouse	WB: 1:2000	Sigma-Aldrich, Taufkirchen, GER
IgG	Rabbit	ChIP: 3 µg for 10 µg chromatin	Cell Signalling Technology, Massachusetts, USA

Secondary antibody	Host species	Reactivity against	Dilution	Manufacturer
HRP labeled	Rabbit	Mouse	1:2000	Abcam
HRP labeled	Goat	Rabbit	1:2000	Abcam

### 2.1.10 Primers

Primer	Sequence	Species
HPRT-F	GACCAGTCAACAGGGGACAT	Human
HPRT-R	GTGTCAATTATATCTTCCACAATCAAG	Human
LSD1-F	CCCTTAAGCACTGGGATCAG	Human
LSD1-R	ACACGAGTAGCCATTCTTACTG	Human
PLK1-F	GCAGCGTGCAGATCAACTTC	Human
PLK1-R	AGGAGACTCAGGCGGTATGT	Human
FABP5-F	CAGTTCAGCAGCTGGAAGGAA	Human
FABP5-R	ATTGCGCCCATTTTTCGCA	Human
FASN-F	CAGGCACACACGATGGAC	Human

FASN-R	CGGAGTGAATCTGGGTTGAT	Human
LDHA-F	AGGCCCGTTTGAAGAAGAGTG	Human
LDHA-R	TACAGTGAAATGATATGACATCAGAAGA	Human
PDK4-F	CTGAGAATTATTGACCGCCTCTTT	Human
PDK4-R	GCAAGCCGTAACCAAAACCAG	Human
ACACA-F	TCAAACCTGCAGGTATCCCAACTC	Human
ACACA-R	CATTTTCCTGCCAGTCCACAC	Human
ESRRA-F	GGCGGCAGAAGTACAAGCG	Human
ESRRA -R	GCATTCACTGGGGCTGCTGT	Human
ANKRD1-F	CCAGATCGAATTCCGTGATATGC	Human
ANKRD1-R	AAACATCCAGGTTTCCTCCACG	Human
GPAM-F	GGAAAGTTTATCCAGTATGGCATTTC	Human
GPAM-R	CTGATATCTTCCTGGTCATCGTG	Human
PIK3R3-F	TGATGCCCTATTCGACAGAA	Human
PIK3R3-R	GGCTTAGGTGGCTTTGGTG	Human
NDRG1-F	GGCGCCTACATCCTAACTCG	Human
NDRG1-R	GCACAAGGGTTCACGTTGAT	Human
LOXL2-F	GGAGAGGACATACAATACCAAAGTGT	Human
LOXL2-R	CCATGGAGAATGGCCAGTAG	Human
FABP5 promoter-F	GCAAGAGGAGCTGGTTAGCA	Human
FABP5 promoter-R	GGCGCTATGCGGCCAATG	Human
PLK1 promoter-F	TTTTAAATCCCCGCGGCCAATC	Human
PLK1 promoter-F	CTCCTCCCCGAATTCAAACG	Human

### 2.1.11 Sequences of siRNAs

LSD1 targeted siRNA sequences were used as follows:

Name	Sequence
siRNA seq2	5'-UGAAUUAGCUGAAACACAA-3'
siRNA seq3	5'-CACAAGGAAAGCUAGAAGA-3'
siRNA seq4	5'-AGGCCUAGACAUUAAACUG-3'

### 2.1.12 Cell lines

Cell line	Cell type	Species	Source
Huh7	Hepatocellular carcinoma	Human	DSMZ <sup>1</sup>
HepG2	Hepatocellular carcinoma	Human	DSMZ <sup>1</sup>
Hep3B	Hepatocellular carcinoma	Human	DSMZ <sup>1</sup>
HEK293	Embryonic kidney cells	Human	DSMZ <sup>1</sup>
PC9	Non-small cell lung cancer	Human	Roman Thomas <sup>2</sup>

1- Deutsche Sammlung von Mikroorganismen und Zellkulturen GmbH, Germany

2- Kind gift from Dr. Roman Thomas (Department of Translational Genomics, University of Cologne, Cologne, Germany)

## 2.2 Methods

### 2.2.1 Cell culture

Pre-warmed culture media DMEM supplemented with 10% FBS and 0.05% Trypsin to 37°C. Cells were split into other plates or frozen for later use when the cells reached the point of growth in a culture where it covers most of the bottom of the plate, or about a 90% *confluency*. Cells were detached with 0.05% Trypsin and incubated at 37°C in the CO<sub>2</sub> incubator. All the steps were performed under the laminar flow hood.

#### 2.2.1.1 Thawing and freezing of cells

Cryopreserved cells were taken from liquid nitrogen and thawed in 37°C water bath for a minute till the ice melted. Gently transferred the cryopreserved cells and thawing media into 3 ml fresh medium and mix well. Finally transferred all the medium with cells into a 10 cm plate with 7 ml fresh medium. Changed to 10 ml fresh medium the next day when the cells attached.

For cell cryopreservation, cells were trypsinized and collected in a falcon tube and centrifuged at 1500 rpm for 5 min. Resuspended the cell pellet in fresh medium with supplemented with 10% DMSO and aliquoted 1 ml of the solution into cryo-vials. Frozen the cells slowly by reducing the temperature to approximately 1°C per minute and later stored the vials in the – 80°C freezer. Transferred the vials to the liquid nitrogen storage area the next day, where the

vials will be stored until further use.

### **2.2.1.2 Determination of cell number**

Cells were detached with 0.05% Trypsin and incubated for 2 min at 37°C in the CO<sub>2</sub> incubator. Fresh medium is added and mixed gently to make sure all the cells are in suspension. Cells were counted using Countess chamber slides (Thermo Fisher Scientific, GER) by adding 10 µL of the cell suspension to 10 µL of 0.4% trypan blue stain. After leaving the mixture for 30 seconds at room temperature, the slides were inserted into the slide port of the cell counter. Cell counting was performed according to the manufacturer's instructions.

### **2.2.1.3 Mycoplasma test**

For the Mycoplasma test, 100 µl culture medium was collected from cells that were already with 90% confluency and were heated in 95°C water bath for 10 min. The supernatant was collected after short centrifugation at 12,000 rpm for 10 seconds. Mycoplasma contaminations were detected by a real-time PCR (qPCR) using Venor®GeM mycoplasma PCR Detection Kit according to the manufacturer's protocol.

## **2.2.2 Cells treated with compounds**

Cells were treated with LSD1 inhibitors (2.2.2.1) or were transduced with various siRNAs (2.2.2.2) or with plasmids constructs as shown in Figure 4 (2.2.2.3).

### **2.2.2.1 Treatment of cells with LSD1 inhibitors**

The reversible Lysine Specific Demethylase-1 (LSD1) inhibitor HCl-2509 (C12) and HCl-2577 were dissolved in DMSO to 50 mM and stocked in the fridge. Cells were seeded with the same cell density in the control group and treatment group one day before treatment to reach a 40% confluency the next day. Diluted the drugs to 1 µM, 2 µM and 4 µM with fresh medium. Cells were washed once with 1xPBS and changed to fresh medium and fresh medium with drugs, respectively, then incubated for 72 hours for the analysis.

### **2.2.2.2 Transfection of cells with small interfering RNA (siRNA)**

Cells were seeded in 6-well plates one day before transfection to reach 50% confluency the next day. SiRNA was transfected to cells using Lipofectamine 2000 according to the manufacturer's instructions. To achieve maximum effectiveness of siRNA, 4 different siRNA concentrations were performed as a pre-experiment for transfection optimization experiments. Transfection was performed for the gene specific siRNA and scrambled siRNA simultaneously with a final concentration of 50 nM and 100 nM, respectively. Cells were washed once after 6 hours of transfection and changed to a fresh medium. Cells were harvested for RNA and protein after 72 hours of growth.

### 2.2.2.3 Conditional shLSD1 knockdown plasmids

Conditional shLSD1 knockdown plasmids were kindly provided by Zhefang Wang ( Department of General, Visceral and Tumor Surgery in University Hospital of Cologne). ShLSD1 includes the following target sequence (CCGGAGGAAGGCTCTTCTAGCAATACTC GAGTATTGCTAGAAGAGCCTTCCTTTTTTG) is expressed by the Tet-On system (Figure 4). Hepatoma cells were cultured and changed fresh medium with 1 µg/ml of doxycycline (Dox) every day to induce knockdown LSD1 expression. Therefore, in the presence of Dox, reverse tet transactivators (rtTAs) bind to the TetO to induce shLSD1 expression and finally get LSD1 mutant protein. In contrast, rtTAs cannot bind to the TetO in the absence of Dox, thus, shLSD1 expression does not occur.

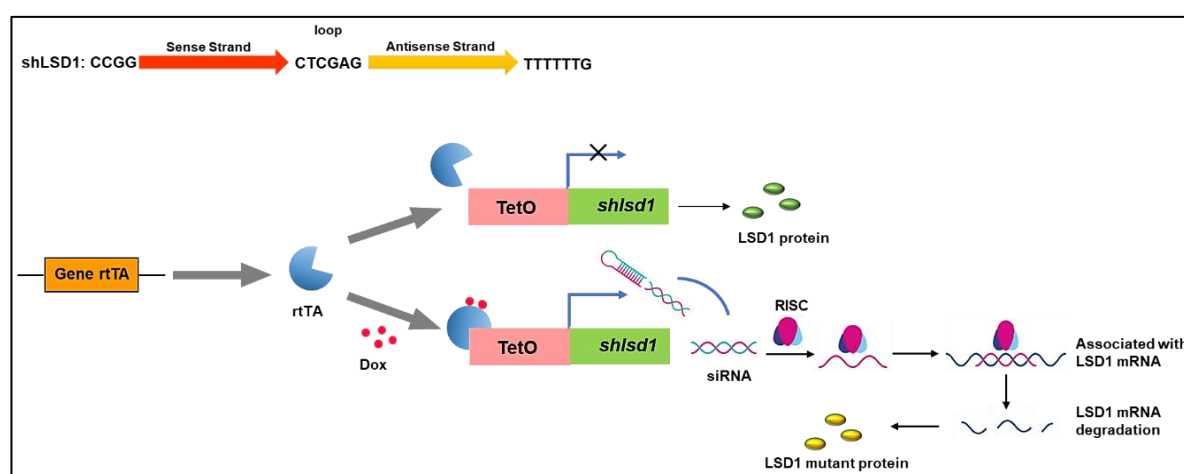


Figure 4. schematic illustration of LSD1 knockdown construct as explained in the main text.

#### **2.2.2.4 Transfection of cells with plasmids**

Transfection was performed using lipofectamine 2000 according to the manufacturer's instructions. Mostly transfection was carried out in 6-well plates. 500,000 cells were seeded the day before transfection in 6-well plates that reach 70-80% confluency 24 hours later at the time of transfection. The Lipofectamine 2000 and the DNA were diluted in separate tubes with Opti-MEM® Medium in a 1:1 ratio and after a 5 min mix and incubated another 5 min at room temperature. Finally, each well had 4 µg of DNA and 10 µl of Lipofectamine 2000. Incubated cells for 2 days at 37°C.

#### **2.2.3 Lentiviral transduction**

For the generation of LSD1 knockdown cells, lentiviral transduction was performed to generate cells stably expressing short hairpin RNA (shRNA). The addition of puromycin was used to select cells that stably express shRNA against LSD1.

##### **2.2.3.1 Preparation of lentiviruses**

HEK293T cells were plated in plates and incubated at 37°C, 5% CO<sub>2</sub> overnight until the cells reached 80% confluency the next day. HEK293T cells were co-transfected with shLSD1 and shNTC plasmids, respectively and 2nd generation packaging vectors (pMD2.G and psPAX2, Addgene, LGC Standards Teddington, UK) using Lipofectamine 2000 according to the manufacturer's instructions. Briefly, a cocktail was made from the vectors and transfection reagent and incubated at room temperature for 10 min. Afterward, the mixture was added to the HEK293T cells and the medium was replaced with fresh medium after 6 hours in order to remove the transfection reagent. The supernatant (virus) was collected and filtered with 0.45 µm filters at 48 hours and 72 hours. The virus was frozen at -80°C for long-term storage.

##### **2.2.3.2 Treatment of lentivirus to hepatoma cells**

The filtered supernatant was mixed 1:1 with a fresh complete culture medium and applied to Huh7 and HepG2 cells to generate the shLSD1 and shNTC constructs. After 72 hours of incubation, the cells were selected by 2 µg/ml puromycin for at least 6 passages. Finally, the

LSD1 knockdown Huh7 and HepG2 clones were established after being selected by puromycin resistance which can successfully generate the shLSD1 and shNTC constructs. Cells were cultured in fresh medium and induced by 1 µg/ml doxycycline to induce the knockdown of LSD1.

## **2.2.4 In vitro analysis of cell viability and proliferation**

### **2.2.4.1 Determination of cell viability using the MTT test**

Cells were seeded the day before treatment at a density of 10,000 cells/well in a 96-well plate. Cells were treated with drugs or transfected with siRNAs for 72 hours at 37°C in the CO<sub>2</sub> incubator. The experiments were performed with biological triplicates. For the 96-well assay plate, 20 µl of CellTiter 96® AQueous One Solution Reagent were pipetted into each well containing the samples in 100µl of culture medium. Then the plate was Incubated at 37°C for 1.5 hours in a humidified, 5% CO<sub>2</sub> incubator. Recorded the absorbance at 490nm using a 96-well plate reader for analysis.

### **2.2.4.2 Incucyte live-cell imaging and analysis**

Images were acquired using ImageXpress Micro 4 High-Content Imaging System in CECAD Imaging Facility (Cologne, GER) with transmitted light every hour for 96 hours. Huh7 and HepG2 transduced cells were plated into 6-well black, clear-bottom plates at of density of 400,000 cells per well and cultured in the environment control chamber for 96 hours at 37°C and 4% CO<sub>2</sub>. Doxycyclin treatment was performed every 24 hours with a final concentration of 1 µg/ml. Image analysis was performed during image acquisition using a transmitted light cell count general analysis protocol. The analysis provided measurements for numbers of cells, average cell area, and total cell-covered area.

## **2.2.5 Analysis of gene expression**

Gene expression analysis was performed using real-time PCR (quantitative PCR, qPCR) to detect and quantify messenger RNA (mRNA) levels of a specific gene. Moreover, RNA sequencing (RNA-Seq) was used for the transcriptome analysis.

### 2.2.5.1 RNA isolation

Cells were washed with ice-cold 1XPBS and harvested from the 6-well plates. Cells were lysed directly in a culture dish by adding 400  $\mu$ l TRIZOL Reagent and scraped with cell scrapers. Chloroform was used to separate the phases, at room temperature for 5-10 min and then centrifuged at 12,000 rpm, 4°C for 15 min. Transferred the aqueous phase in another 1.5 ml Eppendorf tube. RNA was precipitated from the aqueous phase by mixing with isopropanol at 14,000 rpm, 4°C for 30 min. The RNA pellet was washed twice with 75% ethanol and dried at room temperature. Finally, the RNA pellet was resuspended in diethylpyrocarbonate (DEPC) treated RNase-free water to be stored at -80°C.

### 2.2.5.2 Reverse transcription of RNA

For real-time PCR, mRNA was reverse transcribed into cDNA using the SuperScript III Reverse Transcriptase (RT) (Invitrogen, Waltham, Massachusetts, USA) according to the manufacturer's protocol. 500 ng RNA was used to prepare cDNA in a volume of 10  $\mu$ l reaction mix. The reaction was performed by the following steps.

#### Step 1: Mix 1

Total Volume ( $\mu$ l)	6.5
RNA ( $\mu$ l)	5.5
Aqua ( $\mu$ l)	
Random Primer ( $\mu$ l)	0.5
dNTP-Mix (10mM) ( $\mu$ l)	0.5

The heated mixture to 65°C for 5 min and incubate on ice for at least 1 min.

#### Step 2: Mix 2

Total Volume ( $\mu$ l)	3.5
5x FirstStrandBuffer ( $\mu$ l)	2
0.1M DTT (10 mM) ( $\mu$ l)	0.5
RNaseInhibitor ( $\mu$ l)	0.5
SuperScript III ( $\mu$ l)	0.5

Added Mix 2 to Mix 1, then the concentration of RNA is 50ng/ $\mu$ l

25°C for 5 min

50°C for 60 min

70°C for 15 min

### 2.2.5.3 Real-time PCR

Real-time PCR was performed using GoTaq qPCR Master Mix (Promega) and the assay was mixed following the manufacturer's instructions. Forward primer and reverse primer for the gene of interest are available to the samples. A single reaction consisted of a maximum of 10 ng DNA. The amplification efficiency of all the primers used for the reaction was tested by plotting a standard curve. Just 15  $\mu$ l volume when 96-well plates were used and 10  $\mu$ l volume when 384-well plates were used for the quantitative real-time PCR. HPRT gene used for housekeeping gene. The efficiency of each qPCR assay was evaluated before being applied to transcript quantification. For this PCR mixes were set up using a dilution series of cDNA ( 25, 12.5, 6.25, 3.125, 1.56, 0.78 ng/ $\mu$ l ) was set up. After PCR the Ct values of the dilution series were monitored and efficiency determined. Only assays with an efficiency between 90–100% were used for transcript quantification.

PCR was performed at the conditions listed below:

Total Volume ( $\mu$ l)	96-well plate	384-well plate
	15	10
Aqua ( $\mu$ l)	5.3	2.2
10 mM Primer Forward ( $\mu$ l)	0.6	0.4
10 mM Primer Reverse ( $\mu$ l)	0.6	0.4
SYBR Green ( $\mu$ l)	7.5	5
cDNA ( $\mu$ l)	1	2

Cycler:

95°C 2 min

95°C 30 sec

60°C 30 sec

72°C 30 sec 49 cycles

72°C 5 min

Melting curve 65°C to 95°C

#### **2.2.5.4 Pathway analysis using transcriptome data**

To identify the relationship between the biological function and differential expressed genes (DEGs), the Database for Annotation, Visualization and Integrated Discovery (DAVID) was used to investigate the Kyoto Encyclopedia of Genes and Genomes (KEGG) pathways and Gene Ontology (GO) terms. Gene set enrichment was analyzed by GSEA software to rank the significant DEGs between the control and HCI-2509 treated or LSD1 knockdown group. Normalized enriched score (NES) was determined for each gene set. The HCI-2509 treated data from RNA sequencing were kindly provided by my colleague Lingyu Wang. *P* value <0.5 was considered as statistically significant enrichment.

#### **2.2.6 Analysis of protein expression**

Quantification of relative expression levels for specific proteins is accomplished by Western blot and Dot slot immunoblotting analysis from extracted cell proteins.

##### **2.2.6.1 Cell lysis**

Cells were washed with ice-cold 1XPBS and harvested from the 6-well plates. Cells were lysed directly in a culture dish by adding 100 µl RIPA buffer and scraped with cell scrapers. Cell lysates were incubated on ice for 5 min, followed by sonication for 5 min to disrupt the cell membrane completely. The lysates were centrifuged at 14,000 rpm for 15 min at 4°C. The supernatant was transferred to a new tube and quickly frozen into liquid nitrogen, stored at -80°C for further analysis.

##### **2.2.6.2 Determination of protein concentration**

The concentration of protein was measured by BCA Protein Assay Kit which was purchased from Thermo Fisher Scientific. For the albumin (BSA) standards, diluting the contents of

albumin standard (BSA) into a gradient concentration. The final concentration of all the points are 2000 µg/mL, 1500 µg/mL, 1000 µg/mL, 750 µg/mL, 500 µg/mL, 250 µg/mL, 125µg/mL, 0 µg/mL. Dilutions were made in the same buffer as in which the sample was resolved. Prepared working reagent by mixing 50 parts of BCA Reagent A with 1 part of BCA Reagent B (50:1, Reagent A: B), then added to each well of 96-well plate 200 µl reagent with 5 µl standards or samples. Incubated the plate at 37°C for 30 min. Measured the absorbance of the samples at 570 nm wavelength by an Optima reader.

### **2.2.6.3 Western blot analysis**

SDS-polyacrylamide gel electrophoresis (SDS-PAGE) was used for Western blot analysis. 10% Running Gel and 12% Stacking Gels were prepared according to the standard operating protocols in the lab. 4x laemmli buffer supplemented with β-mercaptoethanol was used to dilute the protein samples and heated at 95°C for 5 min and directly loaded onto the gels. 10-15 µg protein was used in 12 µl volume. A prestained protein ladder was used to estimate the protein sizes. The protein samples were resolved by running the gels using the Bio-Rad Mini protein gel system. the electrophoresis was carried out at 90V for 20 min and then increased to 110V for 60 min. Proteins were transferred from the gel to a 0.2 micron PVDF membrane at 90V for 60 min. To block the unspecific region on the membranes. The membranes were incubated in 5% milk powder in PBST for an hour. The primary antibody was diluted in block solution and incubated at 4°C overnight. After primary antibody incubation, the membranes were washed three times with 1X PBST for 5 min each and then incubated with the appropriate HRP labeled secondary antibodies diluted in blocking solution for an hour at room temperature. The washing step was repeated and the membranes were incubated with Pierce™ ECL western blotting substrate for 1 min and developed in the ChemiDoc™ Imaging System. Images obtained were processed using the Image lab.

### **2.2.6.4 Dot slot immunoblotting**

Bio-Dot SF blotting apparatus was performed for protein detection. 100 µl TBS was used twice per well to prewet the nitrocellulose membrane and made sure that all the screws had been

tightened under vacuum to ensure that there will not be any cross-well contamination. 8 µg protein was diluted in TBS with a total 50 µl volume and added to each well. After 5 min under a gentle vacuum, the membrane was washed twice with 200 µl TBS. The membranes were blocked in 0.5% milk solution for one hour. the primary antibody was diluted in block solution and incubated for 3 hours. The primary antibodies and the secondary antibodies were applied the same as the Western blots. The membranes were developed in the ChemiDoc™ Imaging System. Images obtained were processed using the Image lab.

### **2.2.7 Chromatin immunoprecipitation**

Chromatin immunoprecipitation (ChIP) assays were performed by using SimpleChIP® enzymatic chromatin IP Kit (Cell Signaling Technology, Danvers, Massachusetts, USA) according to the manufacturer's instructions. The steps of chromatin immunoprecipitation are shown in Figure 5. Cells were harvested from 15 cm culture dishes containing cells that were 90% confluent and fixed with 1% formaldehyde. The DNA fragments were sonicated. DNA fragmentation was controlled and should be approximately 150-900bp. Genomic DNA was purified after ribonuclease (RNase) treatment, proteinase K, and heat for decross-linking, followed by ethanol precipitation. DNA concentration was measured utilizing the PicoGreen dsDNA assay kit according to the manufacturer's instructions. The working solution was prepared by diluting the Qubit® dsDNA HS Reagent 1:200 in Qubit® dsDNA HS Buffer. Each sample for measurement containing 1 µl DNA and 199 µl working solution, concentration was measured by Qubit® 2.0 Fluorometer. The DNA fragments (10 µg) were immunoprecipitated with 3 µg of antibody against LSD1 or 2 µg of antibody against H3K4me2 and 3 µg of antibody against IgG as a negative control, using genomic DNA as positive input. ChIP analysis was performed using the free source Galaxy platform with the help of Dr. Priya S. Dalvi. The enrichment of LSD1 and histone marks on gene promoters was quantified by ChIP-qPCR.

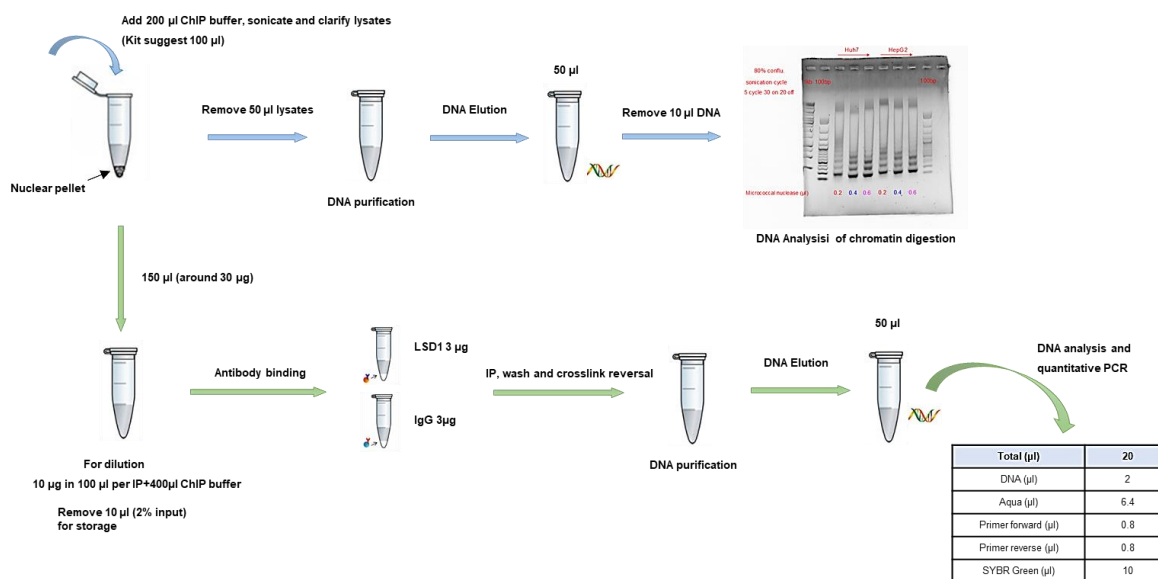


**Figure 5. Schematic representation of ChIP workflow and crucial steps for effective crosslinking and immunoprecipitation.**

## 2.2.8 Induction of NAFLD in mice and inhibition of LSD1 by HCI-2509 treatment

For *in vivo* experiments, the high-fat diet mouse model was used to mimic the development of steatohepatitis and HCC in humans [91]. LSD1 was inhibited by the pharmacological inhibitor HCI-2509. The wild-type mouse C57BL/6J was used for the experiments and purchased from Charles River.

### 2.2.8.1 Experimental design of drug-mediated inhibition of LSD1 *in vivo*

Sixteen wildtype C57BL/6J mice were randomized into two groups so that 8 mice were used in each group. All the mice received an intraperitoneal injection (IP) of 25 mg/kg diethylnitrosamine (DEN) at two weeks old to induce liver disease occurrence. After additional four weeks, beginning at 6 weeks, all the mice were raised on the high-fat diet (HFD), consisting of 60% fat, 20% carbohydrate, and 20% protein (D12492) (ssniff-Spezialdiäten GmbH, Soest, GER). When the mice grew up to 12 weeks, one group received an IP injection of 60 mg/kg LSD1 inhibitor HCI-2509 three times a week for six weeks. The other group received an IP injection of the vehicle. The body weight (BW) was determined once a week. The blood was collected from all the mice for liver enzyme measurement (aspartate aminotransferase (AST) and alanine aminotransferase (ALT) to monitor the development of

the disease every three weeks since the mice were 12 weeks old. At 18 weeks, all the mice were sacrificed by cervical dislocation for organ removal (Figure 6). The histopathological analysis will be performed using histology and immunohistology.

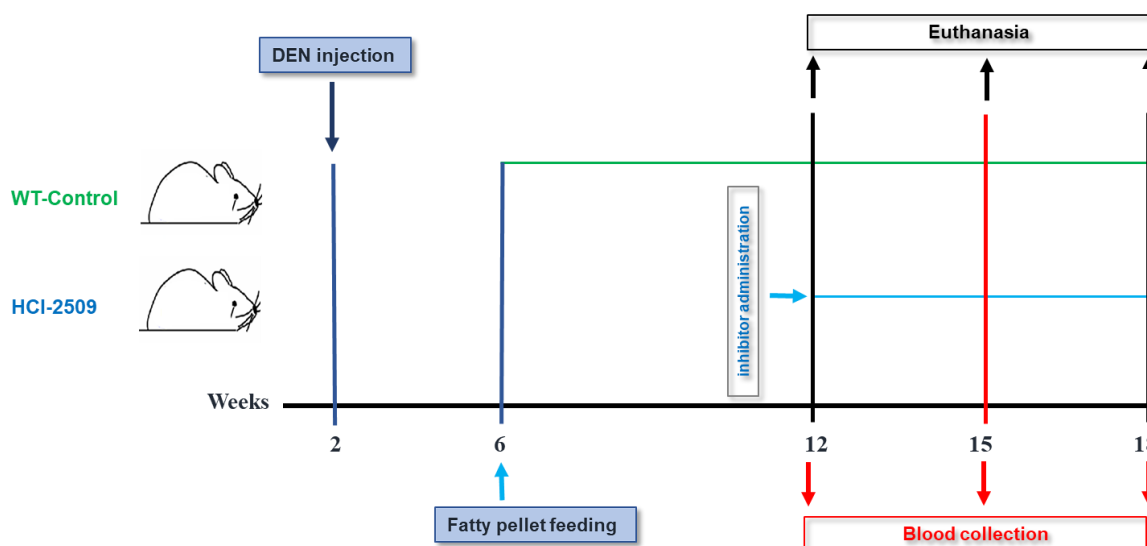


**Figure 6. Experimental design of the treatment with HCl-2509 in NAFLD mouse model.**

At the age of 2 weeks, C57BL/6J mice were treated with 25 mg/kg diethylnitrosamine (DEN). At the age of 6 weeks, all the mice were fed with high-fat diet (HFD). At the age of 12 weeks, all the mice were separated randomly into two groups: Control and HCl-2509 treatment. Blood was collected every three weeks and mice were euthanized at the age of 18 weeks.

### 2.2.8.2 Application of LSD1 inhibitor HCl-2509

For the dose of 60 mg/kg body weight, the LSD1 inhibitor HCl-2509 was dissolved with a final concentration of 7.5 mg/ml in solution. Firstly, the HCl-2509 was dissolved in sterilized DMSO, then the same volume of ethanol was added as stock solution. Kalliphor solution mixture passed through the 0.22  $\mu$ M filter consisting of Kalliphor, Ethanol and PBS with the volume ratio of 1:1:3 was used as diluting solvent. Thus, the final concentration of HCl-2509 is 7.5 mg/ml in the solution with 4% DMSO, 14% Ethanol and 10% Kalliphor. After the 6-week high fat diet, the experimental mice were injected with 60 mg/kg every other day, the control mice are injected with the vehicle solution only. Getting the inhibitor injected represents a moderate additional burden. The score sheet has been adjusted accordingly.

#### **2.2.8.3 Determination of serum ALT and AST values**

The submandibular was used for serial blood collection. Mice were properly fixed with one hand to ensure the submandibular vein was exposed obviously. The 4 mm lancets (MEDpoint, Inc., Mineola, USA ) were used to puncture the submandibular vein for blood collection. Quickly collected 5 drops of blood in the tube and gently stopped the bleeding with the gauze pad. The blood was put on the table at room temperature for up to 2 hours and then collected the serum by centrifuged at 13,000 rpm for 15 min. The liver enzyme AST and ALT were from the serum using the Reflotron system (Roche, Mannheim, GER).

#### **2.2.8.4 Sacrificing of mice and isolation of organs**

For sacrificing, mice were euthanized on the second day after the last injection by cervical dislocation. The abdomen of the mice was immediately opened and the liver, kidney and intestine were taken out. The liver was divided into five parts: one part for paraffin-embedded (FFPE) tissue, two parts in the cryogenic vessels for RNA extraction and two parts in the cryogenic vessels for protein isolation. The tissues for RNA and protein were quickly put into liquid N<sub>2</sub> and stored at -80°C.

For FFPE tissue, the fresh liver tissues were immediately put into 4% paraformaldehyde overnight and water in the tissues was removed automatically by the routine diagnostic of the Institute for Pathology, University Hospital Cologne, Cologne, GER. Samples were embedded in paraffin and processed in immunohistochemistry.

### 3. Results

In order to investigate the function of LSD1 in the development of HCC, especially in HCC based on non-alcoholic fatty liver disease, the role of LSD1 was aimed to be studied in vitro and in vivo. For In vitro experiments, hepatoma cell systems were used. In vivo, a high-fat diet (HFD) experimental mouse model was established to mimic human HCC, which has developed from non-alcoholic liver disease. LSD1 was inhibited pharmacologically utilizing the inhibitors HCI-2509 and HCI-2577 or by RNA interference using different species of siRNAs or conditional shRNA constructs.

#### 3.1 LSD1 regulates the level of di-methylation at H3K4

To evaluate the effect of LSD1 on histone methylation in various hepatoma cell types, the substrate H3K4me2 was evaluated after LSD1 inhibition by different pharmacological LSD1 inhibitors or siRNA or conditional shRNA expression.

##### 3.1.1 Enhancement of H3K4me2 by LSD1 pharmacological inhibition

Firstly, the LSD1 inhibitors HCI-2509 and HCI-2577, which have a similar structure, were used in the following experiments to investigate the role of LSD1 in hepatoma cells. Huh7 and HepG2 cells were treated with 2  $\mu$ M HCI-2509 or HCI-2577 for 72 hours. The transcriptional level of LSD1 expression was studied in response to HCI-2509 and HCI-2577 treatment in Huh7 and HepG2 cells. Interestingly, LSD1 expression is significantly downregulated at the transcriptional level after pharmacological LSD1 inhibition (Figure 7A). In addition, after LSD1 inhibition using these two inhibitors, the overall methylation of H3K4me2 was increased (Figure 7B).

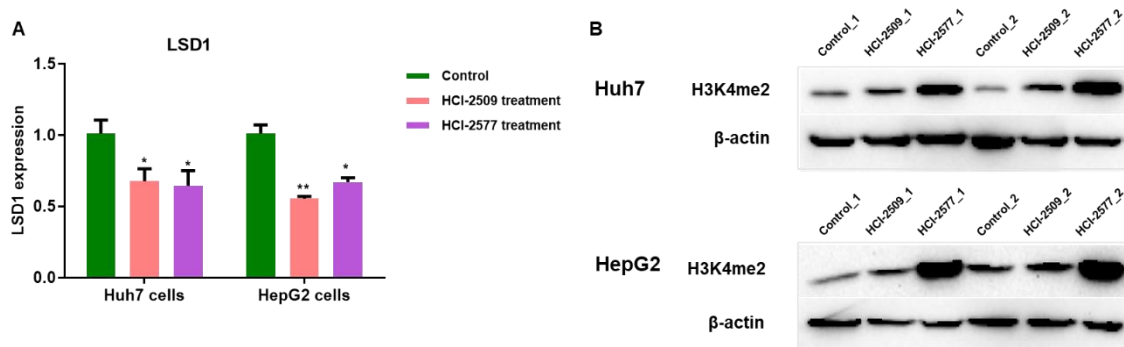


**Figure 7. Enhancement of H3K4me2 by HCI-2509 and HCI-2577 inhibitors.**

(A) LSD1 expression was analyzed by real-time qPCR in Huh7 and HepG2 cells which were treated with 2  $\mu$ M HCI-2509 or HCI-2577 for 72h. All the experiments were performed in triplicates. \* $P < 0.05$ , \*\* $P < 0.01$ . (B) Western Blot analysis of protein isolated from Huh7 and HepG2 cells which were treated with inhibitors using antibodies against LSD1 and H3K4me2. Protein contents were normalized to  $\beta$ -actin.

### 3.1.2 Enhancement of H3K4me2 by LSD1 siRNA

To further examine LSD1 expression in hepatoma cell lines, Huh7, HepG2 and Hep3B cells were transfected with scrambled or different LSD1-targeted siRNA oligonucleotides for 72h. The transcriptional level of LSD1 was measured by qPCR using the relative expression value to hypoxanthine phosphoribosyltransferase (HPRT). Transfection of siRNAs targeting LSD1 resulted in a significant decrease in the expression of LSD1. In Huh7 cells, LSD1 was inhibited by 61% in response to treatment with LSD1-targeting siRNA sequence 2, by 57% using LSD1-targeting siRNA sequence 3 and by 51% using LSD1-targeting siRNA sequence 4. In HepG2 cells, LSD1 was inhibited by 24% with LSD1-targeting siRNA sequence 2, by 23% with LSD1-targeting siRNA sequence 3 and by 54% with LSD1-targeting siRNA sequence 4. In Hep3B cells, all the siRNAs were highly efficient. LSD1 expression was downregulated to 8% after LSD1-targeting siRNA sequence 2 and LSD1-targeting siRNA sequence 3 treatments. Moreover, when the cells were treated with LSD1-targeting siRNA sequence 4, LSD1 expression was even less, only 6% left (Figure 8A). Next, proteins isolated from transfected cells were subjected to quantitative immunoblotting with antibodies against LSD1 and H3K4me2. Exposure of Huh7, HepG2 and Hep3B cells for 72 h to LSD1-targeting siRNA

resulted in a significant decrease in LSD1 protein, which was accompanied by an increase in the overall H3K4me2 status. Especially, in HepG2 cells, LSD1-targeting siRNA sequence 4 showed the most efficient inhibition for LSD1 expression (Figure 8B).

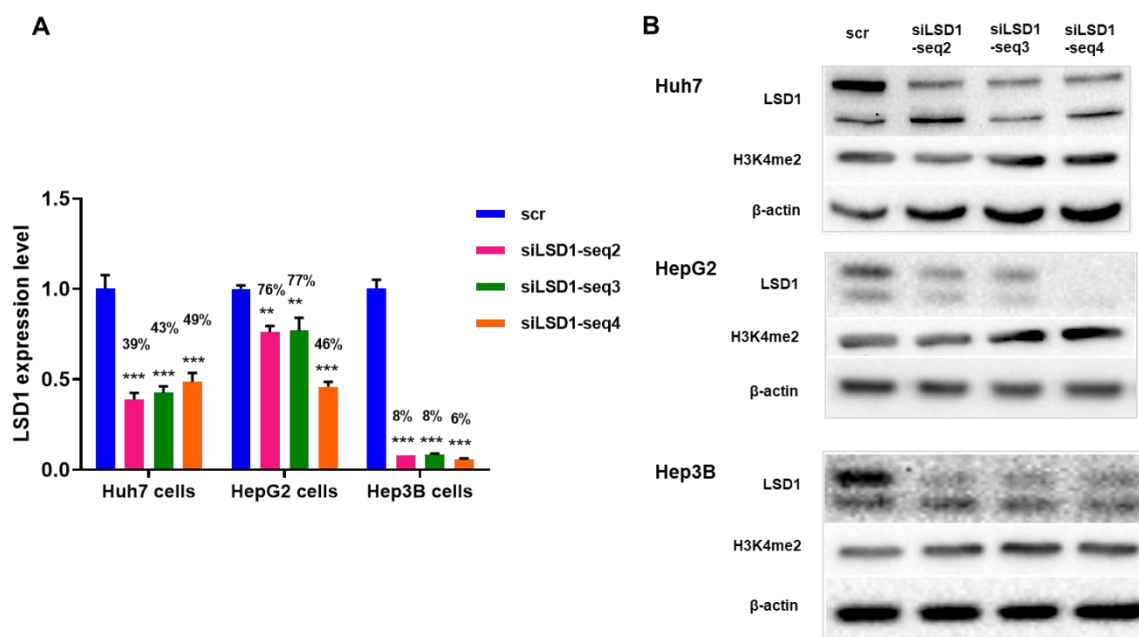


**Figure 8. Inhibition of LSD1 by small interfering RNA.**

(A) Cell viability after LSD1 inhibited by siRNA. Hepatoma cell samples which are Huh7, HepG2 and Hep3B were treated with 100 nM scrambled siRNA and 50 nM different LSD1-targeting siRNAs for 72 h. Cell viability was measured by MTT test. (B) LSD1 expression was analyzed by real-time q-PCR using the hepatoma cell samples which are treated with siRNAs for 72h. \* $P < 0.05$ , \*\* $P < 0.01$ . (C) Western Blot analysis of protein isolated from Huh7, HepG2 and Hep3B cells after treatment with siRNA against LSD1 or with scramble (scr) RNA is shown using antibodies against LSD1 and H3K4me2. Detection of  $\beta$ -actin by anti- $\beta$ -actin antibodies was used as the loading control.

To assess the gene expression profile after LSD1 inhibition, except for PLK1, p21 is also selected because it represents a major target of p53 activity and thus is associated with linking DNA damage to cell cycle arrest (Figure 9A and B). When I analyzed the RNA-seq data from hepatoma cells, I found the metabolic genes BNIP3 and BNIP3L, which are important in inducing cell death and mitophagy [92, 93], were highly regulated by LSD1. Therefore, I used these genes as marker genes of LSD1 to show the efficiency of siRNAs on LSD1 inhibition (Figure 9A-D). The results showed the expression of these genes changed after LSD1 was

inhibited by all different species of LSD1-targeting siRNAs. In addition, in agreement with the previous Western results of LSD1 inhibition, LSD1-targeting siRNA sequence 4 showed the best results on PLK1, p21, BNIP3 and BNIP3L, all of these marker genes, in HepG2 cells.

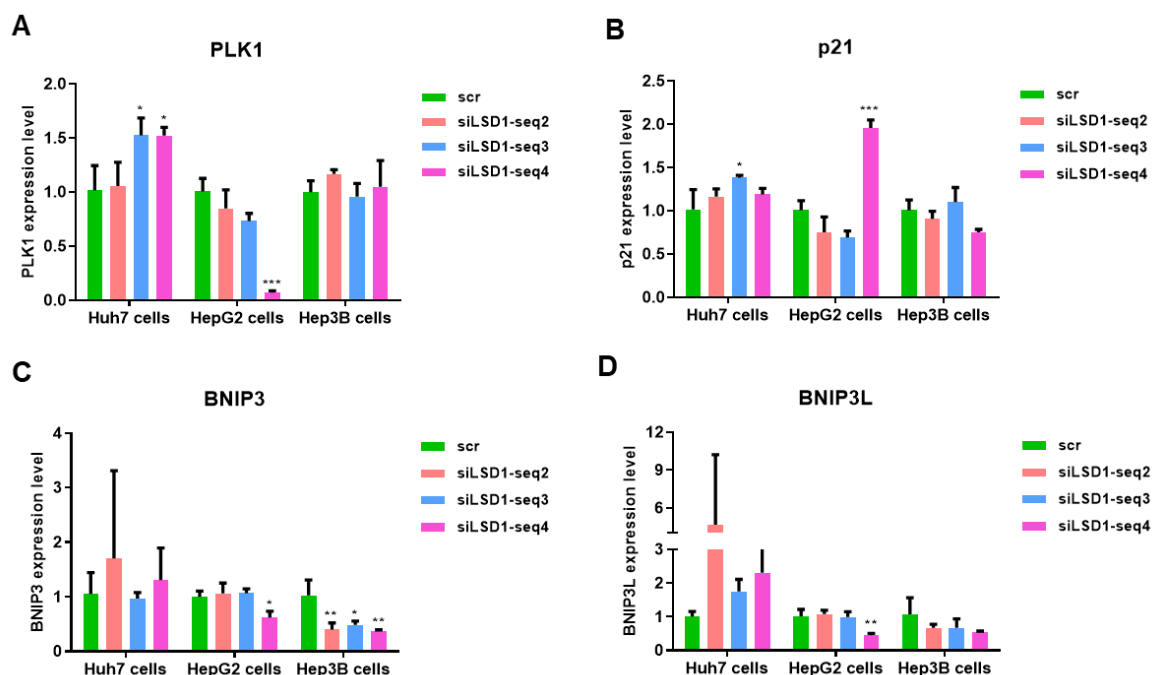


**Figure 9. Alteration of cell cycle and mitophagy sensors involved genes by LSD1 inhibition.**

Huh7, HepG2 and Hep3B cells are treated with different LSD1-targeting siRNAs for 72 hours. LSD1 related genes were analyzed by q-PCR. Values of each gene were normalized to the expression level of HPRT. \* $P < 0.05$ , \*\* $P < 0.01$ .

Because the LSD1 inhibition was not enough with siRNAs treated at the protein level, only HepG2 cells treated with LSD1-targeting siRNA sequence 4 showed significantly LSD1 downregulate. I hypothesized that LSD1 has a long turnover in hepatoma cells. In order to confirm that hypothesis, I used normal cells like HEK cells and liver cancer cells Huh7, which were treated with 50 $\mu$ g/ml cycloheximide (CHX) for 48 hours. The results showed that the expression of LSD1 in HEK cells started to obviously degrade at 20h point and gradually decreased to an invisible level. However, the LSD1 expression seemed not to change along the time in Huh7 cells but at 48h point likely started to degrade (Figure 10). These results confirmed that the LSD1 in liver cancer cells takes more time to degrade than other cell types, which validated the hypothesis that LSD1 has a longer turnover in liver cancer cells.

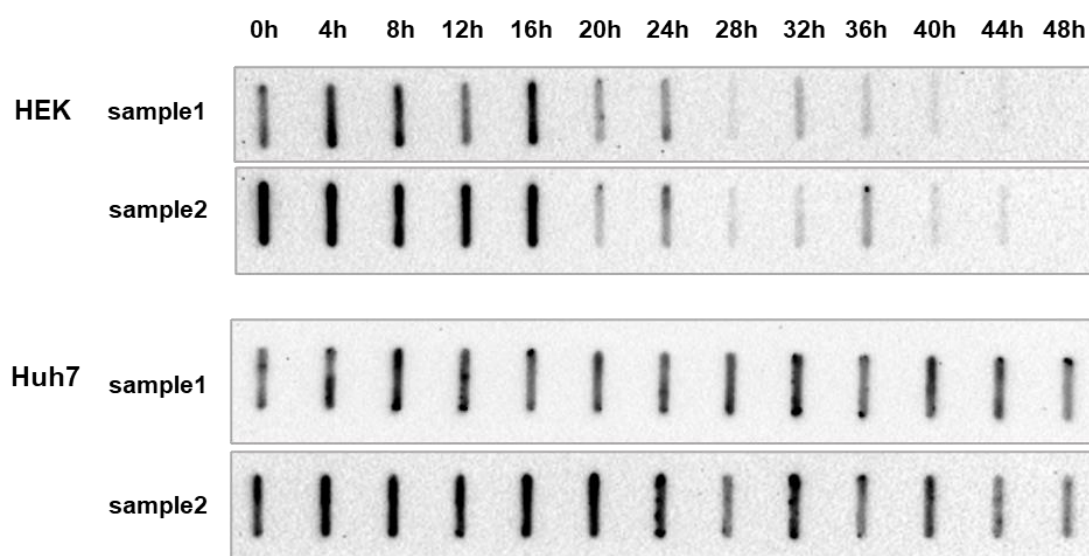


**Figure 10. Determination of LSD1 turnover in different cell types.**

HEK cells and Huh7 cells were treated with 50 $\mu$ g/ml cycloheximide (CHX) for 48 hours. Cells were harvested every 4 hours and the protein was isolated for determination. Each point had a replicate. Dot slot blot was used to detect the LSD1 expression at each point.

### 3.1.3 Enhancement of H3K4me2 by LSD1 knockdown construct

To further confirm the methylation sites on H3 associated with LSD1, LSD1 was knocked down by shRNA in lentivirus transduced stable Huh7 and HepG2 cells. Cells were induced by 1  $\mu$ g/ml doxycycline, hence the knockdown of LSD1 expressed. After doxycycline treatment for 4, 8, 12 and 16 days, in Huh7 cells, LSD1 expression was significantly downregulated both at the transcription and translation levels. In agreement, the methylation status of histone 3 lysine 4 residues was increased (Figure 11A-B). The knockdown of LSD1 was accompanied by a downregulation of the LSD1 target gene PLK1, but interestingly, p21 was also significantly downregulated (Figure 11A). In HepG2 cells, after the cells were treated with doxycycline for 8 and 16 days. LSD1 expression was significantly inhibited at the transcriptional level which is subjected to real-time qPCR analysis (Figure 11C). However, on protein level, the LSD1 decreased in response to 8 days of doxycycline treatment was not obvious in all biological replicates results, besides, only in the first and second of the three independent experiments, there was a significant decrease in LSD1 accompanied by an increase in H3K4me2. In contrast to the 8 days treatment approach, after 16 days of treatment with doxycycline, LSD1

was decreased with an accumulation of H3K4me2 in the first and the third of the three independent experiments ( Figure 11D).

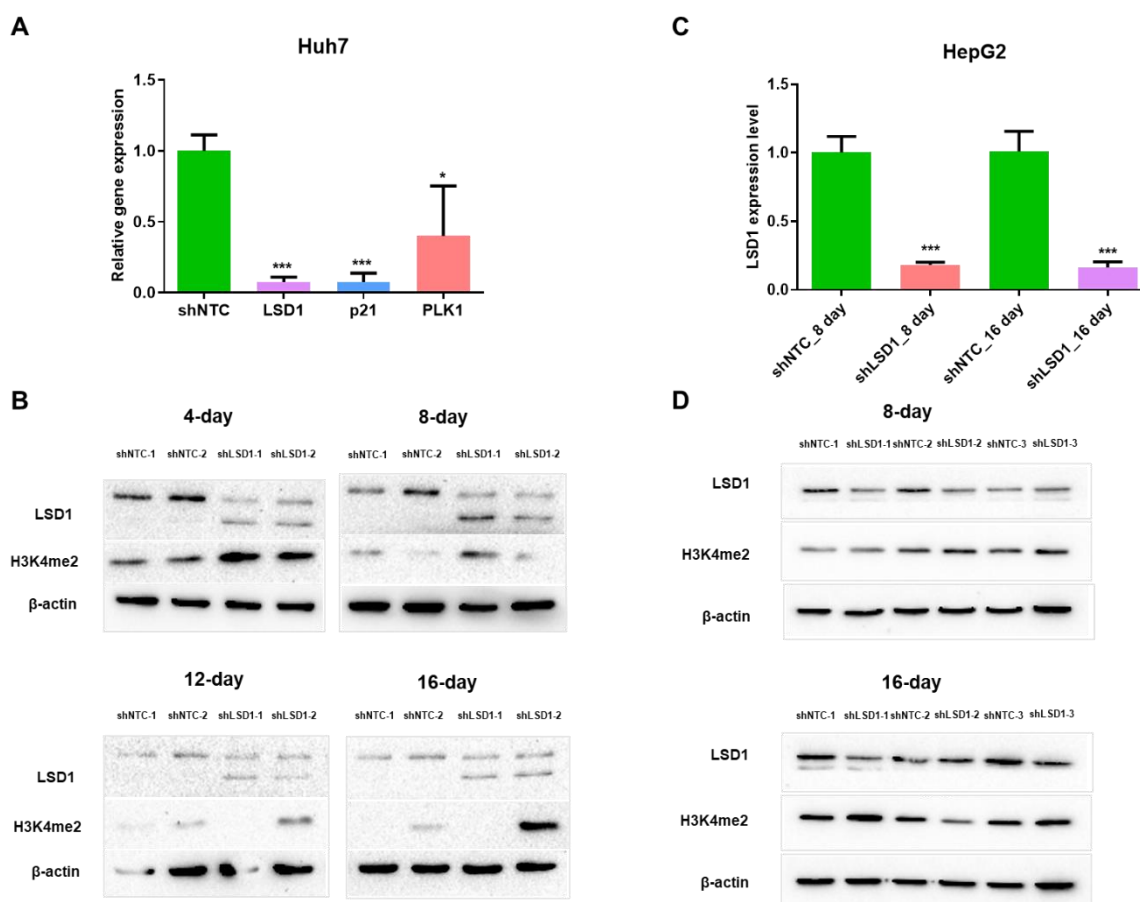


**Figure 11. Increase of di-methylation levels of H3K4 by LSD1 knockdown construct.**

(A-B) Huh7 stable cell line was transduced with shRNA against scramble or LSD1. Cells were induced by 1  $\mu$ g/ml doxycycline for 4, 8, 12 and 16 days. The expression of LSD1 was measured by real-time qPCR and immunoblot. (C-D) HepG2 stable cell line was transduced with shRNA against scramble or LSD1. Cells were induced by 1  $\mu$ g/ml doxycycline for 8 and 16 days. The expression of LSD1 was measured by real-time qPCR and immunoblot. \* $P$  < 0.05, \*\* $P$  < 0.01.

### 3.2 LSD1 inhibition decreases cell viability

To evaluate the effect of LSD1 on cell viability in various hepatoma cell types, LSD1 was inhibited by RNA interference using siRNA or conditional shRNA expression or pharmacologically by means of different LSD1 inhibitors.

#### 3.2.1 Cell viability is reduced by LSD1 pharmacological inhibition

Firstly, the cell viability was analyzed by MTT assays. The monoamine oxidase inhibitor (MAO) GSK2879552 was previously described to inhibit cell growth in acute myeloid leukemia (AML) and some SCLC cell lines [83]. Huh7 and HepG2 cells were treated with increasing concentrations of GSK2879552, ranging from 0.5 to 32  $\mu\text{M}$  and cell viability was measured. The cell viability of both hepatoma cell lines was not altered by GSK2879552 even when a high concentration of 32  $\mu\text{M}$  was used (Figure 12).

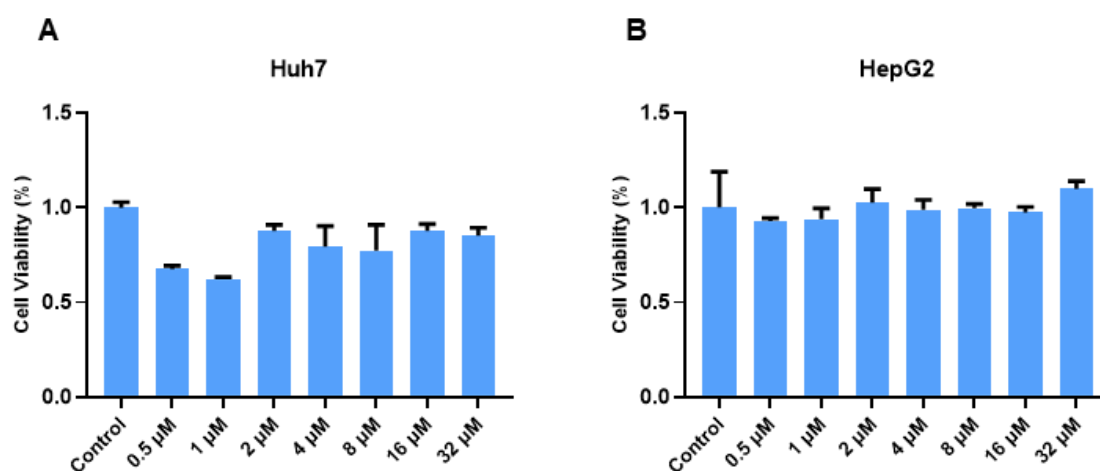


**Figure 12. The effect of monoamine oxidase inhibitor (MAO) GSK2879552 on the viability of hepatoma cells.**

Huh7 or HepG2 cells were exposed to 0.5 to 32  $\mu\text{M}$  GSK2879552 for 72 h, cell viability was determined using MTT assays. Values are the percentage of cell viability compared to control. All the experiments were performed in triplicates.

Since the MAO inhibitor GSK2879552 didn't affect cell viability in hepatoma cells, we used non-MAO LSD1 inhibitors. The LSD1 inhibitor HCI-2509 is a reversible LSD1 inhibitor, which is developed from a novel series of LSD1 inhibiting N'-(1-phenylethylidene)-benzo hydrazide compounds [94]. Huh7, HepG2 and Hep3B cells were seeded in 96-well plates with 10,000 cells in each well and treated with different concentrations of HCI-2509 for 72 h. Viability assays proved a significant reduction in cell viability. Furthermore, the results showed a viability reduction of more than 50% since the cells were treated with more than 2  $\mu\text{M}$  inhibitors (Figure 13). In addition, HCI-2509 made a progressively increasing effect on various cell types, that was dose-dependent.

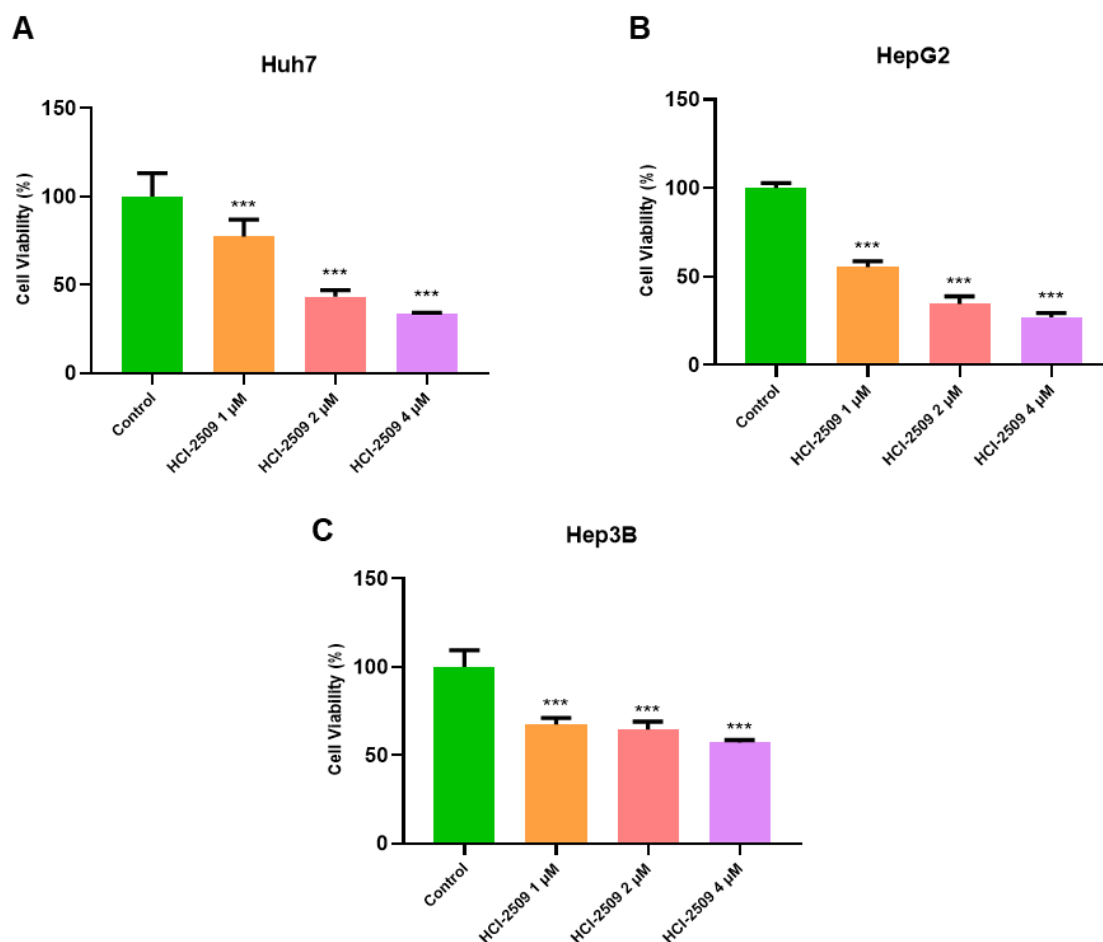


**Figure 13. Reduction of cell viability by LSD1 inhibitor HCl-2509.**

Huh7, HepG2 and Hep3B cells were seeded with 10,000 each well in 96-well plates and exposed to 1, 2 and 4  $\mu\text{M}$  HCl-2509 for 72 h. Histograms represented the percentage of cell viability above the control (100%) as the mean  $\pm$  SD of three independent experiments. Asterisks indicate statistical significance ( $*P < 0.05$ ,  $**P < 0.01$ ).

In order to find the most efficient LSD1 inhibitors, we tested another inhibitor HCl-2577 which has a similar structure to HCl-2509. Therefore I compared the efficacy of these two inhibitors on cell viability. Huh7 and HepG2 cells were treated with different doses of HCl-2509 and HCl-2577 for 72 hours. The viability of the cells was performed by the MTT test. Both inhibitors affected equally cell viability on Huh7 cells. Huh7 cells (Figure 14A). In HepG2 cells, a low dose of 0.5  $\mu\text{M}$  HCl-2577 showed no effect on cell viability, but higher doses of HCl-2577 reduced cell viability in an equal manner as HCl-2509 did. (Figure 14B).

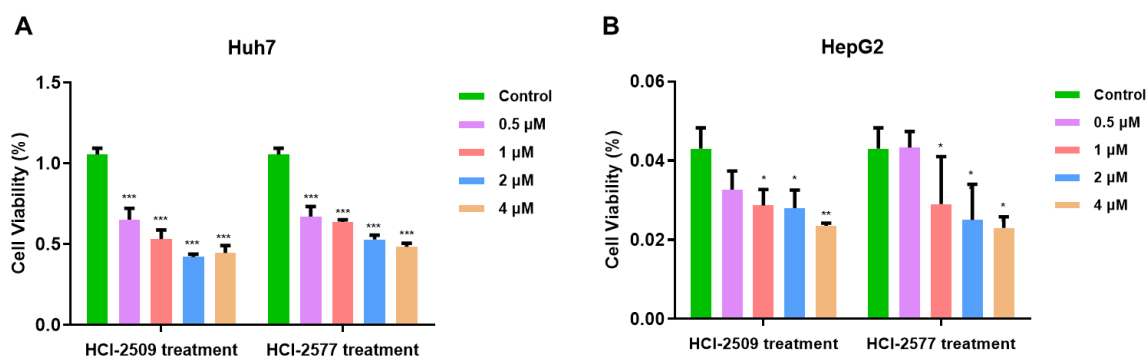


**Figure 14. Cell viability upon different pharmacological LSD1 inhibition.**

Hepatoma cells ( $3 \times 10^4$  cells/cm<sup>2</sup>) were treated with different doses of HCl-2509 and HCl-2577 (0, 0.5, 1, 2, and 4 μM) and incubated for 72h. Cell viability was measured by MTT test. \* $P < 0.05$ , \*\* $P < 0.01$ .

We hypothesized that HCl-2509 might be hydrolyzed in an acidic environment resulting in two compounds 5-chloro-2-hydroxyacetophenone and hydrazide, which I will henceforth refer to as drug A and drug B, respectively (Figure 15A). Because the extracellular pH is acidic in the microenvironment of cancer cells, according to the structure of the HCl-2509, Huh7 cells were treated with different doses of HCl-2509 and its putative hydrolyzates A and B for 72 hours. The viability of the cells was investigated by MTT tests. The results showed that only HCl-2509 affected cell viability (Figure 15B). In addition, gene expression of two known LSD1 targets p21 and PLK1, both shown to be involved in the cell cycle [95, 96] were analyzed by qPCR in hepatoma cells upon treatment with HCl-2509 or the compounds A or B. The expression of cell cycle-related genes such as PLK1 and p21 were altered in the HCl-2509 treatment group, but not by the hydrolysis products compound A or B (Figure 15C). Thus, an influence of the acidic hydrolysis products of HCl-2509 on LSD1 targets could be excluded.

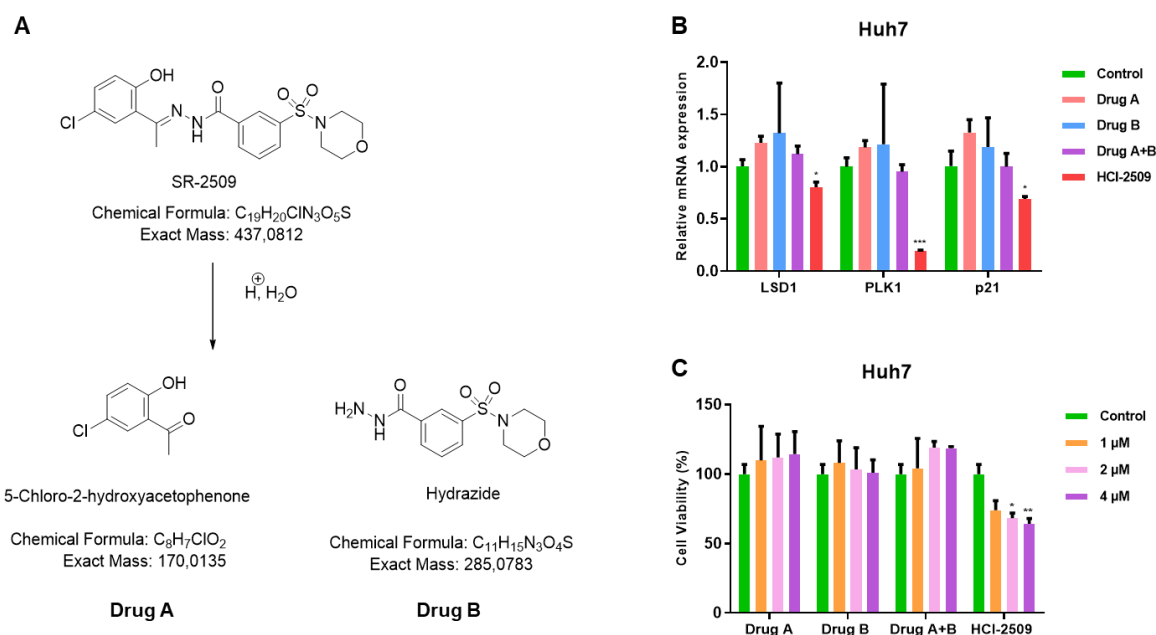


**Figure 15. Inhibition of LSD1 by reversible inhibitor HCl-2509.**

(A) Putative hydrolysis of HCl-2509 in the acidic environment into two compounds, 5-chloro-2-hydroxyacetophenone and hydrazide, which were named drug A and drug B, respectively. (B) MTT test results after 72h. Hepatoma cells were treated with different doses of HCl-2509 and HCl-2509 hydrolyzates (0, 1, 2 and 4  $\mu$ M). (C) LSD1 expression and its target gene were analyzed by quantitative real-time polymerase chain reaction (q-PCR) using the samples treated with 2  $\mu$ M HCl-2509 and hydrolyzates. \* $P$  < 0.05, \*\* $P$  < 0.01.

### 3.2.2 Cell viability is reduced by LSD1 siRNA/shRNA

To further examine the effect of LSD1 expression on cell growth in hepatoma cell lines, Huh7, HepG2 and Hep3B cells were transfected with scrambled or different LSD1-targeted siRNA oligonucleotides for 72h. Cell viability was measured by MTT test (Figure 16). There was no significant difference in cell viability between scrambled and siRNA-treated cells.

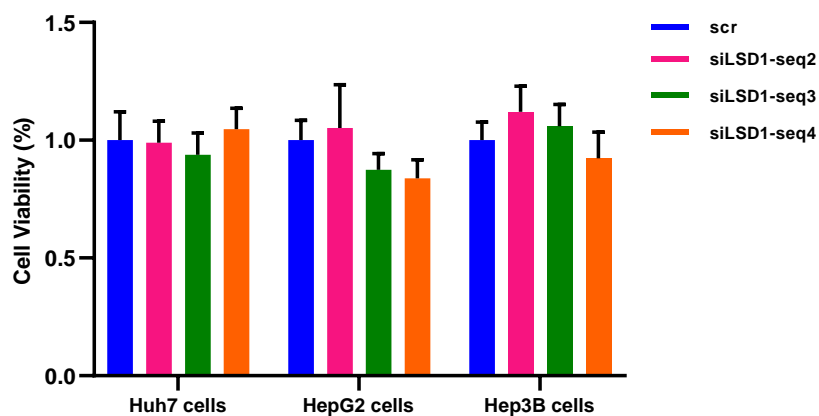


**Figure 16. Inhibition of LSD1 by small interfering RNA.**

Cell viability after LSD1 is inhibited by siRNA. Hepatoma cell samples which are Huh7, HepG2 and Hep3B were treated with 100 nM scrambled siRNA and 50 nM different LSD1-targeting siRNAs for 72 h. Cell viability was measured by MTT test. Data were shown as the mean  $\pm$  SD of three independent experiments.

Due to the no effect of LSD1 inhibition by siRNAs on cell growth, for further functional study, the stable Huh7 and HepG2 cell lines with LSD1 knockdown were used for the subsequent in vitro experiments. To visualize cells and to monitor cell proliferation and cell death, images were acquired using ImageXpress Micro 4 High-Content Imaging System with transmitted light every hour for 96 hours under doxycycline treatment. As shown in Figure 17, on the fourth day of doxycycline treatment, LSD1 knockdown significantly inhibited cell growth in Huh7 and HepG2 cells.

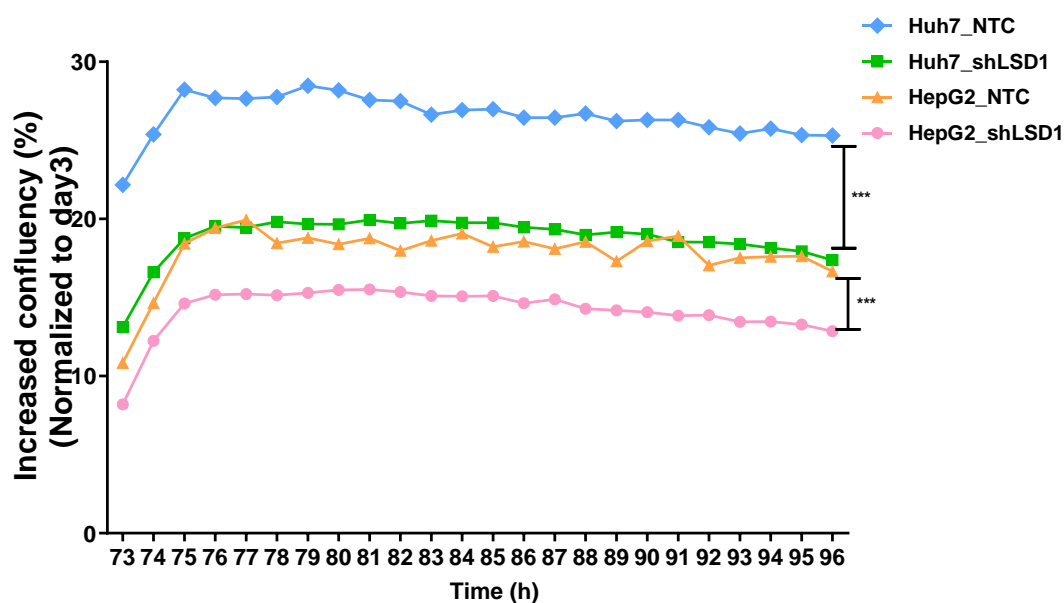


**Figure 17. Reduction of cell viability by LSD1 knockdown in vitro.**

Cell proliferation was monitored with a live cell imaging system. Huh7 and HepG2 cells were seeded in 6-well plates at a density of 400,000 cells. Cells were induced by 1  $\mu$ g/ml doxycycline for 96 hours. \* $P$  < 0.05, \*\* $P$  < 0.01.

### 3.3 LSD1 inhibition results in an alteration of gene expression

In order to identify differentially expressed genes after LSD1 inhibition, RNA seq was performed using Huh7 and HepG2 cells treated with pharmacological inhibitor HCI-2509 or conditional LSD1 knockdown construct.

First, the RNA-seq from HCI-2509 treated versus control in both Huh7 and HepG2 cells was analyzed. In the process of differential expression analysis, relative gene expression levels calculated using FPKM (Fragments Per Kilobase Million), and remarkably differentially expressed genes in triplicate samples were identified by a corrected  $P$ -value ( $p_{adj}$  < 0.05) and  $\log_2$  Fold Change ( $|FC|$ ) > 1. After Huh7 was treated with HCI-2509, 6930 genes were differentially expressed, there were 3371 up-regulated genes and 3559 down-regulated genes (Figure 18A). In HepG2 cells, 8126 genes were differentially expressed, including 4238 up-regulated genes and 3888 down-regulated genes (Figure 18B).

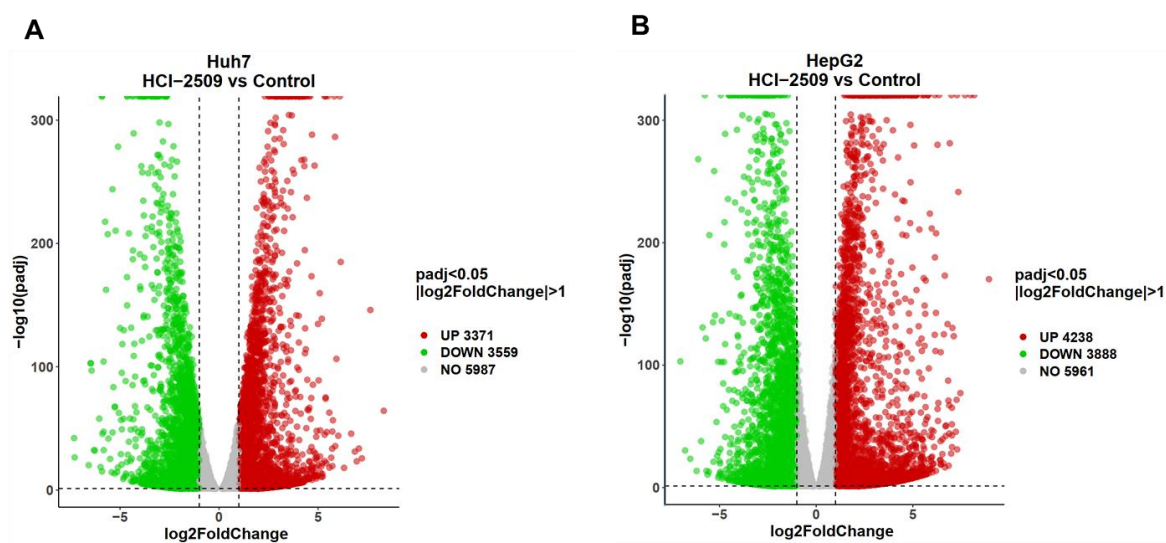


**Figure 18. Identification of differentially expressed genes between the HCI-2509 treated group and the untreated group in Huh7 and HepG2 cells.**

(A) Volcano plot of DEGs in Huh7 cells. (B) Volcano plot of DEGs in HepG2 cells. The green dots represent the expression of down-regulated genes, the red dots represent the expression of up-regulated genes.

Furthermore, the differentially expressed genes were also identified by RNA-seq from the Huh7 LSD1 knockdown compared to Huh7 control cells. Cells were treated with doxycycline for 4 days, 8 days and 16 days. The genes with an adjusted  $P$ -value ( $\text{padj} < 0.05$ ) and  $\log_2$  Fold Change ( $|\text{FC}| > 1$ ). Gene expression profiles were shown in volcano plots as shown in Figure 19A. There were 904 significant differentially expressed genes after 4 days of treatment including 211 up-regulated genes and 693 down-regulated genes. 2424 genes were significantly differentially regulated after 8 days of treatment, 743 genes were significantly up-regulated, and 1681 genes were significantly down-regulated. After 16 days of treatment, there were 811 significant differentially expressed genes including 168 up-regulated genes and 643 down-regulated genes. In addition, Venn diagrams were performed to identify the specific genes and co-expressed genes expression regulation in these three different LSD1 inhibition conditions. The results showed that 109, 584 and 81 genes were up-regulated in 4 days of treatment, 8 days of treatment and 16 days of treatment, respectively. In addition, 25 genes were up-regulated in all of these three different treatment conditions (Figure 19B). For the down-regulated genes, 135 genes were specifically expressed in 4 days of treatment, 891

were only expressed in 8 days of treatment and 148 genes were specifically expressed in 16 days of treatment. Furthermore, 261 genes were down-regulated in all of these three different treatment conditions (Figure 19C). All the coexpressed 286 differentially expressed genes in 4 days, 8 days and 16 days of treatment were presented in a clustered heatmap as shown in Figure 19D.

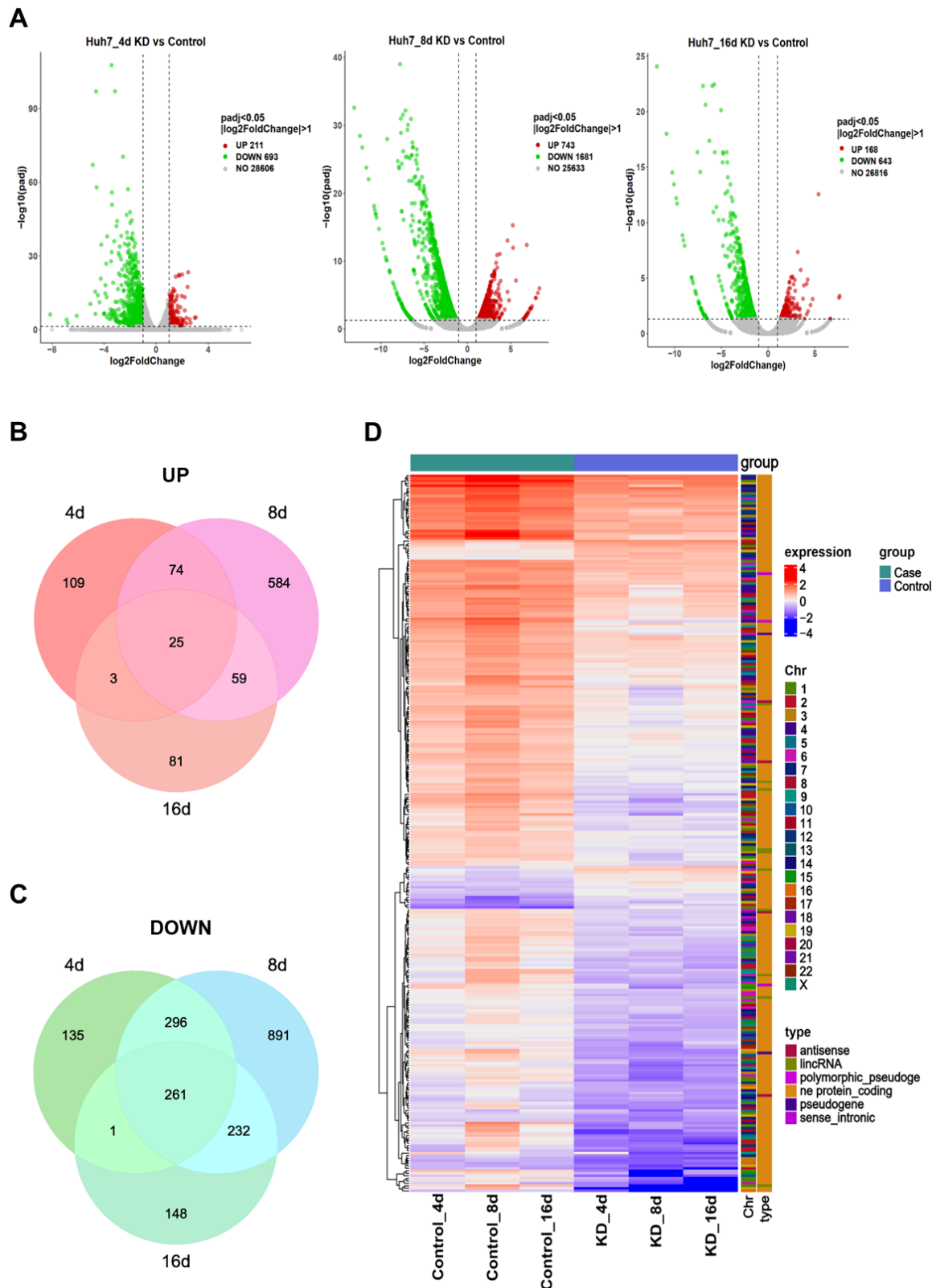


**Figure 19. RNA-seq differential gene expression analysis in the Huh7 LSD1 knockdown versus Huh7 control cells.**

Huh7 LSD1 knockdown and control cells were treated with doxycycline for 4 days (4d), 8 days (8d) and 16 days (16d). (A) Volcano plots show the differentially expressed genes (DEGs) ( $\log_2$  Fold Change (IFC)  $>1$ ,  $\text{padj} <0.05$ ). The red dots show the upregulated genes and the green dots show the

downregulated genes. The x-axis represents the log<sub>2</sub>-transformed gene expression in LSD1 knockdown cells divided by that into control cells. (B) and (C) Venn diagram of the differentially expressed genes. The number in each circle represents the amount of differentially expressed genes between the LSD1 knockdown and control cells. The overlapping number stands for the mutual differentially expressed genes among 4 days, 8 days and 16 days of doxycycline treatment and the non-overlapping numbers specify the genes unique to each different treatment. (D) Heatmap shows the co-expressed DEGs in 4 days, 8 days and 16 days of doxycycline treatment. All the experiments were in triplicates.

### 3.3.1 The expression of liver disease-related genes was altered upon LSD1 inhibition

To gain insight into the molecular basis of the alteration in LSD1 regulated mechanism of related disease, the DisGeNET database was further used to identify DEGs related diseases. The results showed that DEGs participated in the progression of various diseases, such as hepatocarcinogenesis, non-alcoholic fatty liver disease, cholangiocarcinoma, cirrhosis and tumor angiogenesis, which were all related to the common liver disease (Figure 20A). When we performed the enrichment analysis with downregulated DEGs in the DisGeNET database. The DEGs were also shown in the bubble chart (Figure 20B) as shown in the bar chart. Taken together, the above results indicated that the DEGs were mostly associated with liver-related functions.

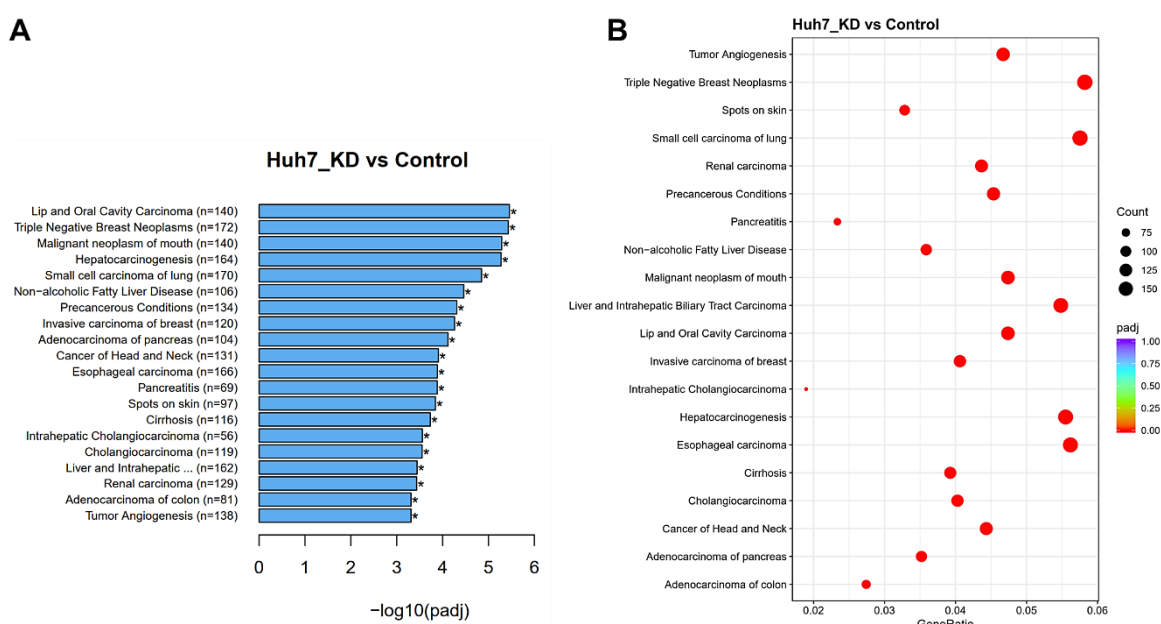


**Figure 20. Functional annotations involved in liver disease.**

Enrichment analysis of all DEGs in the DisGeNET database as a bar chart (A) or as the bubble chart (B).

**3.3.2 Cell cycle pathway enrichment upon LSD1 inhibition**

After showing in which disease genes, upregulated and downregulated upon LSD1 inhibition were involved, I next analyzed which pathways might be affected by differential gene expression due to LSD1 inhibition. To this end, the gene ontology (GO) enrichment analysis as well as the Kyoto encyclopedia of genes and genomes (KEGG) tool, was applied by means of the DAVID database platform. Signaling pathway analysis of the DEGs was performed and data were presented in Figure 21. The DEGs were mainly enriched for the GO terms DNA replication, mitotic nuclear division, nuclear division, organelle fission and regulation of mitotic cell cycle phase transition (Figure 21A and B). Additionally, three KEGG pathways were identified for the DEGs, including cell cycle, cellular senescence and the p53 signaling pathway (Figure 21C and D).

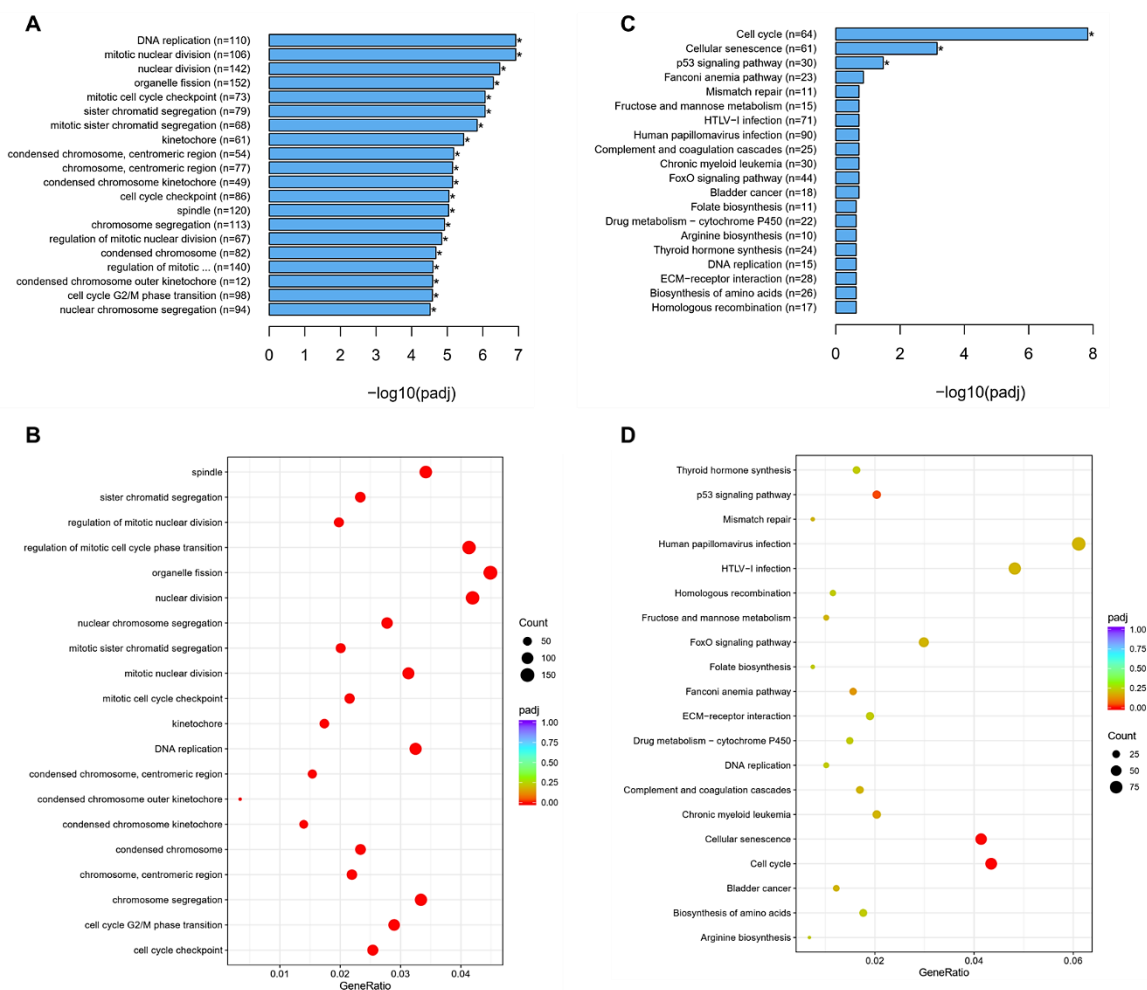


**Figure 21. GO and KEGG signaling pathway analysis of DEGs in LSD1 knockdown cells.** (A-B) GO enrichment analysis of DEGs was shown in the bar chart and bubble chart. (C-D) KEGG signaling pathway analysis of DEGs was shown in the bar chart and bubble chart. DEGs, differentially expressed genes; GO, Gene Ontology; KEGG, Kyoto encyclopedia of genes and genomes.

### 3.3.3 LSD1 inhibition represses pathways in cell cycle progression

From our primary data in lung cancer cells, it was previously shown that PLK1 is a direct target of LSD1 H3K4 demethylation. In addition, ChIP followed by ultra-deep DNA sequencing demonstrated LSD1 interaction with the PLK1 promoter region [96]. Furthermore, Gene Set Enrichment Analysis (GSEA) was subsequently performed to investigate the potential downstream signaling pathways that may be regulated by LSD1. GSEA indicated PLK1 mitotic pathway was most significantly downregulated upon LSD1 inhibition. Polo-like kinase 1 (PLK1) is a serine/threonine kinase that plays a key role in cell cycle progression and division [97]. In addition, the G2 checkpoint signaling pathway was also significantly downregulated upon

LSD1 inhibition (Figure 22A and B). Differential PLK1 expression in response to LSD1 inhibition was verified by RT-qPCR analysis (Figure 22C and D). The results showed that PLK1 was significantly downregulated after LSD1 was inhibited by HCI-2509 and HCI-2577 both in Huh7 and HepG2 cells.

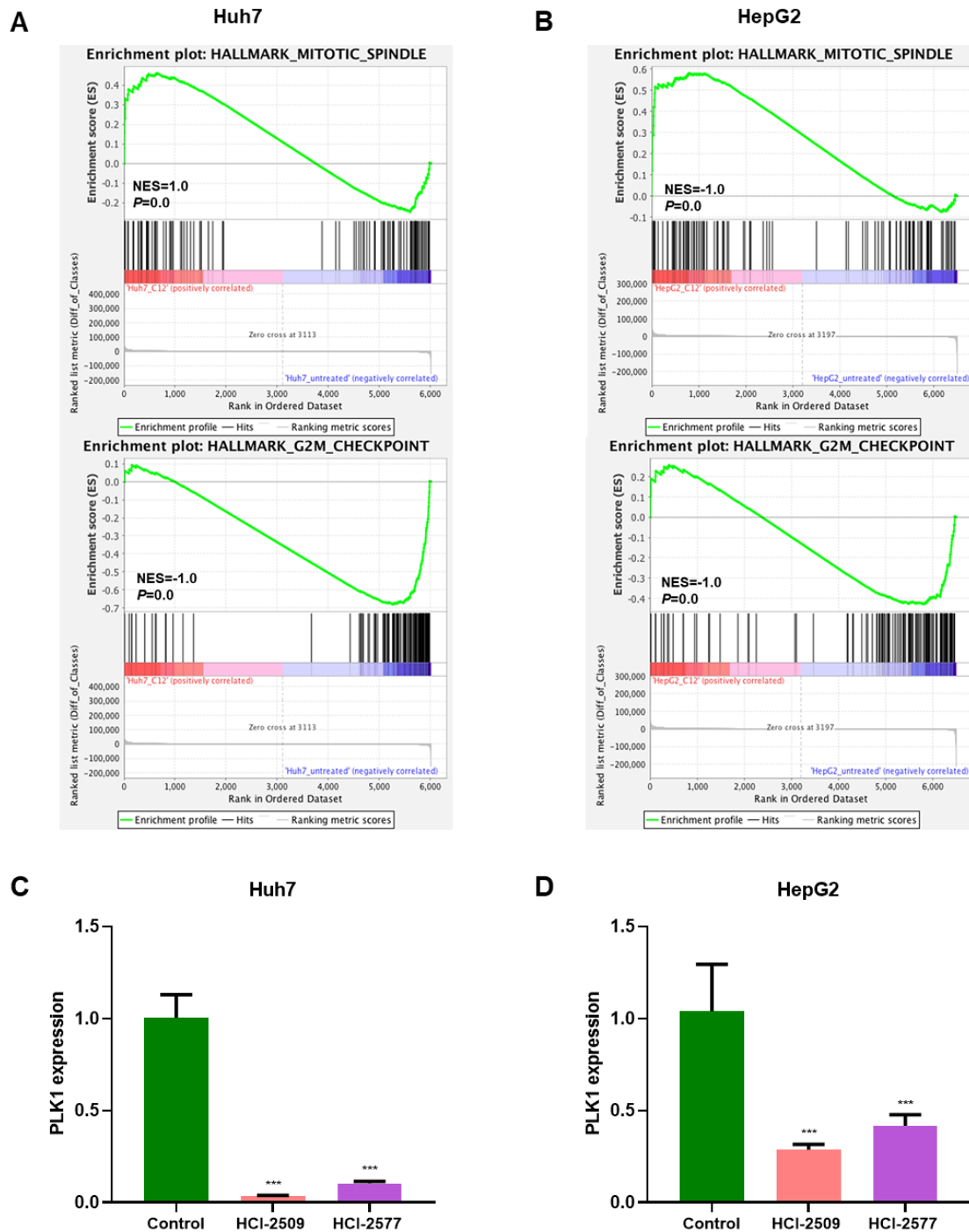


Figure 22. The cell cycle regulation by LSD1 through the PLK1 mediator.

---

GSEA indicated that the mitotic and G2 checkpoint signaling pathways were enriched in (A) Huh7 cells and (B) HepG2 cells. (C) and (D) PLK1 repression upon pharmacologic LSD1 inhibition using the HCl-2509 and HCl-2577 inhibitors. The results were analyzed by real-time qPCR. \* $P < 0.05$ , \*\* $P < 0.01$ .

### **3.3.4 LSD1 inhibition results in the alteration of metabolic genes**

To get a better understanding of how LSD1 may be influencing lipid metabolism, a differential gene expression analysis of the HCl-2509 treated compared to the untreated group was carried out on the RNA-seq data from Huh7 and HepG2 cells. Gene Set Enrichment Analysis (GSEA) was subsequently performed to clarify the genes in lipid metabolism pathways. The results showed that in the HCl-2509 treated group in both Huh7 and HepG2 cells, FATTY ACID METABOLISM and CHOLESTEROL HOMEOSTASIS were enriched pathways (normalized enrichment score=-1.0,  $p=0.0$ ) (Figure 23A and B).

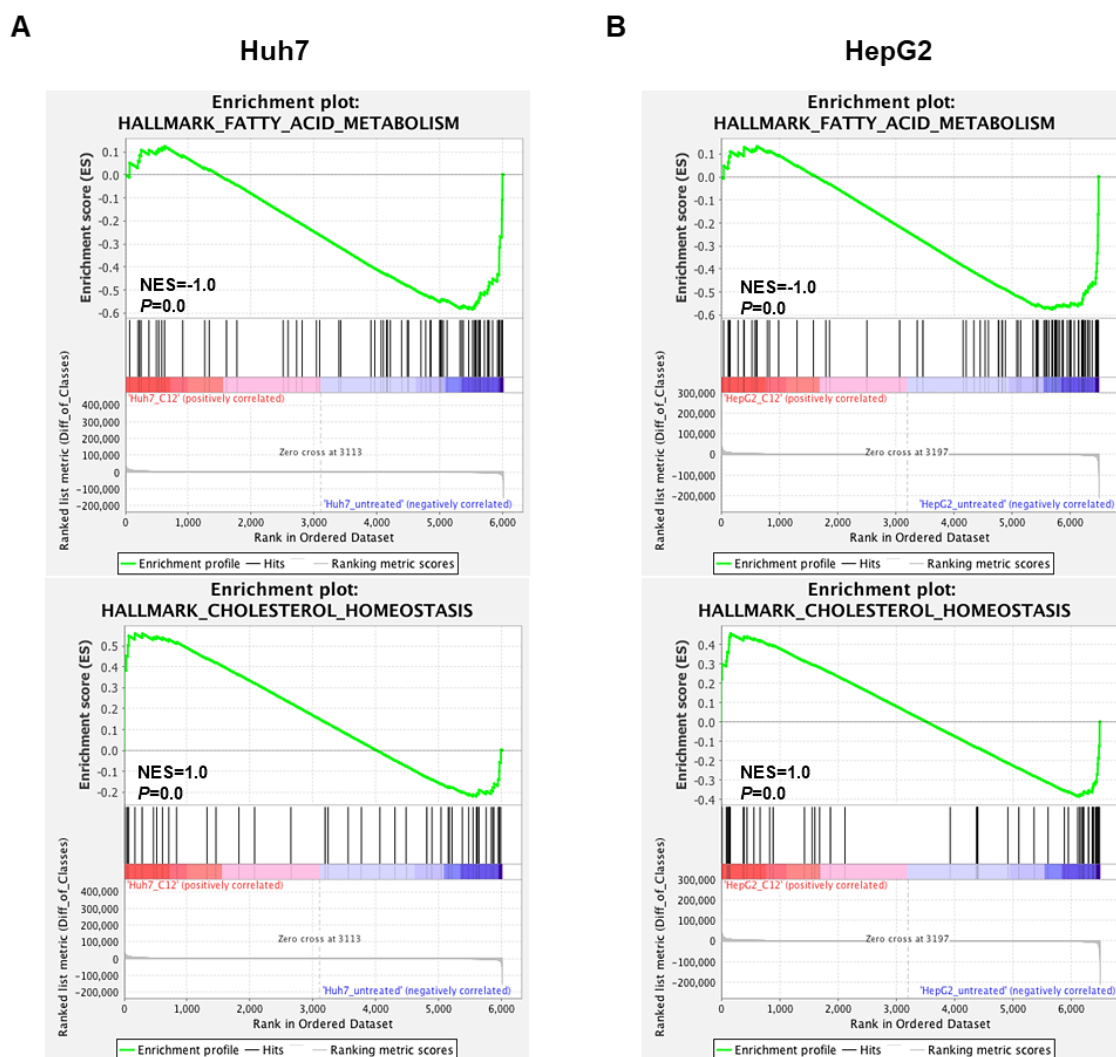


**Figure 23. GSEA plot showing the lipid metabolism pathways.**

lipid metabolism pathways enriched in Huh7 cells (A). Similarly, GSEA plot for lipid metabolism pathways enriched in in HepG2 cells (B).

Based on the signaling pathways from Gene Set Enrichment Analysis, 56 significantly modulated genes that may relate to the metabolic metabolism were plotted as a heatmap, including the genes of the citrate cycle and lipid metabolism (Figure 24A). In Huh7 cells, 19 genes were upregulated and 37 genes were downregulated upon LSD1 inhibition compared to the control group. While in HepG2 cells, 17 genes were upregulated and 39 genes were downregulated. We observed that in both cell lines, PDK4, ANKRD1 and PYGM were the top 3 positively regulated genes. GPAM, HMGCS2 and FABP5 were the top 3 negatively regulated genes. The expression of 11 candidate metabolic genes after LSD1 inhibition in Huh7 and

HepG2 cells was validated by quantitative RT-PCR (Figure 24B), including gene FABP5, FASN, LOXL2, NDRG1, PIK3R3, GPAM, ANKRD1, ESRRA, ACACA, PDK4 and LDHA. Among these genes, 6 genes including FABP5, FASN, PIK3R3, GPAM, ACACA and LDHA showed significant downregulation upon LSD1 inhibition not only by pharmacological inhibitors but also by LSD1 knockdown construct. NDRG1, ANKRD1 and PDK4 showed different regulations in LSD1 knockdown Huh7 cells. Interestingly, the gene ESRRA showed different expression in Huh7 and HepG2 cells, it was upregulated in Huh7 cells but downregulated in HepG2 cells. The HPRT gene was used as a reference gene to normalize the expression levels of 11 DEGs. The results showed the genes involved in lipid metabolism changed after LSD1 was inhibited not only by HCI-2509 and HCI-2577 inhibitors but also by LSD1 knockdown construct, which means LSD1 also plays an important role in lipid metabolism reprogramming in the development of HCC.

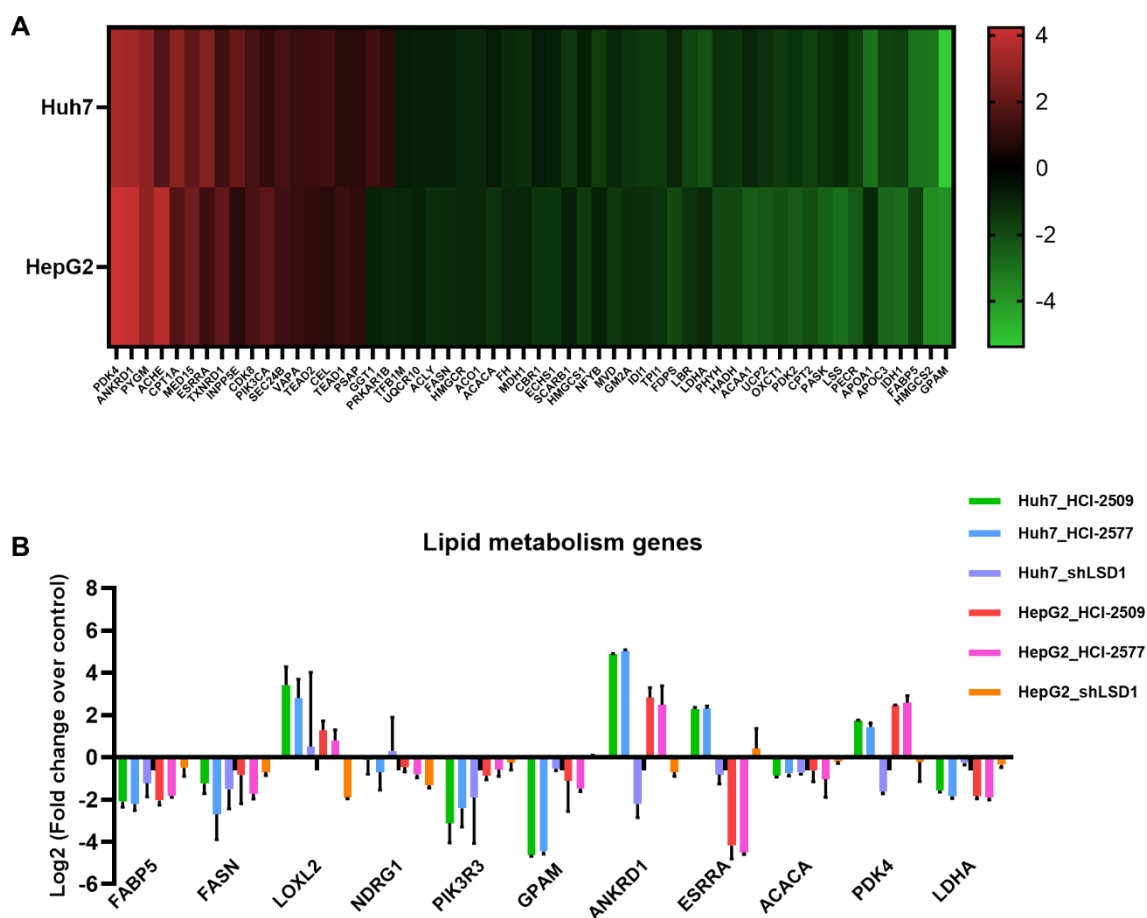


**Figure 24. Heat map visualization and relative quantification of differentially expressed metabolic genes by real-time PCR for verification.**

(A) RNA-Seq heatmap showing the top 56 genes differentially expressed in Huh7 and HepG2 cells upon LSD inhibition. (B) The log<sub>2</sub> of the fold-change (Log<sub>2</sub>FC) expression of metabolic genes in LSD1 inhibition Huh7 and HepG2 cells compared to normal Huh7 and HepG2 cells, respectively. Values of each gene were normalized to the expression level of HPRT. The y-axis refers to the relative expression level for each gene, with the mean  $\pm$  SD of three replicates.

**3.4 Promoter interactions of LSD1 in liver cancer cells**

In order to assess the promoter regulation by LSD1 and to find direct targets. ChIP was performed and binding sites were studied by subsequent qPCR and whole-genome DNA sequencing.

**3.4.1 LSD1 regulates PLK1 by binding its promoter**

The polo-like kinase 1 (PLK1) is a serine/threonine kinase that plays a key role in cell cycle progression and division and it is highly expressed in proliferative cells [97]. In lung cancer cells, it was previously shown that PLK1 is a direct target of LSD1 H3K4 demethylation [96]. Since I have shown by RNA seq followed by pathway analysis i. that the PLK1 pathway is predominantly affected by pharmacological LSD1 inhibition and ii. that PLK1 transcript levels were significantly repressed, I first addressed the question of if PLK1 is also a direct target in liver cancer cells. To assess the direct involvement of LSD1 in the regulation of PLK1, I examined the occupancy of LSD1 on the PLK1 genomic region by ChIP analysis followed by qPCR. The results showed a lower enrichment for LSD1 and higher enrichment for H3K4me<sub>2</sub> at the promoter region of PLK1 in samples upon LSD1 inhibition compared to non-treated control (Figure 25A). To validate this, I performed a qPCR analysis from chromatin immunoprecipitates of antibodies against IgG, LSD1 and H3K4me<sub>2</sub>. The results showed that LSD1 binds to the PLK1 promoter region and that inhibition of LSD1 using either the pharmacological inhibitor HCI-2509 or the conditional knockdown construct, both significantly reduced the PLK1 promoter interaction of LSD1 in Huh7 cells. Moreover, the H3K4me<sub>2</sub> occupancy at the PLK1 promoter region increased upon LSD1 inhibition. In HepG2 cells, the binding of LSD1 to the PLK1 promoter region also decreased after LSD1 inhibition by HCI-2509. However, after LSD1 knockdown LSD1 interaction with the PLK1 promoter was not

affected and also no change in the H3K4me2 status was observed (Figure 25B and C). Though there was no significant change in LSD1 binding or H3K4 methylation status after LSD1 inhibition, these results demonstrate that LSD1 binds at the PLK1 promoter site and thereby potentially regulates PLK1 expression.

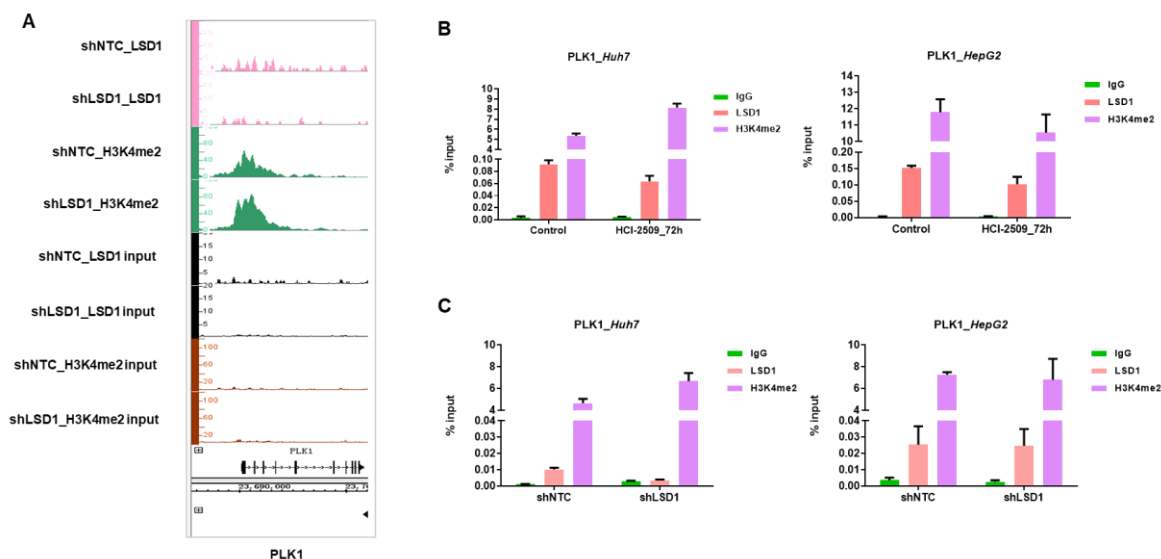


**Figure 25. Visualization and validation of the ChIP-seq data for PLK1-binding sites with LSD1 enrichment in hepatoma cells upon LSD1 inhibition using ChIP-qPCR.**

(A) Exemplary visualization of the LSD1 and H3K4me2 ChIP-Seq data obtained from triplicate samples of hepatoma cells. The binding site for the PLK1 gene is displayed above the peak density plots. (B) ChIP-qPCR analysis of LSD1 and H3K4me2 at the PLK1 gene loci in Huh7 cells and HepG2, respectively. The cells were cultured either in the presence of HCI-2509 (2  $\mu$ M) or under vehicle control for 72 h. (C) ChIP-qPCR analysis of LSD1 and H3K4me2 at PLK1 gene loci in LSD1 knockdown Huh7 and HepG2 cells, respectively. The cells were cultured under 1  $\mu$ g/ml Dox induction for 16 days. Data are presented as mean values  $\pm$  SD of three independent experiments (n = 3).

### 3.4.2 Enrichment of H3K4me2 to promoters of metabolic genes

To investigate the genome-wide distribution of H3K4me2, the chromatin immunoprecipitations using an antibody against H3K4me2 and chromatin isolated from HCI-2509 treated and non-treated Huh7 cells were performed. Genome-wide analysis of H3K4me2 binding after pharmacologically LSD1 inhibition by chromatin immunoprecipitation followed by sequencing (ChIP-seq) revealed the prevalence of recruitment of H3K4me2 to the promoters of most differential expressed genes, especially 56 metabolic genes which I selected from the previous

RNA-seq data (Figure 26). The results showed the methylation status of H3K4me2 on targets genes markedly increased upon LSD1 inhibition.

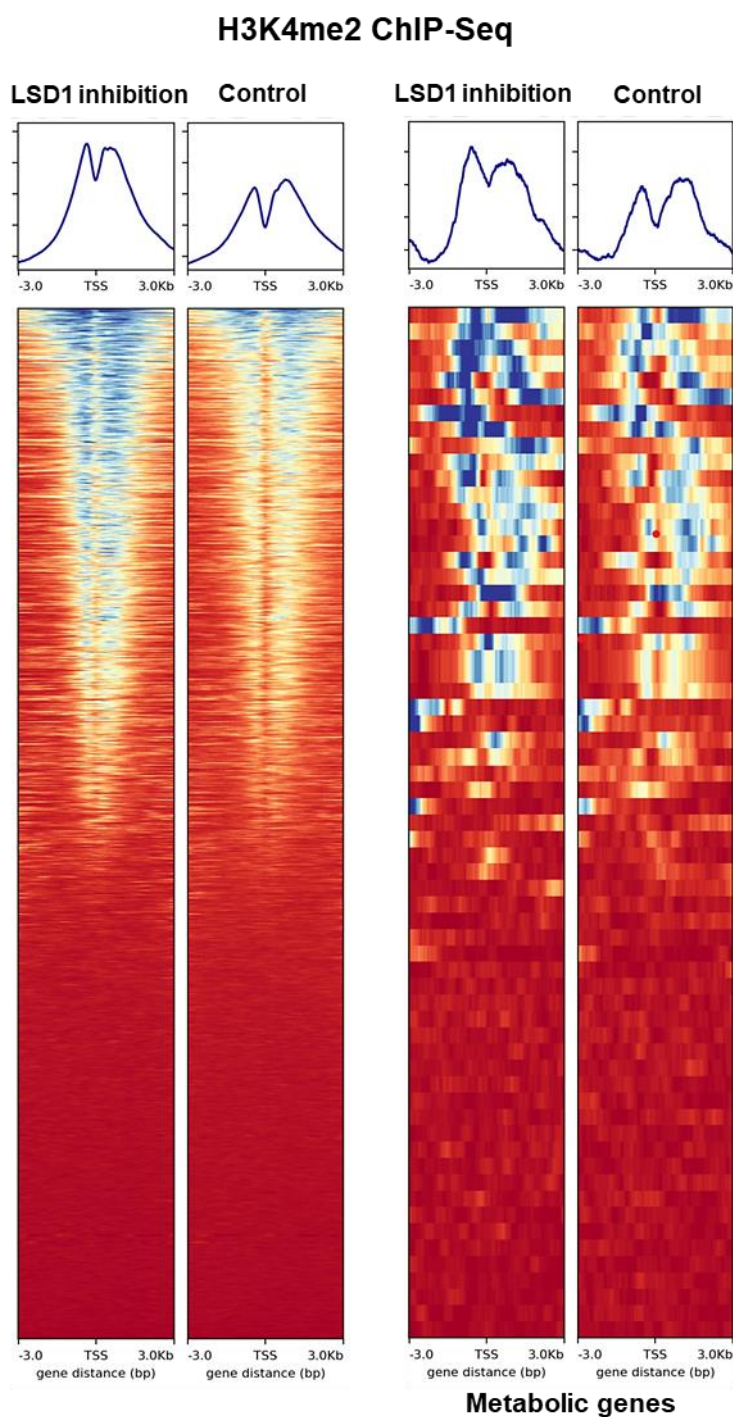
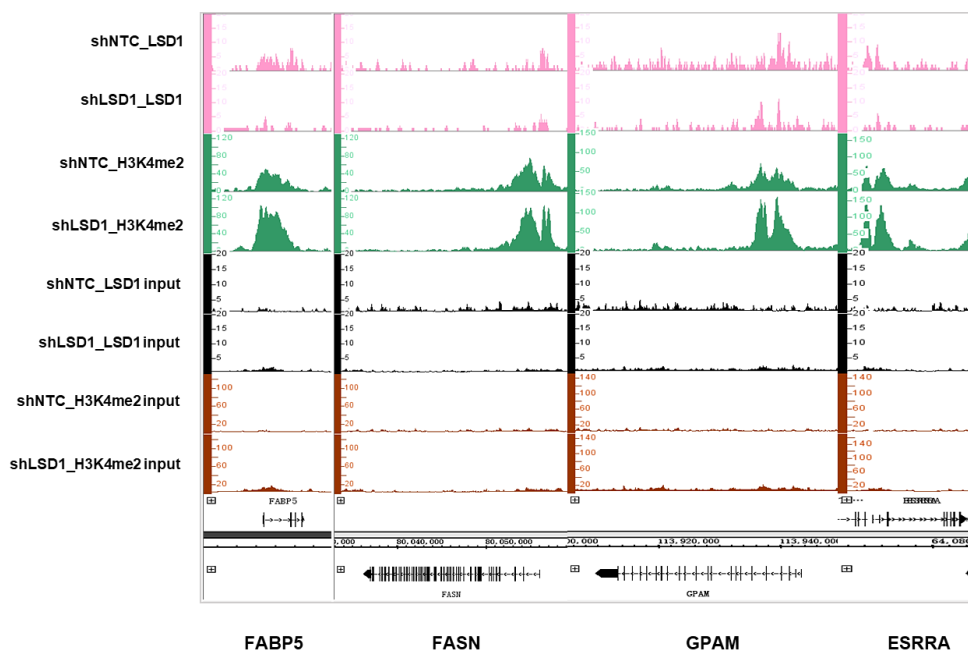


**Figure 26. The methylation status of H3K4me2 on targets genes.**

H3K4me2 histone mark enrichment near individual TSS ( $\pm 3.0$  kbp) genome-wide was ranked by the overall fold enrichment for individual genes in HCI-2509 treated Huh7 cells versus control, 56 metabolic genes were presented.

### 3.4.3 LSD1 mediates lipid metabolic reprogramming by directly regulating the metabolic genes

In order to investigate whether LSD1 affects lipid metabolism by its interaction with the metabolic genes, next a detailed view was performed to analyze the binding pattern of LSD1 and H3K4me2 with the 11 metabolic sensors which were chosen from RNA-seq and validated by qPCR in previous experiments. The data revealed that LSD1 can directly regulate gene FABP5, FASN, GAPM, ESRRA, ACACA, PDK4 and LDHA by occupying their promoter regions. Strikingly, LSD1 knockdown causes less binding of LSD1 at the metabolic gene loci. Furthermore, the H3K4me2 level is increased in the absence of LSD1 relative to shNTC samples (Figure 27).



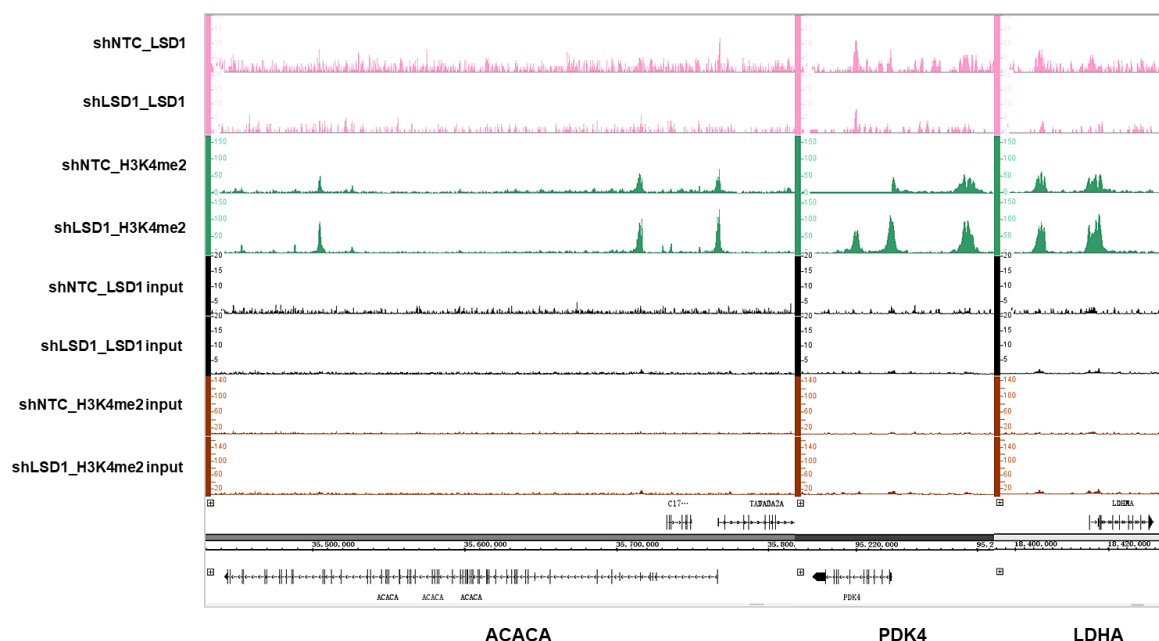


**Figure 27. Promoter binding of metabolic genes in Huh7 cells.**

Binding patterns of LSD1 and H3K4me2 at FABP5, FASN, GAPM, ESRRA, ACACA, PDK4 and LDHA gene loci after shNTC and shLSD1 in Huh7 cells. The profile of LSD1 is shown in pink and the profile of H3K4me2 is marked in green. The y-axis shows read coverage; the x-axis shows the gene loci. The peaks are visualized with the Integrated Genome Browser.

### 3.4.4 LSD1 regulates FABP5 by binding its promoter

RNA seq data revealed that FABP5 is one of the most prominent divergently expressed genes after LSD1 inhibition. Since FABP5 is not only involved in lipid metabolism but also in cell growth progression [98], I further analyzed its promoter binding by quantitative ChIP-PCR. To this end, independent ChIP PCR assays were carried out. The results showed that LSD1 binding at the FABP5 promoter decreased upon LSD1 inhibition by HCI-2509 treatment relative to IgG in Huh7 cells. Consistently, the occupancy of H3K4me2 at FABP5 promoter enriched in Huh7 cells (Figure 28A). In LSD1 knockdown Huh7 cells, the binding of LSD1 to the FABP5 promoter region significantly decreased after LSD1 inhibition but with a decreased H3K4me2 occupancy (Figure 28C). Strikingly, ChIP assay results revealed that less enrichment of both LSD1 and H3K4me2 was observed on the FABP5 promoter after LSD1 pharmacological inhibition compared to IgG in HepG2 cells (Figure 28B). However, the ChIP assay showed the FABP5 interactions after LSD1 inhibition by knockdown construct were moderate in HepG2 cells (Figure 28D). This data confirmed that LSD1 might involve in lipid

metabolic reprogramming by directly regulating FABP5 expression.

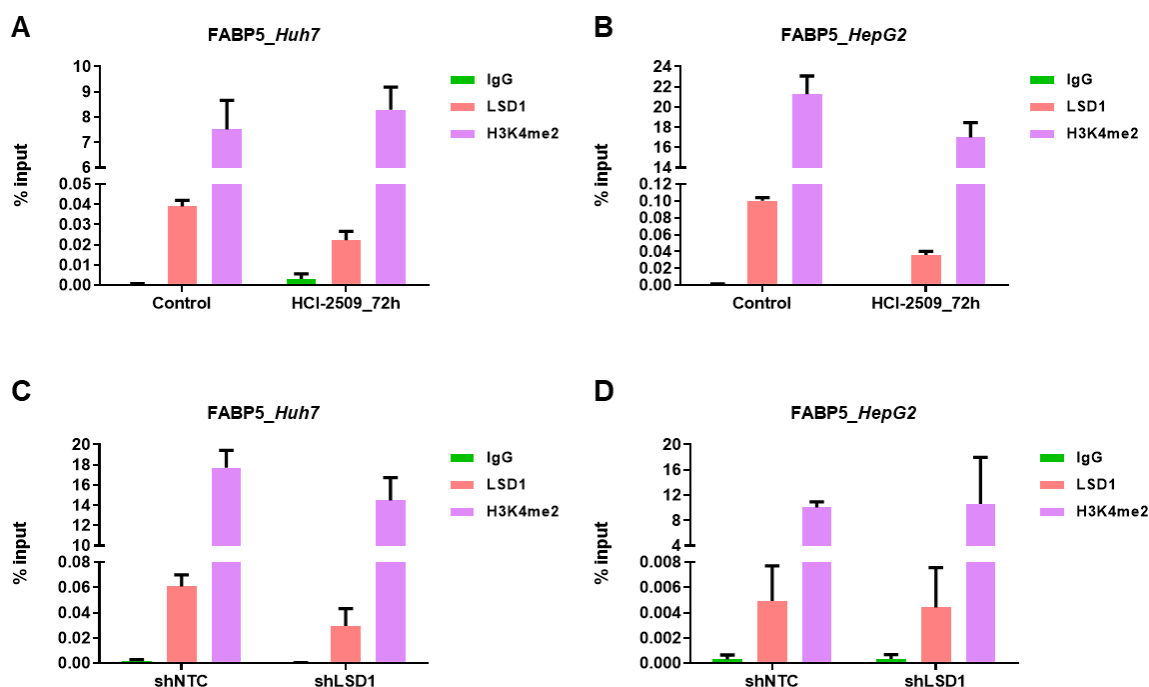


**Figure 28. Analysis of the FABP5 promoter region for binding of LSD1 and H3K4me2 in hepatoma cells upon LSD1 inhibition by ChIP-qPCR.**

(A) and (B) ChIP-qPCR analysis of LSD1 and H3K4me2 at FABP5 gene loci in Huh7 cells and HepG2, respectively. The cells were cultured either in the presence of HCI-2509 (2  $\mu$ M) or under vehicle control for 72 h. (C) and (D) ChIP-qPCR analysis of LSD1 and H3K4me2 at FABP5 gene loci in LSD1 knockdown Huh7 and HepG2 cells, respectively. The cells were cultured under 1  $\mu$ g/ml Dox induction for 16 days. Data are presented as mean values  $\pm$  SD of three independent experiments (n = 3).

### 3.4.5 Overexpression of FABP5 contributes to HCC

Due to the prominent role of FABP5 in some cancer types, I investigated its putative role in HCC. Firstly, I performed a large-scale analysis of HCC patient data from the TCGA dataset. These data showed FABP5 was higher expressed in tumor tissues than in non-tumor liver areas (Figure 29A). Accordingly, the survival data from 364 patients for 120 months also showed short survival was associated with high FABP5 expression and long survival with low FABP5 expression (Figure 29B). Moreover, the correlation analysis of FABP5 and LSD1 showed a significance ( $P=0$ ) with a strong positive correlation coefficient ( $R=0.56$ ) (Figure 29C)

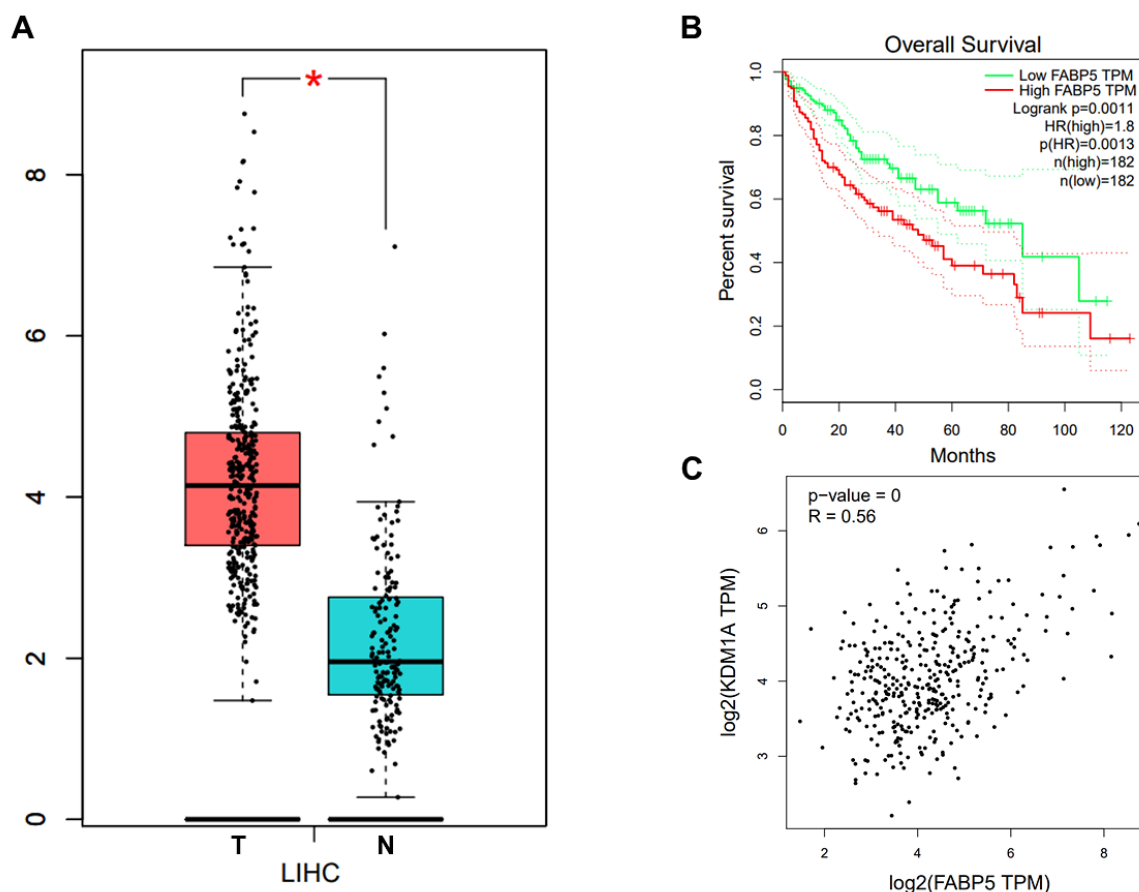


**Figure 29. TCGA data analysis for FABP5. FABP5 mRNA expression levels were obtained from the TCGA database with HCC.**

(A) Comparison of FABP5 expression in tumor tissues and non-tumor liver areas. (B) Survival analysis based on the patients with high expression of FABP5 and low expression of FABP5. (C) Correlation analysis of FABP5 and LSD1.

### 3.4.6 LSD1 inhibition downregulates FABP5 expression

As shown in the previous data, quantitative PCR analysis revealed that most of the lipid metabolic genes, including FABP5, were downregulated upon LSD1 inhibition. To further investigate the FABP5 expression on protein level, Western blots using Huh7 and HepG2 cells with LSD1 inhibition under pharmacological inhibitor treatment or by LSD1 knockdown construct were carried out. Compared to the control cells, LSD1 inhibition showed substantial downregulation of FABP5 at the protein level in HCI-2509 and HCI-2577 treated Huh7 cells (Figure 30A). Similar effects on the expression of FABP5 were observed in Huh7 cells after doxycycline induction of the LSD1 knockdown. Especially after 8-day and 16-day doxycycline induction, the FABP5 was significantly reduced (Figure 30B). Interestingly, in HepG2 cells, the

FABP5 expression was not altered after LSD1 inhibition by pharmacological inhibitors in HCl-2509 and HCl-2577 treated cells when compared to control cells (Figure 30C). However, the expression of FABP5 was significantly decreased in LSD1 knockdown HepG2 cells when induced by doxycycline for 8 days and 16 days (Figure 30D).

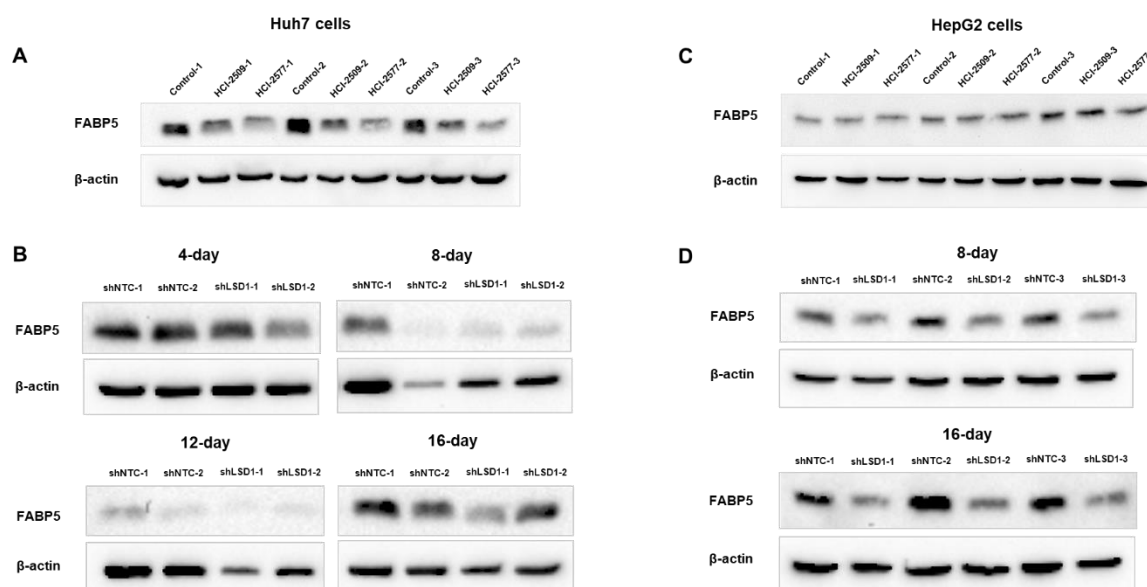


**Figure 30. Downregulation of FABP5 expression by LSD1 inhibition.**

(A) Immunoblot showing protein levels of FABP5 in untreated Huh7 cells and cells treated with HCl-2509 and HCl-2577. (B) LSD1 knockdown Huh7 cells were induced by 1  $\mu$ g/ml doxycycline for 4, 8, 12 and 16 days. The expression of FABP5 was analyzed immunoblot. (C) Immunoblot showing protein levels of FABP5 in untreated HepG2 cells and cells treated with HCl-2509 and HCl-2577. (D) LSD1 knockdown HepG2 cells were induced by 1  $\mu$ g/ml doxycycline for 8 and 16 days. The expression of FABP5 was analyzed immunoblot.

### 3.5 LSD1 inhibition with HCl-2509 using rodent NAFLD model

After showing the role of LSD1 in lipogenic gene expression in hepatoma cells, next I studied the influence of LSD1 on lipid metabolism in vivo. To this end, I chose murine non-alcoholic fatty liver disease (NAFLD) as an ideal model to show changes in lipid metabolism and fat accumulation.

#### 3.5.1 Effect of LSD1 inhibition on mice body weight

NAFLD was induced by a high-fat diet (HFD) in wildtype C57BL/6J mice and LSD1 was inhibited by pharmacological treatment of the mice with the inhibitor HCI-2509. To follow up on the weight gain and development of obesity, mice were regularly weighted from the age of 6 weeks when starting the HFD, until the age of 18 weeks. As shown in Figure 31A and B, both female and male mice gained body weight, the female mice showed a gain of nearly 30% and the male mice presented to gain double weight within the first 6 weeks after HFD without HCI-2509 treatment. After the mice received HCI-2509 treatment, the male mice exhibited reduced body weight and there was a significant difference in weight loss compared to vehicle treated male mice (Figure 31A). In addition, there also was a significant difference in body weight change in female mice when treated with HCI-2509 compared to vehicle treatment (Figure 31B). Interestingly, although all the mice showed a significant reduction of body weight under HCI-2509 treatment. According to the data sets of Jackson Laboratory, the body weights in response to LSD1 inhibition were still not significantly under the normal body weights of mice which were the same age and which were fed with the standard diet (Figure 31 and Supplementary Table 1).

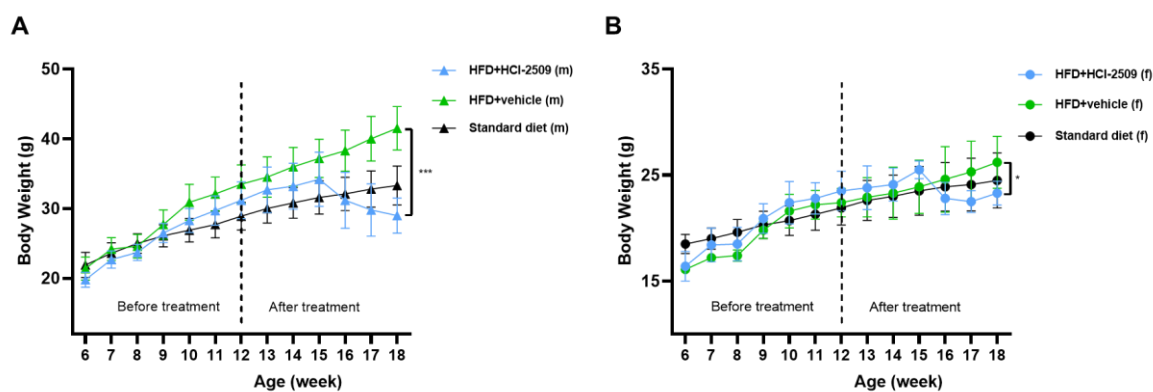


**Figure 31. Body weight reduction in HCI-2509 treated mice.**

The HCI-2509 treated mice present lower body weight compared to vehicle treated mice. The body weight curve in blue and green shows the body weight changes with time after receiving a high-fat diet (HFD). Mice in the blue curve received an IP injection of 60 mg/kg HCI-2509 ( $n=8$ ) after getting 8 weeks high-fat diet (at the age of 14 weeks). Mice in the green curve received 60 mg/kg vehicle (PBS) as the control group ( $n=8$ ). The number of female and male mice was equal in each group ( $n=4$ ). Mice in the black curve show the normal body weight from standard diet and cited from Jackson Laboratory. Data are represented as mean $\pm$ SD.  $P$ -value was calculated by ANOVA analysis,  $***P < 0.001$ .

### 3.5.2 Effect of LSD1 inhibition on serum AST and ALT

To evaluate the effect of LSD1 inhibition by HCI-2509 on NAFLD progression, aspartate transaminase (AST) and alanine aminotransferase (ALT) were measured to monitor the liver injury. After 18 weeks treatment with of HFD, the AST values were moderately increased and levels of around 120 IU/L when the control group was measured, whereas the normal reference values of AST and ALT are  $56.07 \pm 14.14$  and  $28.79 \pm 9.00$ , respectively [99]. Notably, HCI-2509 treated mice showed a decrease in serum values of AST compared to the control group. Importantly, reduced AST levels were observed in both male and female mice (Figure 32A). Moreover, there were significantly decreased ALT values in HCI-2509 treated male mice. However, in female mice after 18 weeks of HFD, ALT values were not elevated, neither in untreated nor in the HCI-2509 treated mice suggesting that no liver injury was yet induced by the HFD (Figure 32B).

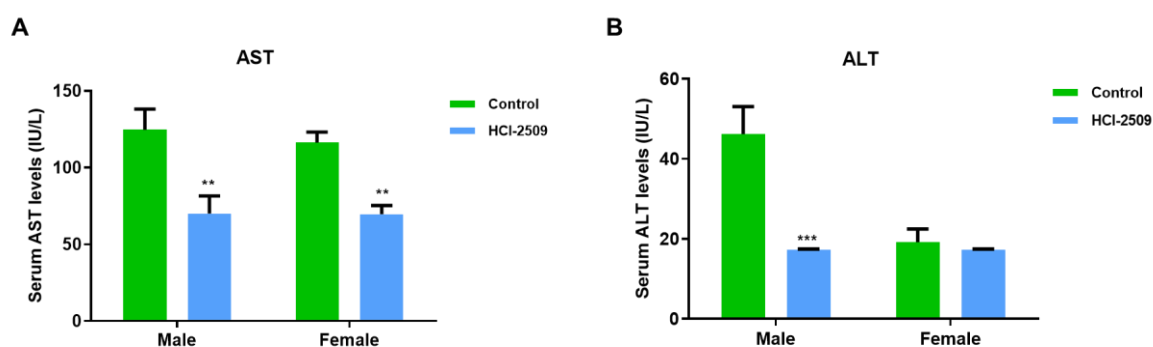


**Figure 32. Changes of serum AST and ALT in liver injury mice.**

C57BL/6J mice were fed with the high-fat diet (HFD) as control or HFD with 60 mg/kg HCI-2509 treatment for 6 weeks. Serum levels of (A) aspartate transaminase (AST) and (B) alanine aminotransferase (ALT) were measured by the Reflotron system. All values are expressed as the mean  $\pm$  SD ( $n = 8$ /group, 4 male mice and 4 female mice). \*\* $P < 0.01$ , \*\*\* $P < 0.001$ .

### 3.5.3 Effect of LSD1 inhibition on fat accumulation

The HFD-induced NAFLD model was established after the mice were fed with HFD for 18 weeks. Hematoxylin-eosin-stained (HE) liver sections are shown in Figure 33. The HE staining displayed an abundant accumulation of fat droplets in control HFD mice but no fat accumulation in HCI-2509 treated mice. In addition, more fat droplets were shown in male

mice than female mice. The steatosis grade of the liver tissues was higher in male mice than in female mice. These results indicated that LSD1 inhibition reduced fat accumulation in HFD mice.

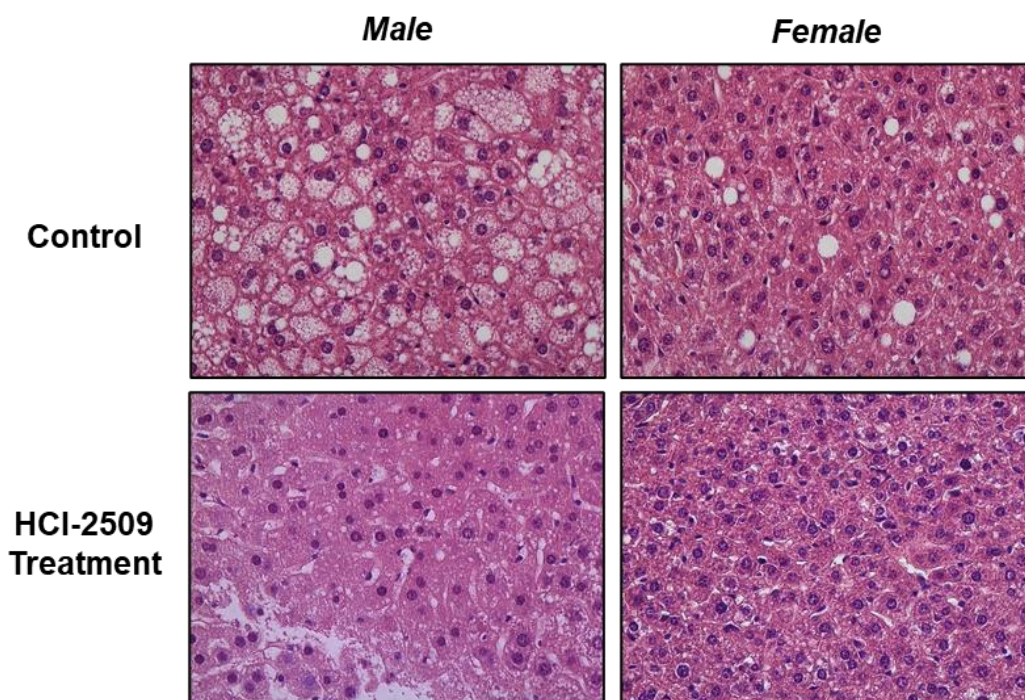


**Figure 33. Liver histopathology in NAFLD model from HFD mice.**

C57BL/6J mice were fed with the high-fat diet (HFD) as control or HFD with 60 mg/kg HCl-2509 treatment. Liver histopathology showed hematoxylin and eosin-stained sections of liver tissues from representative mice from each group, the original magnification is  $\times 40$ .

## 4. Discussion

Hepatocarcinogenesis is a multistep process associated with multiple different signaling pathway changes [57] due to dysregulation of gene expression caused by genetic and epigenetic alterations. In the present study, different approaches to LSD1 inhibition in hepatoma cells were established and the impact of LSD1 inhibition on gene expression was determined. Importantly, my findings revealed that after LSD1 inhibition, genes involved in proliferative and metabolic regulation were altered. Cell cycle interruption caused by LSD1 inhibition was evident due to the downregulation of PLK1. Furthermore, genes related to the cell cycle progression and lipid metabolism were affected. Noteworthy, for the first time FABP5 was demonstrated to be a novel target of LSD1 and was downregulated following LSD1 inhibition.

### 4.1 LSD1-mediated H3K4me2 demethylation regulates cell cycle

Histone methylation at specific lysine residues plays a critical role in regulating chromatin structure, gene expression and subsequent cellular activities. Fine control of the balance of histone methyltransferase and demethylase activities is essential for cell cycle progression and maintenance of genome integrity [100]. In the present study, different approaches were applied to inhibit LSD1 using pharmacologic inhibitors or RNA interference using either siRNA or conditional shRNA constructs.

Pharmacological inhibitors and conditional LSD1 knockdown constructs reduced cell viability and inhibited cell growth. Furthermore, expression profiles after LSD1 inhibition revealed a differential expression pattern of genes associated with the cell cycle. Notably, the alterations of gene expression were mostly linked to DNA replication, regulation of mitotic progression, cell cycle checkpoints, spindles and cell cycle G2/M transition. In addition, a role for LSD1 in the DNA damage response has been proposed by Nima et al. [101]. Moreover, studies on the effect of HCI-2509 on AML cell lines and AML primary cells have indicated that HCI-2509 inhibits cell proliferation and promotes cell differentiation and apoptosis [102]. However, cell viability was not reduced upon LSD1 inhibition by different species of siRNAs, which indicates

that treating cells by RNA interference for only 72 h might be not enough. This finding was further confirmed when the Tet-On system with the LSD1 knockdown construct was used for LSD1 inhibition for 4 days. After 4 days of doxycycline treatment, cell growth was inhibited upon LSD1 inhibition compared to control cells. LSD1 is also known to control gene expression in different complexes with the substrate H3K4me2 [103]. Here, I demonstrated that inhibition of LSD1 not only inhibited cell growth but also increased the level of H3K4me2. In contrast, Y He et al. did not find significant differences in H3K4me2 though the authors found that depletion of LSD1 led to downregulation of the cell cycle-promoting genes SKP2 and CDC25A and increased H3K9me2 at the SKP2 and CDC25A promoters in prostate cancer cells [104]. However, previous findings on AML cells indicated that LSD1 mediates demethylation of H3K4me1/2 but not H3K9me1/2 and in this study, the authors have shown that inhibition of LSD1 by HCI-2509 increased dimethylation and trimethylation of H3K4 levels in the promoter of the LSD1 target genes [102]. Additionally, recent reports have suggested that high levels of LSD1 can maintain the undifferentiated state and the high proliferation rate of human and mouse embryonic stem cells by removing H3K4 methylation [105, 106]. Furthermore, previous work from our lab on lung cancer cells provides evidence of downregulation of PLK1 mRNA expression in response to LSD1 inhibition. Downregulation was accompanied by increased levels of the LSD1 substrate H3K4me2, which supports the data of my study. Taken together, these results suggest that LSD1 might inhibit the cell cycle by primarily promoting H3K4 demethylation-dependent transcription repression of cell cycle genes.

ChIP-seq analysis and ChIP-PCR demonstrated that PLK1 is a direct target of LSD1 in liver cancer cells. In addition, knockdown of LSD1 enriched H3K4me2 and reduced LSD1 occupation on the PLK1 promoter. PLK1 is a well-known mitotic kinase with an important role in cell cycle progression and is a crucial gene in the mitotic process [107, 108]. Notably, there is increasing evidence, demonstrating that PLK1 overexpression can be a marker of cancer prognosis based on the fact that PLK1 is commonly upregulated in a variety of tumors [109-112]. Signaling pathway analysis revealed that genes involved in G2/M-phase arrest and PLK1 mitotic pathways were mostly significantly downregulated upon pharmacological LSD1 inhibition. Real-time PCR also validated the downregulation of PLK1 expression after LSD1

was inhibited by pharmacological inhibitors and the LSD1 knockdown construct, This finding is consistent with the decreased cell proliferation in hepatoma cells, indicating that LSD1 inhibited cell growth and triggered G2/M-phase arrest by downregulating PLK1 expression. Moreover, PLK1 can be transcriptionally regulated by the forkhead transcription factor FOXM1 during cell cycle progression, leading to peak expression during the G2/M phase of the cell cycle [113].

However, when endogenous LSD1 was inhibited by different species of siRNAs, PLK1 unexpectedly experienced almost no significant downregulation after LSD1 inhibition. However, in our previous study on LUAD, we observed a significantly reduced PLK1 expression accompanied by a decrease in expression of other members of this pathway such as AURKA. In contrast, here the cyclin-dependent kinase inhibitor 1A (CDKN1A) increased after LSD1 knockdown using different siRNAs [96]. Compared to other cell types, in hepatoma cells, LSD1 might have a longer turnover. Therefore, here I investigated the LSD1 turnover in different cell types, including normal human HEK cells, and liver cancer Huh7 cells. Indeed, LSD1 degradation had a longer half-time in Huh7 cells than in HEK cells. This result indicates that transient transfection using siRNAs for LSD1 inhibition is not as efficient in liver cancer cells as in other cell types. Furthermore, transduced LSD1 knockdown stable Huh7 and HepG2 cell lines further confirmed that LSD1 inhibition hindered the activity of PLK1 thus affecting the cell cycle progression.

Taken together, these findings support the role of LSD1, as a modulator of the methylation/demethylation dynamic of PLK1, in the cell cycle regulatory mechanism and hepatocarcinogenesis.

## **4.2 LSD1 inhibition by pharmacological inhibitors**

In my study, LSD1 inhibition was investigated by utilizing different LSD1 pharmacological inhibitors. However, when various hepatoma cells were treated with a serious concentration of GSK2879552, LSD1 inhibition did not affect cell proliferation. Since LSD1 is considered a homology protein of monoamine oxidase (MAO), in the past, small-molecular inhibitors of MAOs were applied for LSD1 inhibition, such as tranylcypromine (TCP or 2-PCPA), pargyline,

phenelzine, [114] as well as ORY-1001 [115], GSK-2879552 [83], IMG-7289, CC-90011 and INCB059872 [86]. Some of these inhibitors are currently undergoing clinical trials. Kimberly N. Smitheman et al. found that combined inhibition of LSD1 with both all-trans retinoic acid and GSK2879552 produced a synergistic effect on cell proliferation in patients with acute myeloid leukemia (AML) [116]. Nevertheless, a proliferation screen of 165 cell lines by Helai P. Mohammad et al. that considered many tumor types indicated that only small cell lung carcinoma (SCLC) and AML were sensitive to LSD1 inhibition by GSK2879552 treatment [83]. In agreement, my study revealed that LSD1 inhibition by GSK2879552 does not affect cell proliferation in liver cancer cells, these data demonstrate that GSK2879552 is not effective at inhibiting LSD1 in most cells.

When pharmacological LSD1 inhibitors HCl-2509 and HCl-2577 were applied to hepatoma cells, both inhibitors had strong effects of LSD1 inhibition on cell growth and cell viability in hepatoma cells. HCl-2509 is a non-covalent reversible and highly selective inhibitor of LSD1 but has no effect against MAO-A and B [102]. Some studies have presented promising data concerning HCl-2509 mediated LSD1 inhibition in preclinical non-leukemic tumor lesions [117]. Furthermore, HCl-2509 has been shown preclinical efficacy in Ewing's sarcoma, acute myeloid leukemia and endometrial cancer [87, 89, 102]. Similarly, previous data from our lab has also demonstrated an effect of HCl-2509 on LSD1 inhibition in lung cancer cells [95]. My studies demonstrated that inhibition of LSD1 by HCl-2509 led to a significant reduction in cell growth, which is consistent with previous studies. Moreover, LSD1 inhibition caused increased H3K4me2 accumulation in hepatoma cells. Interestingly, LSD1 was downregulated at the transcriptional level with the inhibitors treatment, which indicates that inhibition of LSD1 might regulate its own gene expression. In addition, considering that extracellular pH is acidic in the microenvironment of cancer cells, HCl-2509 might be hydrolyzed in an acidic environment due to its structure, two compounds presumed to be hydrolysates of HCl-2509. Neither the single compound nor the combination of two compounds had an effect on LSD1 inhibition and the marker genes. In addition, cell growth was not inhibited by the treatment of the compounds. Furthermore, molecular docking performed by Sorna et al. has also confirmed that HCl-2509 can block the FAD-binding region of LSD1 and reversibly for LSD1 inhibition [94], which

supports my results that HCI-2509 can directly bind to LSD1 thus reducing cell growth.

A comparison of the cell viability reduction between HCI-2509 and HCI-2577 showed that these two inhibitors had a similar efficacy on LSD1 inhibition. Sorna et al. found that HCI-2577 (SP-2577), a clinical analogue of HCI-2509, acted as a potent reversible LSD1 inhibitor by Sorna et al. [94]. Like HCI-2509, HCI-2577 does not inhibit MAO-A/B and is ineffective at inhibiting the activity of cytochrome P450 monooxygenases (CYPs) and hERG. [118]. Furthermore, the alteration of metabolic genes expression from qPCR also demonstrated that HCI-2577 and HCI-2509 have nearly the same effect on LSD1 inhibition. Currently, HCI-2577 is being evaluated in phase I/II clinical trials in Ewing sarcoma (NCT03600649). In addition to this, the effect of HCI-2577 on tumor cell proliferation has also been reported in ovarian cancer. Moreover, the proliferation of cancer cells has also been suppressed in colorectal and breast cancer. Besides, HCI-2577 improves antitumor immune mechanisms in ovarian cancer with mutations in the switch/sucrose nonfermentable (SWI/SNF) complex [119]. All these data support the HCI-2577 effects observed in my study. Of note, the protein level of H3K4me2 showed stronger enhancement upon LSD1 inhibition by HCI-2577 than by HCI-2509 in both hepatoma cells, indicating that HCI-2577 might have a greater effect on LSD1 histone substrates.

### **4.3 LSD1 involvements in lipid metabolic reprogramming**

Expression profiling and CHIP analysis indicated that genes involved in lipid metabolism were significantly downregulated by LSD1 inhibition, especially in fatty acid metabolism and cholesterol homeostasis pathways. The various mechanisms of LSD1 in the regulation of cancer progression have been widely investigated and increasing evidence indicates that lipids play critical roles in tumorigenesis and progression [120], but the underlying mechanism of LSD1 and lipid metabolism is still poorly understood. In the present data obtained by RNA-seq analysis, I showed that, in addition to lipogenic genes such as FASN and FABP5, many mitochondrial-related genes were differentially expressed after LSD1 inhibition, such as BNIP3 and BNIP3L. Importantly, this result is apparent in both pharmacologically and transgenically inhibited hepatoma cells. Moreover, DisGeNet revealed that alterations of gene

expression were associated with tumor angiogenesis and hepatocarcinogenesis as well as non-alcoholic fatty liver disease (NAFLD). ChIP followed by genome-wide sequencing (ChIP-seq) studies have indicated that LSD1 binds to the promoter regions of multiple genes. Furthermore, in the present study, ChIP-seq analysis revealed that LSD1 peaks coincided with H3K4me2 peaks in the promoter and enhancer regions of the downregulated lipid metabolic genes FABP5, FASN, GAPM, ESRRA, ACACA, PDK4 and LDHA. These findings were of particular interest because they revealed the link between LSD1 and cancer cell lipid metabolism, especially in fatty acid metabolism. LSD1 can evidently regulate the “BAT” gene program in brown adipose tissue (BAT) by catalyzing the demethylation of mono- and dimethylated H3K9 [121]. In addition, an increased methylation pattern of H3K9me1/me2 at the proximal Ucp1 promoter was found in LSD1 knockout mice after Ucp1 expression was downregulated [121]. However, Hino et al. have found that in adipocytes, transcription repression triggered by LSD1-dependent demethylation of H3K4me at promoters of genes involved in energy expenditure, such as PGC-1 $\alpha$  and the pyruvate dehydrogenase kinase 4 (PDK4) [122]. LSD1 has also been shown to coincide with H3K4 methylation but not with H3K9 peaks in cultured lymph node carcinoma of the prostate cells and myoblasts [123, 124]. These findings support my results that LSD1 occupies the promoters of metabolic genes accompanied by methylation of H3K4.

Among the metabolic genes in this study, PDK4 and GPAM were shown to be highly upregulated and downregulated by LSD1 inhibition. Importantly, ChIP analysis demonstrated that LSD1 can directly regulate PDK4 and GPAM expression both by binding their promoters and through increased methylation of H3K4me2. PDK4 is an important regulator of pyruvate dehydrogenase complex (PDC) activity, and it has been shown to alter fatty acid metabolism in HCC cells, knockdown of PDK4 leads to upregulation of FASN and stearoyl-CoA desaturase (SCD) [125]. In addition, loss of the fatty acid translocase inhibited starvation-induced PDK4 expression, suggesting that fatty acid uptake is a major factor in the induction of PDK4 expression [126]. Similar results of PDK4 enhanced lipogenesis have been shown in lung cancer cells [127]. However, a recent study revealed a protective effect of high PDK4 expression in PCa in a transcriptomic patient dataset [128], which is thought to support the

upregulated PDK4 after LSD1 inhibition in hepatoma cells in my study. Moreover, qPCR validation for the metabolic genes selected from lipid metabolism pathways showed that GPAM was downregulated upon LSD1 inhibition. GPAM is important for triglyceride synthesis during lipid biosynthesis, but its role in cancer is not well understood. A recent study in ovarian carcinoma has reported that high GPAM expression promotes tumor cell migration and is associated with poor survival [129]. These data are consistent with my data about the downregulation of metabolic genes by LSD1 inhibition.

In carcinogenesis, tumor tissues require a surge in lipid metabolism to accommodate the increased requirements for the synthesis of membranes, energy storage, and signaling functions [130]. In my study, qPCR was used to validate the lipid metabolic genes, and FASN was shown to be downregulated after LSD1 was inhibited not only by inhibitors but also with endogenous knockdown LSD1. In addition, FABP5, as lipid chaperones, also shows the downregulation in LSD1 inhibited hepatoma cells. Furthermore, ChIP analysis revealed that LSD1 could directly bind to the promoter of FASN and FABP5 thus regulating their expression. Fatty acids are the major components of cell membrane lipids [131] and are critical for energy metabolism. Fatty acid synthase (FASN), a key activator of the lipogenic gene, is vital to the synthesis of these all-important fatty acids *de novo*. FASN overexpression has been detected in many cancer types [132-137] and it has been shown to enhance lipogenesis and increased cell growth and proliferation [138]. LSD1 has been shown to regulate triglyceride levels in hepatocytes by regulating the expression of the fatty acid synthase FASN [73]. In addition, the high expression of LSD1 has been associated with the accumulation of lipid drops and high FASN expression [139]. Furthermore, past work has indicated that LSD1 knockdown mice have increased FASN activity and increased fatty acid uptake in BAT [75]. The results of the studies are consistent with those of my study.

TCGA data analysis indicated a higher expression of FABP5 in tumor-related tissues than in non-tumor tissues. Accordingly, higher FABP5 expression was associated with a lower survival rate. Excitingly, a strong positive correlation between LSD1 and FABP5 was observed. Moreover, results from ChIP-seq analysis suggested that LSD1 inhibition downregulated FABP5 expression by binding its promoter with an enrichment of H3K4me2 at gene loci. This

is also the first study to show the mechanisms of histone modifiers of LSD1 and FABP5. FABP5 has a generic role in fatty acid-binding and trafficking, lipid metabolism, and regulating cell growth [140]. Past work has suggested that upregulation of FABP5 is induced by NF-kappaB (NF-kB) through two response elements in the promoter of the EGFR and the activation of PPARG [141]. Morgan et al. also found that FABP5 expression (cytoplasmic and nuclear) was increased in patients with PC compared to patients with benign hyperplasia and this was associated with decreased survival time [142]. These existing findings support my finding that high FABP5 expression leads to low survival rates. These data indicate that FABP5 might be a new target of LSD1 in the regulation of lipid metabolism. All these results indicate the value of LSD1 inhibition in the regulation of lipid metabolism in new strategies of cancer therapy.

#### **4.4 LSD1 inhibition reduced fat accumulation in NAFLD in vivo**

Since the in vitro data pointed to a prominent role of LSD1 in fat metabolism, I investigated the links between LSD1 and fat metabolism in NAFLD. NAFLD is a slowly progressive condition characterized by the accumulation of excess hepatic lipids [143]. Some individuals go on to develop NASH, which drives fibrosis that can in turn lead to cirrhosis and HCC [144]. Given the increasing incidence of NAFLD proceeding to HCC, there is an urgent need to identify biomarkers as well as treatments to prevent negative outcomes. To elucidate this, animal models have played a vital role in showing the pathophysiological mechanisms of NAFLD and its progression to HCC. In the present study, the HCC mouse model was established based on NAFLD, a high-fat diet as exposed to DEN-induced C57BL/6J mouse led to HCC for 32 weeks. The C57BL/6 strain in mice is generally preferred because of their intrinsic predilection to develop obesity, T2DM and NAFLD [145]. Due to the limited time, the progression of HCC is still ongoing. Therefore, in this study, I only show limited data at 18 weeks indicating that the mice had NAFLD.

Along with the HFD-induced obesity, both male and female mice rapidly gained body weight and high levels of liver enzyme AST values. These data are in line with human data that indicate rapid development of hepatic steatosis and abnormal liver enzymes following the

initiation of an obesogenic diet [146]. In HFD-induced female mice, I observed no elevated ALT values. Moreover, both male and female mice showed a significant reduction in body weight after receiving HCI-2509, but there was no significant difference when compared to normal body weight according to the Jackson Laboratory datasets. My findings provide evidence that LSD1 inhibition by HCI-2509 can prevent mice from developing obesity. In addition, lower AST values were also found in HCI-2509 treated male and female mice, while lower ALT was only shown in HCI-2509 treated male mice. Although AST and ALT are the two most reliable markers of liver injury, ALT is more reliable than AST because it mainly exists in the cell membranes of the liver and is more specific to liver damage [147]. The results thus indicate that the female mice have less liver injury than male mice, confirming previous data. Histology staining showed fat accumulation in HFD-induced mice but fewer lipid drops in female mice also confirmed this. Furthermore, transgenic adult mice with a high-fat diet have been reported to express the human cholesterol transporter APOE2 (hAPOE2) gene and exhibit significantly elevated hepatic lipid accumulation [148].

In the present study, I demonstrated that HCI-2509, the potent LSD1 inhibitor, induced less fat accumulation and decreased AST and ALT values during the development of NAFLD *in vivo*. HCI-2509 has been shown to induce differentiation of AML cell lines and primary AML, and prolonged overall survival in AML mouse models [102]. Furthermore, a novel combination of LSD1 inhibitor HCI-2509 and EZH2 inhibitor EPZ6438 exhibited a strong synergistic anti-AML effect *in vitro* and *in vivo* [149]. Moreover, hypoxia-treated HCC827 cells demonstrated more aggressive tumor growth *in vivo* compared with cells grown in normoxia, but inhibition of LSD1 function by shRNA-mediated knockdown or by the small-molecular inhibitor HCI-2509 suppressed tumor growth and enhanced gefitinib response *in vivo* [150]. These findings indicated that HCI-2509 had a good effect on LSD1 inhibition *in vivo*. The features of histology and biomarkers as well as the further mechanism links between genes involved in lipid metabolism and LSD1 during the whole progression of HCC will be addressed in future studies.

In conclusion, the presented data reveal that LSD1 plays important roles not only in cell cycle control but also in the metabolism and in lipid regulation to promote the progression of HCC. Due to the novel function of LSD1 in metabolic regulation, LSD1 has been shown to bind to

the promoter of metabolic genes and regulate their expression. Notably, from the downregulation of FABP5 upon LSD1 inhibition, this is the first study to prove that FABP5 is a novel direct target of LSD1 due to the downregulation of FABP5 upon LSD1 inhibition. Because of the important function of FABP5 in cell proliferation and lipid metabolism regulation, FABP5 provides a new sight for future studies to investigate its role in the progression of cancer.

## 5. References

1. Torre, L.A., et al., *Global cancer statistics, 2012*. CA Cancer J Clin, 2015. 65(2): p. 87-108.
2. Parkin, D.M., et al., *Global cancer statistics, 2002*. CA Cancer J Clin, 2005. 55(2): p. 74-108.
3. Kumar, V., et al., *Robbins and Cotran pathologic basis of disease*. 7th ed. 2005, Philadelphia: Elsevier Saunders. xv, 1525 p.
4. Baffy, G., E.M. Brunt, and S.H. Caldwell, *Hepatocellular carcinoma in non-alcoholic fatty liver disease: an emerging menace*. J Hepatol, 2012. 56(6): p. 1384-91.
5. Beasley, R.P., et al., *Hepatocellular carcinoma and hepatitis B virus. A prospective study of 22 707 men in Taiwan*. Lancet, 1981. 2(8256): p. 1129-33.
6. Parkin, D.M., *The global health burden of infection-associated cancers in the year 2002*. Int J Cancer, 2006. 118(12): p. 3030-44.
7. Imai, M., et al., *Free and integrated forms of hepatitis B virus DNA in human hepatocellular carcinoma cells (PLC/342) propagated in nude mice*. J Virol, 1987. 61(11): p. 3555-60.
8. Lavanchy, D., *Hepatitis B virus epidemiology, disease burden, treatment, and current and emerging prevention and control measures*. J Viral Hepat, 2004. 11(2): p. 97-107.
9. Huang, Y.T., et al., *Lifetime risk and sex difference of hepatocellular carcinoma among patients with chronic hepatitis B and C*. J Clin Oncol, 2011. 29(27): p. 3643-50.
10. Asham, E.H., A. Kaseb, and R.M. Ghobrial, *Management of hepatocellular carcinoma*. Surg Clin North Am, 2013. 93(6): p. 1423-50.
11. Bowen, D.G. and C.M. Walker, *Adaptive immune responses in acute and chronic hepatitis C virus infection*. Nature, 2005. 436(7053): p. 946-52.
12. Seitz, H.K. and F. Stickel, *Molecular mechanisms of alcohol-mediated carcinogenesis*. Nat Rev Cancer, 2007. 7(8): p. 599-612.
13. Abnet, C.C., *Carcinogenic food contaminants*. Cancer Invest, 2007. 25(3): p. 189-96.
14. Vakevainen, S., et al., *High salivary acetaldehyde after a moderate dose of alcohol in ALDH2-deficient subjects: strong evidence for the local carcinogenic action of acetaldehyde*. Alcohol Clin Exp Res, 2000. 24(6): p. 873-7.
15. Herrmann, S.S., K. Granby, and L. Duedahl-Olesen, *Formation and mitigation of N-nitrosamines in nitrite preserved cooked sausages*. Food Chem, 2015. 174: p. 516-26.
16. Hengstler, J.G., et al., *Challenging dogma: thresholds for genotoxic carcinogens? The case of vinyl acetate*. Annu Rev Pharmacol Toxicol, 2003. 43: p. 485-520.
17. Tsuda, S., et al., *DNA damage induced by red food dyes orally administered to pregnant and male mice*. Toxicol Sci, 2001. 61(1): p. 92-9.
18. Yang, C.S., et al., *Cytochrome P450IIE1: roles in nitrosamine metabolism and mechanisms of regulation*. Drug Metab Rev, 1990. 22(2-3): p. 147-59.
19. Verna, L., J. Whysner, and G.M. Williams, *N-nitrosodiethylamine mechanistic data and risk assessment: bioactivation, DNA-adduct formation, mutagenicity, and tumor initiation*.

- Pharmacol Ther, 1996. 71(1-2): p. 57-81.
20. Jakszyn, P., et al., *Intake and food sources of nitrites and N-nitrosodimethylamine in Spain*. Public Health Nutr, 2006. 9(6): p. 785-91.
  21. Naugler, W.E., et al., *Gender disparity in liver cancer due to sex differences in MyD88-dependent IL-6 production*. Science, 2007. 317(5834): p. 121-4.
  22. El-Serag, H.B., *Hepatocellular carcinoma*. N Engl J Med, 2011. 365(12): p. 1118-27.
  23. Magee, P.N. and J.M. Barnes, *The production of malignant primary hepatic tumours in the rat by feeding dimethylnitrosamine*. Br J Cancer, 1956. 10(1): p. 114-22.
  24. Rao, K.V. and S.D. Vesselinovitch, *Age- and sex-associated diethylnitrosamine dealkylation activity of the mouse liver and hepatocarcinogenesis*. Cancer Res, 1973. 33(7): p. 1625-7.
  25. Wang, J., et al., *Mutual interaction between endoplasmic reticulum and mitochondria in nonalcoholic fatty liver disease*. Lipids Health Dis, 2020. 19(1): p. 72.
  26. Sayiner, M., et al., *Epidemiology of Nonalcoholic Fatty Liver Disease and Nonalcoholic Steatohepatitis in the United States and the Rest of the World*. Clin Liver Dis, 2016. 20(2): p. 205-14.
  27. Kanwar, P. and K.V. Kowdley, *The Metabolic Syndrome and Its Influence on Nonalcoholic Steatohepatitis*. Clin Liver Dis, 2016. 20(2): p. 225-43.
  28. Poonawala, A., S.P. Nair, and P.J. Thuluvath, *Prevalence of obesity and diabetes in patients with cryptogenic cirrhosis: a case-control study*. Hepatology, 2000. 32(4 Pt 1): p. 689-92.
  29. Andrade, A., et al., *Nonalcoholic steatohepatitis in posttransplantation liver: Review article*. Rev Assoc Med Bras (1992), 2018. 64(2): p. 187-194.
  30. Buzzetti, E., M. Pinzani, and E.A. Tsochatzis, *The multiple-hit pathogenesis of non-alcoholic fatty liver disease (NAFLD)*. Metabolism, 2016. 65(8): p. 1038-48.
  31. Bugianesi, E., et al., *Insulin resistance in nonalcoholic fatty liver disease*. Curr Pharm Des, 2010. 16(17): p. 1941-51.
  32. Guilherme, A., et al., *Adipocyte dysfunctions linking obesity to insulin resistance and type 2 diabetes*. Nat Rev Mol Cell Biol, 2008. 9(5): p. 367-77.
  33. Boden, G., *Role of fatty acids in the pathogenesis of insulin resistance and NIDDM*. Diabetes, 1997. 46(1): p. 3-10.
  34. Cusi, K., *Role of insulin resistance and lipotoxicity in non-alcoholic steatohepatitis*. Clin Liver Dis, 2009. 13(4): p. 545-63.
  35. Vonghia, L., P. Michielsen, and S. Francque, *Immunological mechanisms in the pathophysiology of non-alcoholic steatohepatitis*. Int J Mol Sci, 2013. 14(10): p. 19867-90.
  36. Stienstra, R., et al., *Kupffer cells promote hepatic steatosis via interleukin-1beta-dependent suppression of peroxisome proliferator-activated receptor alpha activity*. Hepatology, 2010. 51(2): p. 511-22.
  37. Tosello-Tramont, A.C., et al., *Kupffer cells trigger nonalcoholic steatohepatitis development in diet-induced mouse model through tumor necrosis factor-alpha production*. J Biol Chem, 2012. 287(48): p. 40161-72.

38. Marra, F. and F. Tacke, *Roles for chemokines in liver disease*. *Gastroenterology*, 2014. 147(3): p. 577-594 e1.
39. Arrese, M., et al., *Innate Immunity and Inflammation in NAFLD/NASH*. *Dig Dis Sci*, 2016. 61(5): p. 1294-303.
40. Ganz, M. and G. Szabo, *Immune and inflammatory pathways in NASH*. *Hepatology Int*, 2013. 7 Suppl 2: p. 771-81.
41. Kang, M.J., et al., *Inhibition of Hepatic Stellate Cell Activation Suppresses Tumorigenicity of Hepatocellular Carcinoma in Mice*. *Am J Pathol*, 2021. 191(12): p. 2219-2230.
42. Chen, H.F., P. Chen, and C.Y. Li, *Risk of malignant neoplasms of liver and biliary tract in diabetic patients with different age and sex stratifications*. *Hepatology*, 2010. 52(1): p. 155-63.
43. Sung, K.C., S.H. Wild, and C.D. Byrne, *Development of new fatty liver, or resolution of existing fatty liver, over five years of follow-up, and risk of incident hypertension*. *J Hepatol*, 2014. 60(5): p. 1040-5.
44. Marra, F. and G. Svegliati-Baroni, *Lipotoxicity and the gut-liver axis in NASH pathogenesis*. *J Hepatol*, 2018. 68(2): p. 280-295.
45. Feldstein, A.E., et al., *Free fatty acids promote hepatic lipotoxicity by stimulating TNF- $\alpha$  expression via a lysosomal pathway*. *Hepatology*, 2004. 40(1): p. 185-94.
46. Han, M.S., et al., *Lysophosphatidylcholine as a death effector in the lipoapoptosis of hepatocytes*. *J Lipid Res*, 2008. 49(1): p. 84-97.
47. Kakisaka, K., et al., *Mechanisms of lysophosphatidylcholine-induced hepatocyte lipoapoptosis*. *Am J Physiol Gastrointest Liver Physiol*, 2012. 302(1): p. G77-84.
48. Osawa, Y., et al., *Roles for C16-ceramide and sphingosine 1-phosphate in regulating hepatocyte apoptosis in response to tumor necrosis factor- $\alpha$* . *J Biol Chem*, 2005. 280(30): p. 27879-87.
49. Ioannou, G.N., et al., *Cholesterol crystallization within hepatocyte lipid droplets and its role in murine NASH*. *J Lipid Res*, 2017. 58(6): p. 1067-1079.
50. Hirsova, P., et al., *Lipotoxic lethal and sublethal stress signaling in hepatocytes: relevance to NASH pathogenesis*. *J Lipid Res*, 2016. 57(10): p. 1758-1770.
51. Begriche, K., et al., *Mitochondrial dysfunction in NASH: causes, consequences and possible means to prevent it*. *Mitochondrion*, 2006. 6(1): p. 1-28.
52. Cusi, K., *Nonalcoholic fatty liver disease in type 2 diabetes mellitus*. *Curr Opin Endocrinol Diabetes Obes*, 2009. 16(2): p. 141-9.
53. Paradies, G., et al., *Oxidative stress, cardiolipin and mitochondrial dysfunction in nonalcoholic fatty liver disease*. *World J Gastroenterol*, 2014. 20(39): p. 14205-18.
54. Zhang, X.Q., et al., *Role of endoplasmic reticulum stress in the pathogenesis of nonalcoholic fatty liver disease*. *World J Gastroenterol*, 2014. 20(7): p. 1768-76.
55. Akazawa, Y. and K. Nakao, *Lipotoxicity pathways intersect in hepatocytes: Endoplasmic reticulum stress, c-Jun N-terminal kinase-1, and death receptors*. *Hepatology Res*, 2016. 46(10): p. 977-84.

56. Baiceanu, A., et al., *Endoplasmic reticulum proteostasis in hepatic steatosis*. Nat Rev Endocrinol, 2016. 12(12): p. 710-722.
57. Villanueva, A., et al., *Genomics and signaling pathways in hepatocellular carcinoma*. Semin Liver Dis, 2007. 27(1): p. 55-76.
58. Zhao, Z.K., et al., *Overexpression of LSD1 in hepatocellular carcinoma: a latent target for the diagnosis and therapy of hepatoma*. Tumour Biol, 2013. 34(1): p. 173-80.
59. Brown, R., et al., *Poised epigenetic states and acquired drug resistance in cancer*. Nat Rev Cancer, 2014. 14(11): p. 747-53.
60. Tao, R., et al., *Methylation profile of single hepatocytes derived from hepatitis B virus-related hepatocellular carcinoma*. PLoS One, 2011. 6(5): p. e19862.
61. Meng, F., et al., *MicroRNA-21 regulates expression of the PTEN tumor suppressor gene in human hepatocellular cancer*. Gastroenterology, 2007. 133(2): p. 647-58.
62. Kutay, H., et al., *Downregulation of miR-122 in the rodent and human hepatocellular carcinomas*. J Cell Biochem, 2006. 99(3): p. 671-8.
63. Dawson, M.A. and T. Kouzarides, *Cancer epigenetics: from mechanism to therapy*. Cell, 2012. 150(1): p. 12-27.
64. Shi, Y., et al., *Histone demethylation mediated by the nuclear amine oxidase homolog LSD1*. Cell, 2004. 119(7): p. 941-53.
65. Metzger, E., et al., *LSD1 demethylates repressive histone marks to promote androgen-receptor-dependent transcription*. Nature, 2005. 437(7057): p. 436-9.
66. Amente, S., L. Lania, and B. Majello, *The histone LSD1 demethylase in stemness and cancer transcription programs*. Biochim Biophys Acta, 2013. 1829(10): p. 981-6.
67. Kahl, P., et al., *Androgen receptor coactivators lysine-specific histone demethylase 1 and four and a half LIM domain protein 2 predict risk of prostate cancer recurrence*. Cancer Res, 2006. 66(23): p. 11341-7.
68. Lv, S., et al., *LSD1 is required for chromosome segregation during mitosis*. Eur J Cell Biol, 2010. 89(7): p. 557-63.
69. Agger, K., et al., *The H3K27me3 demethylase JMJD3 contributes to the activation of the INK4A-ARF locus in response to oncogene- and stress-induced senescence*. Genes Dev, 2009. 23(10): p. 1171-6.
70. Kang, M.K., et al., *Epigenetic gene regulation by histone demethylases: emerging role in oncogenesis and inflammation*. Oral Dis, 2017. 23(6): p. 709-720.
71. Scoumanne, A. and X. Chen, *The lysine-specific demethylase 1 is required for cell proliferation in both p53-dependent and -independent manners*. J Biol Chem, 2007. 282(21): p. 15471-5.
72. Schulte, J.H., et al., *Lysine-specific demethylase 1 is strongly expressed in poorly differentiated neuroblastoma: implications for therapy*. Cancer Res, 2009. 69(5): p. 2065-71.
73. Wu, J., et al., *Prognostic role of LSD1 in various cancers: evidence from a meta-analysis*. Onco Targets Ther, 2015. 8: p. 2565-70.
74. Sheng, W., et al., *LSD1 Ablation Stimulates Anti-tumor Immunity and Enables Checkpoint*

- Blockade*. Cell, 2018. 174(3): p. 549-563 e19.
75. Duteil, D., et al., *Lsd1 Ablation Triggers Metabolic Reprogramming of Brown Adipose Tissue*. Cell Rep, 2016. 17(4): p. 1008-1021.
76. Kim, Y., et al., *Methylation-dependent regulation of HIF-1alpha stability restricts retinal and tumour angiogenesis*. Nat Commun, 2016. 7: p. 10347.
77. Sakamoto, A., et al., *Lysine Demethylase LSD1 Coordinates Glycolytic and Mitochondrial Metabolism in Hepatocellular Carcinoma Cells*. Cancer Res, 2015. 75(7): p. 1445-56.
78. Kim, D., K.I. Kim, and S.H. Baek, *Roles of lysine-specific demethylase 1 (LSD1) in homeostasis and diseases*. J Biomed Sci, 2021. 28(1): p. 41.
79. Liu, W., et al., *Knockdown of LSD1 ameliorates the severity of rheumatoid arthritis and decreases the function of CD4 T cells in mouse models*. Int J Clin Exp Pathol, 2018. 11(1): p. 333-341.
80. Janzer, A., et al., *Lysine-specific demethylase 1 (LSD1) and histone deacetylase 1 (HDAC1) synergistically repress proinflammatory cytokines and classical complement pathway components*. Biochem Biophys Res Commun, 2012. 421(4): p. 665-70.
81. Mack, C.P., *An epigenetic clue to diabetic vascular disease*. Circ Res, 2008. 103(6): p. 568-70.
82. Wang, Q., et al., *Host-secreted antimicrobial peptide enforces symbiotic selectivity in Medicago truncatula*. Proc Natl Acad Sci U S A, 2017. 114(26): p. 6854-6859.
83. Mohammad, H.P., et al., *A DNA Hypomethylation Signature Predicts Antitumor Activity of LSD1 Inhibitors in SCLC*. Cancer Cell, 2015. 28(1): p. 57-69.
84. Schenk, T., et al., *Inhibition of the LSD1 (KDM1A) demethylase reactivates the all-trans-retinoic acid differentiation pathway in acute myeloid leukemia*. Nat Med, 2012. 18(4): p. 605-11.
85. Kong, L., et al., *KDM1A promotes tumor cell invasion by silencing TIMP3 in non-small cell lung cancer cells*. Oncotarget, 2016. 7(19): p. 27959-74.
86. Zheng, Y.C., et al., *A Systematic Review of Histone Lysine-Specific Demethylase 1 and Its Inhibitors*. Med Res Rev, 2015. 35(5): p. 1032-71.
87. James, N.D., et al., *Survival with Newly Diagnosed Metastatic Prostate Cancer in the "Docetaxel Era": Data from 917 Patients in the Control Arm of the STAMPEDE Trial (MRC PR08, CRUK/06/019)*. Eur Urol, 2015. 67(6): p. 1028-1038.
88. Fiskus, W., et al., *Highly effective combination of LSD1 (KDM1A) antagonist and pan-histone deacetylase inhibitor against human AML cells*. Leukemia, 2017. 31(7): p. 1658.
89. Theisen, E.R., et al., *Reversible inhibition of lysine specific demethylase 1 is a novel anti-tumor strategy for poorly differentiated endometrial carcinoma*. BMC Cancer, 2014. 14: p. 752.
90. Wang, X., et al., *Medicinal chemistry insights in the discovery of novel LSD1 inhibitors*. Epigenomics, 2015. 7(8): p. 1379-96.
91. Gao, J., et al., *The Adenosine Monophosphate (AMP) Analog, 5-Aminoimidazole-4-Carboxamide Ribonucleotide (AICAR) Inhibits Hepatosteatosis and Liver Tumorigenesis in a High-Fat Diet Murine Model Treated with Diethylnitrosamine (DEN)*. Med Sci Monit, 2018.

- 24: p. 8533-8543.
92. Zhang, J. and P.A. Ney, *Role of BNIP3 and NIX in cell death, autophagy, and mitophagy*. Cell Death Differ, 2009. 16(7): p. 939-46.
93. Li, Y., et al., *BNIP3L/NIX-mediated mitophagy: molecular mechanisms and implications for human disease*. Cell Death Dis, 2021. 13(1): p. 14.
94. Sorna, V., et al., *High-throughput virtual screening identifies novel N'-(1-phenylethylidene)-benzohydrazides as potent, specific, and reversible LSD1 inhibitors*. J Med Chem, 2013. 56(23): p. 9496-508.
95. Macheleidt, I.F., et al., *Preclinical studies reveal that LSD1 inhibition results in tumor growth arrest in lung adenocarcinoma independently of driver mutations*. Mol Oncol, 2018. 12(11): p. 1965-1979.
96. Dalvi, P.S., et al., *LSD1 Inhibition Attenuates Tumor Growth by Disrupting PLK1 Mitotic Pathway*. Mol Cancer Res, 2019. 17(6): p. 1326-1337.
97. van de Weerd, B.C. and R.H. Medema, *Polo-like kinases: a team in control of the division*. Cell Cycle, 2006. 5(8): p. 853-64.
98. Lv, Q., et al., *FABP5 regulates the proliferation of clear cell renal cell carcinoma cells via the PI3K/AKT signaling pathway*. Int J Oncol, 2019. 54(4): p. 1221-1232.
99. Fernandez, I., et al., *Clinical biochemistry parameters in C57BL/6J mice after blood collection from the submandibular vein and retroorbital plexus*. J Am Assoc Lab Anim Sci, 2010. 49(2): p. 202-6.
100. Ning, B., et al., *Targeting epigenetic regulations in cancer*. Acta Biochim Biophys Sin (Shanghai), 2016. 48(1): p. 97-109.
101. Mosammamarast, N., et al., *The histone demethylase LSD1/KDM1A promotes the DNA damage response*. J Cell Biol, 2013. 203(3): p. 457-70.
102. Fiskus, W., et al., *Highly effective combination of LSD1 (KDM1A) antagonist and pan-histone deacetylase inhibitor against human AML cells*. Leukemia, 2014. 28(11): p. 2155-64.
103. Rudolph, T., S. Beuch, and G. Reuter, *Lysine-specific histone demethylase LSD1 and the dynamic control of chromatin*. Biol Chem, 2013. 394(8): p. 1019-28.
104. He, Y., et al., *LSD1 promotes S-phase entry and tumorigenesis via chromatin co-occupation with E2F1 and selective H3K9 demethylation*. Oncogene, 2018. 37(4): p. 534-543.
105. Adamo, A., et al., *LSD1 regulates the balance between self-renewal and differentiation in human embryonic stem cells*. Nat Cell Biol, 2011. 13(6): p. 652-9.
106. Yang, P., et al., *RCOR2 is a subunit of the LSD1 complex that regulates ESC property and substitutes for SOX2 in reprogramming somatic cells to pluripotency*. Stem Cells, 2011. 29(5): p. 791-801.
107. Llamazares, S., et al., *polo encodes a protein kinase homolog required for mitosis in Drosophila*. Genes Dev, 1991. 5(12A): p. 2153-65.
108. Kitada, K., et al., *A multicopy suppressor gene of the Saccharomyces cerevisiae G1 cell cycle mutant gene dbf4 encodes a protein kinase and is identified as CDC5*. Mol Cell Biol, 1993.

- 13(7): p. 4445-57.
109. Cheng, M.W., et al., *Clinicopathological significance of Polo-like kinase 1 (PLK1) expression in human malignant glioma*. *Acta Histochem*, 2012. 114(5): p. 503-9.
110. Donizy, P., et al., *Augmented expression of Polo-like kinase 1 is a strong predictor of shorter cancer-specific overall survival in early stage breast cancer at 15-year follow-up*. *Oncol Lett*, 2016. 12(3): p. 1667-1674.
111. Lin, P., et al., *Comprehensive and Integrative Analysis Reveals the Diagnostic, Clinicopathological and Prognostic Significance of Polo-Like Kinase 1 in Hepatocellular Carcinoma*. *Cell Physiol Biochem*, 2018. 47(3): p. 925-947.
112. Yamada, S., et al., *Expression profiling and differential screening between hepatoblastomas and the corresponding normal livers: identification of high expression of the PLK1 oncogene as a poor-prognostic indicator of hepatoblastomas*. *Oncogene*, 2004. 23(35): p. 5901-11.
113. Laoukili, J., et al., *FoxM1 is required for execution of the mitotic programme and chromosome stability*. *Nat Cell Biol*, 2005. 7(2): p. 126-36.
114. Fu, X., P. Zhang, and B. Yu, *Advances toward LSD1 inhibitors for cancer therapy*. *Future Med Chem*, 2017. 9(11): p. 1227-1242.
115. Fang, Y., G. Liao, and B. Yu, *LSD1/KDM1A inhibitors in clinical trials: advances and prospects*. *J Hematol Oncol*, 2019. 12(1): p. 129.
116. Smitheman, K.N., et al., *Lysine specific demethylase 1 inactivation enhances differentiation and promotes cytotoxic response when combined with all-trans retinoic acid in acute myeloid leukemia across subtypes*. *Haematologica*, 2019. 104(6): p. 1156-1167.
117. Castelli, G., E. Pelosi, and U. Testa, *Targeting histone methyltransferase and demethylase in acute myeloid leukemia therapy*. *Onco Targets Ther*, 2018. 11: p. 131-155.
118. Dai, X.J., et al., *Reversible Lysine Specific Demethylase 1 (LSD1) Inhibitors: A Promising Wrench to Impair LSD1*. *J Med Chem*, 2021. 64(5): p. 2466-2488.
119. Soldi, R., et al., *The novel reversible LSD1 inhibitor SP-2577 promotes anti-tumor immunity in SWI/SNF complex mutated ovarian cancer*. *PLoS One*, 2020. 15(7): p. e0235705.
120. Lisacovitch, M. and L.C. Cantley, *Lipid second messengers*. *Cell*, 1994. 77(3): p. 329-34.
121. Sambeat, A., et al., *LSD1 Interacts with Zfp516 to Promote UCP1 Transcription and Brown Fat Program*. *Cell Rep*, 2016. 15(11): p. 2536-49.
122. Hino, S., et al., *FAD-dependent lysine-specific demethylase-1 regulates cellular energy expenditure*. *Nat Commun*, 2012. 3: p. 758.
123. Anan, K., et al., *LSD1 mediates metabolic reprogramming by glucocorticoids during myogenic differentiation*. *Nucleic Acids Res*, 2018. 46(11): p. 5441-5454.
124. Sehrawat, A., et al., *LSD1 activates a lethal prostate cancer gene network independently of its demethylase function*. *Proc Natl Acad Sci U S A*, 2018. 115(18): p. E4179-E4188.
125. Yang, C., et al., *Downregulation of PDK4 Increases Lipogenesis and Associates with Poor Prognosis in Hepatocellular Carcinoma*. *J Cancer*, 2019. 10(4): p. 918-926.

126. Nahle, Z., et al., *CD36-dependent regulation of muscle FoxO1 and PDK4 in the PPAR delta/beta-mediated adaptation to metabolic stress*. J Biol Chem, 2008. 283(21): p. 14317-26.
127. Li, G., et al., *The microRNA-182-PDK4 axis regulates lung tumorigenesis by modulating pyruvate dehydrogenase and lipogenesis*. Oncogene, 2017. 36(7): p. 989-998.
128. Oberhuber, M., et al., *STAT3-dependent analysis reveals PDK4 as independent predictor of recurrence in prostate cancer*. Mol Syst Biol, 2020. 16(4): p. e9247.
129. Marchan, R., et al., *Glycerol-3-phosphate Acyltransferase 1 Promotes Tumor Cell Migration and Poor Survival in Ovarian Carcinoma*. Cancer Res, 2017. 77(17): p. 4589-4601.
130. Santos, C.R. and A. Schulze, *Lipid metabolism in cancer*. FEBS J, 2012. 279(15): p. 2610-23.
131. Menendez, J.A. and R. Lupu, *Fatty acid synthase and the lipogenic phenotype in cancer pathogenesis*. Nat Rev Cancer, 2007. 7(10): p. 763-77.
132. Walter, K., et al., *Serum fatty acid synthase as a marker of pancreatic neoplasia*. Cancer Epidemiol Biomarkers Prev, 2009. 18(9): p. 2380-5.
133. Witkiewicz, A.K., et al., *Co-expression of fatty acid synthase and caveolin-1 in pancreatic ductal adenocarcinoma: implications for tumor progression and clinical outcome*. Cell Cycle, 2008. 7(19): p. 3021-5.
134. Alo, P.L., et al., *Immunohistochemical expression and prognostic significance of fatty acid synthase in pancreatic carcinoma*. Anticancer Res, 2007. 27(4B): p. 2523-7.
135. Long, Q.Q., et al., *Fatty acid synthase (FASN) levels in serum of colorectal cancer patients: correlation with clinical outcomes*. Tumour Biol, 2014. 35(4): p. 3855-9.
136. Cai, Y., et al., *Expressions of fatty acid synthase and HER2 are correlated with poor prognosis of ovarian cancer*. Med Oncol, 2015. 32(1): p. 391.
137. Di Vizio, D., et al., *Caveolin-1 interacts with a lipid raft-associated population of fatty acid synthase*. Cell Cycle, 2008. 7(14): p. 2257-67.
138. Vazquez-Martin, A., et al., *Overexpression of fatty acid synthase gene activates HER1/HER2 tyrosine kinase receptors in human breast epithelial cells*. Cell Prolif, 2008. 41(1): p. 59-85.
139. Duteil, D., et al., *LSD1 promotes oxidative metabolism of white adipose tissue*. Nat Commun, 2014. 5: p. 4093.
140. Zimmerman, A.W. and J.H. Veerkamp, *New insights into the structure and function of fatty acid-binding proteins*. Cell Mol Life Sci, 2002. 59(7): p. 1096-116.
141. Kannan-Thulasiraman, P., et al., *Fatty acid-binding protein 5 and PPARbeta/delta are critical mediators of epidermal growth factor receptor-induced carcinoma cell growth*. J Biol Chem, 2010. 285(25): p. 19106-15.
142. Morgan, E.A., et al., *Expression of cutaneous fatty acid-binding protein (C-FABP) in prostate cancer: potential prognostic marker and target for tumorigenicity-suppression*. Int J Oncol, 2008. 32(4): p. 767-75.
143. Diehl, A.M. and C. Day, *Cause, Pathogenesis, and Treatment of Nonalcoholic Steatohepatitis*. N Engl J Med, 2017. 377(21): p. 2063-2072.
144. Angulo, P., et al., *Liver Fibrosis, but No Other Histologic Features, Is Associated With Long-*

- 
- term Outcomes of Patients With Nonalcoholic Fatty Liver Disease*. Gastroenterology, 2015. 149(2): p. 389-97 e10.
145. Kohli, R. and A.E. Feldstein, *NASH animal models: are we there yet?* J Hepatol, 2011. 55(4): p. 941-3.
146. Fabbrini, E., S. Sullivan, and S. Klein, *Obesity and nonalcoholic fatty liver disease: biochemical, metabolic, and clinical implications*. Hepatology, 2010. 51(2): p. 679-89.
147. Giboney, P.T., *Mildly elevated liver transaminase levels in the asymptomatic patient*. Am Fam Physician, 2005. 71(6): p. 1105-10.
148. Jun, H.J., et al., *Hepatic lipid accumulation alters global histone h3 lysine 9 and 4 trimethylation in the peroxisome proliferator-activated receptor alpha network*. PLoS One, 2012. 7(9): p. e44345.
149. Wen, S., et al., *Novel combination of histone methylation modulators with therapeutic synergy against acute myeloid leukemia in vitro and in vivo*. Cancer Lett, 2018. 413: p. 35-45.
150. Lu, Y., et al., *Hypoxia Promotes Resistance to EGFR Inhibition in NSCLC Cells via the Histone Demethylases, LSD1 and PLU-1*. Mol Cancer Res, 2018. 16(10): p. 1458-1469.

## 6. Abbreviations

<b>Abbreviation</b>	<b>Explanation</b>
ACACA	Acetyl-CoA carboxylase alpha
ALT	Alanine aminotransferase
AML	Acute myeloid leukemia
ANKRD1	Ankyrin repeat domain-containing protein 1
APOE2	Apolipoprotein E2
APS	Ammonium peroxodisulfate
AST	Aspartate aminotransferase
BNIP3	BCL2 interacting protein 3
BNIP3L	BCL2 interacting protein 3-like
BSA	Bovine serum albumin
BW	Body weight
CDKN1A	Cyclin-dependent kinase inhibitor 1A
cDNA	Copy-deoxyribonucleic acid
ChIP	Chromatin immunoprecipitation
CHX	Cycloheximide
CoREST	REST corepressor 1
CO <sub>2</sub>	Carbon dioxide
CYP2E1	Cytochrome P450 2E1
d	Day
DAVID	Database for Annotation, Visualization and Integrated Discovery
DEGs	Differential expressed genes
DEN	Diethylnitrosamine
DMEM	Dulbecco's Modified Eagle Medium
DMN	Dimethylnitrosamine
DMSO	Dimethyl sulfoxide
DNA	Deoxyribonucleic acid
dNTPs	Deoxynucleosidtriphosphate
Dox	Doxycycline
dsDNA	Double stranded DNA
EDTA	Ethylenediaminetetraacetic acid
EGFR	Epidermal growth factor receptor
EMILIN2	Elastin microfibril interfacier 2

---

EMT	Epithelial-mesenchymal transition
ER	endoplasmic reticulum
ESRRA	Estrogen-related receptor alpha
FABP5	Fatty acid-binding protein 5
FAD	Flavin adenine dinucleotide
FASN	Fatty acid synthase
FBS	Fetal bovine serum
FC	Fold change
FFPE	Paraffin-embedded
FPKM	Fragments Per Kilobase Million
g	Gram
GO	Gene Ontology
GPAM	Glycerol-3-phosphate acyltransferase
GSEA	Gene Set Enrichment Analysis
HBV	Hepatitis B virus
HCC	Hepatocellular carcinoma
HCV	Hepatitis C virus
HDAC	Histone deacetylases
HE	Hematoxylin-eosin-staining
HFD	High-fat diet
HIF-1 $\alpha$	Hypoxia-inducible factor 1-alpha
HPRT	Hypoxanthine phosphoribosyltransferase
HSCs	Hepatic stellate cells
H <sub>2</sub> O	Aqua
H3K4	Histone 3 lysine 4
H3K4me2	Dimethylation of lysine 4 on histone 3
H3K9	Histone 3 lysine 9
H3K9me2	Dimethylation of lysine 9 on histone 3
IgG	Immunoglobulin G
IP	Intraperitoneal
LUAD	Lung adenocarcinoma
KCl	Potassium chloride
KD	Knockdown
KEGG	Kyoto Encyclopedia of Genes and Genomes
kg	Kilogram

---

KH <sub>2</sub> PO <sub>4</sub>	Potassium dihydrophosphate
K <sub>2</sub> HPO <sub>4</sub>	Dipotassium hydrogenphosphate
LDHA	Lactate dehydrogenase A
LDL	Low-density lipoprotein
LOXL2	Lysyl oxidase-like 2
LSD1	Lysine-specific demethylase 1
MAO	Monoamine oxidase
mg	Milligram
MgCl <sub>2</sub>	Magnesium chloride
miR-	Micro-RNA
ml	Milliliter
mM	Millimolar
MYPT1	Myosin phosphatase target subunit 1
n	Number
NAFLD	Non-alcoholic fatty liver disease
NASH	Non-alcoholic steatohepatitis
NaCH <sub>3</sub> COOH	Sodium acetate
NaCl	Sodium chloride
NaOH	Sodium hydroxide
Na <sub>2</sub> HPO <sub>4</sub>	Disodium hydrogenphosphate
NDRG1	N-myc downstream regulated 1
NES	Normalized enriched score
nM	Nanomolar
N <sub>2</sub>	Nitrogen
PBS	Phosphate buffered saline
PBST	Tween 20-containing phosphate buffered saline
PCR	Polymerase chain reaction
PDK4	Pyruvate dehydrogenase kinase 4
PIK3R3	Phosphoinositide-3-kinase regulatory subunit 3
PLK1	Polo-like kinase 1
PMSF	Phenylmethanesulfonyl fluoride
PPARG	Peroxisome proliferator-activated receptor gamma
PVDF	Polyvinylidene difluoride
p21	Cyclin-dependent kinase inhibitor 1A
RIPA	Radioimmunoprecipitation assay buffer

---

RNA	Ribonucleic acid
RNase	Ribonuclease
ROS	Reactive oxygen species
rpm	Revolutions per minute
rtTA	Tetracycline-dependend transactivator
SCLC	Small cell lung carcinoma
scr	Scramble
SDS	Sodium dodecyl sulphate
SDS-PAGE	SDS-polyacrylamide gel electrophoresis
siRNA	Small interfering RNA
shRNA	Short hairpin RNA
TBS	Tris-buffered saline
TCGA	The Cancer Genome Atlas
TCP	Tranylcypromine
TEMED	Tetramethylethylenediamine
Tet	Tetracycline
TG	Triglycerides
TGF- $\beta$	Transforming growth factor $\beta$
TLX3	T-cell leukemia homeobox protein 3
TM6SF1	Transmembrane 6 superfamily member 1
TNF- $\alpha$	Tumor necrosis factor-alpha
T2DM	Type 2 diabetes mellitus
qPCR	Quantitative polymerase chain reaction
$\mu$ l	Microliter
$\mu$ M	Micromolar
V	Voltage
VLDL	Very low-density lipoprotein

## 7. Supplementary information

Supplementary Table 1: Body weight information for aged C57BL/6J from the Jackson Laboratory.

Age (Weeks)	Body Weight (grams; mean $\pm$ st. dev)	
	Females	Males
3	10.1 $\pm$ 1.7	10.6 $\pm$ 1.9
4	14.7 $\pm$ 1.8	16.5 $\pm$ 2.6
5	17.8 $\pm$ 1.1	20.7 $\pm$ 1.8
6	18.5 $\pm$ 0.9	21.9 $\pm$ 1.8
7	19.0 $\pm$ 1.0	23.6 $\pm$ 1.5
8	19.6 $\pm$ 1.2	25.0 $\pm$ 1.4
9	20.3 $\pm$ 1.3	26.1 $\pm$ 1.6
10	20.7 $\pm$ 1.4	26.9 $\pm$ 1.7
11	21.3 $\pm$ 1.5	27.7 $\pm$ 1.9
12	21.9 $\pm$ 1.6	28.9 $\pm$ 2.0
13	22.6 $\pm$ 1.9	30.0 $\pm$ 2.1
14	23.0 $\pm$ 2.0	30.8 $\pm$ 2.2
15	23.5 $\pm$ 2.3	31.6 $\pm$ 2.4
16	23.9 $\pm$ 2.3	32.1 $\pm$ 2.4
17	24.1 $\pm$ 2.5	32.8 $\pm$ 2.6
18	24.5 $\pm$ 2.6	33.3 $\pm$ 2.8
19	24.8 $\pm$ 2.8	33.7 $\pm$ 2.8
20	25.3 $\pm$ 2.8	34.2 $\pm$ 2.9
21	25.8 $\pm$ 3.2	34.6 $\pm$ 2.9
22	26.1 $\pm$ 3.2	35.1 $\pm$ 3.2
23	26.5 $\pm$ 3.3	35.8 $\pm$ 3.2
24	26.9 $\pm$ 3.4	36.3 $\pm$ 3.4

24-08.2022 ingeben

## Acknowledgments

I would like to express my gratitude to all those who helped me during the writing of this thesis. My deepest gratitude goes first and foremost to my supervisor, Prof. Dr. Margarete Odenthal, who has always given me support and guidance in academic studies since 2018. In the preparation of the thesis, she has read my manuscript carefully through each draft, provided me with inspiring advice, and helped me to shape this work through hours of discussion. Without her patient instruction, insightful criticism and expert guidance, the completion of the thesis would be impossible.

I am highly grateful to Prof. Dr. Reinhard Büttner for giving me the opportunity to work in the Institute for Pathology and support me to carry out my research work. I would also like to thank my two tutors from the IPMM program, Prof. Dr. Dr. Michal-Ruth Schweiger and PD. Dr. Thomas Wunderlich, who were always kind to discuss my result and give me valuable suggestions on my project.

I would like to thank all my colleagues for all the support that I received from them over the years. I have learned many skills from Hannah in the beginning and she also helped me a lot. Sonja is very nice and patient and always helped me in need. Dr. Xiaojie Yu, Dr. Priya Dalvi, Dr. Maria Anokhina, Lingyu Wang and Hardik Makawana also helped me a lot during my study. Special thanks to Yefeng Shen, my colleague and best friend, who has given me much support and motivation. There are many lovely moments, thanks to them for creating such nice memories. Besides, I also owe my sincere gratitude to my friends who gave me accompany and help.

Lastly, many thanks would go to my beloved family, especially my parents, for their meticulous care and support, and for their selfless contribution over the years that allowed me to complete my studies and pursue my dream.

## Erklärung

Ich versichere, dass ich die von mir vorgelegte Dissertation selbständig angefertigt, die benutzten Quellen und Hilfsmittel vollständig angegeben und die Stellen der Arbeit – einschließlich Tabellen, Karten und Abbildungen –, die anderen Werken im Wortlaut oder dem Sinn nach entnommen sind, in jedem Einzelfall als Entlehnung kenntlich gemacht habe; dass diese Dissertation noch keiner anderen Fakultät oder Universität zur Prüfung vorgelegen hat; dass sie – abgesehen von unten angegebenen Teilpublikationen – noch nicht veröffentlicht worden ist sowie, dass ich eine solche Veröffentlichung vor Abschluss des Promotionsverfahrens nicht vornehmen werde. Die Bestimmungen dieser Promotionsordnung sind mir bekannt. Die von mir vorgelegte Dissertation ist von Frau Prof. Dr. Margarete Odenthal betreut worden.

### Übersicht der Publikationen:

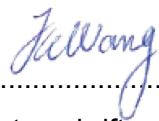
Kanne J, Hussong M, Isensee J, Muñoz-López Á, Wolffgramm J, Heß F, Grimm C, Bessonov S, Meder L, **Wang J**, Reinhardt HC, Odenthal M, Hucho T, Büttner R, Summerer D, Schweiger MR. Pericentromeric Satellite III transcripts induce etoposide resistance. *Cell Death Dis.* 2021;12(6):530.

**Jie Wang**, Lingyu Wang, Marcel Schmiel, Yefeng Shen, Priya Dalvi, Xiaojie Yu, Zhefang Wang, Yue Zhao, Reinhard Büttner, Margarete Odenthal. The impact of histone modifier lysine-specific demethylase 1 (LSD1) in cell metabolism in hepatocellular carcinoma. (manuscript in preparation)

Ich versichere, dass ich alle Angaben wahrheitsgemäß nach bestem Wissen und Gewissen gemacht habe und verpflichte mich, jedmögliche, die obigen Angaben betreffenden Veränderungen, dem Promotionsausschuss unverzüglich mitzuteilen.

24.08.2022

.....  
Datum

  
.....  
Unterschrift

## Curriculum Vitae

Jie Wang

Date of birth: 11.08.1992 in Hebei, China

Nationality: Chinese

Address: Kerpener Str. 62, 50924 Köln

Tel.: 0221/4786351

Email: jie.wang@uk-koeln.de

## Education

2011 NO.1 Middle School of Xinji, Shijiazhuang, China

2011-2015 Bachelor of Science in Pharmacy  
Hebei North University, Zhangjiakou, China

2015-2018 Master of Medicine in Pharmacology  
Zhengzhou University, Zhengzhou, China

2018-present PhD student in Molecular Medicine  
University of Cologne, Cologne, Germany

## Presentations

2021 PO-1629, International Liver Congress 2021-EASL meeting

2021 P05 IPMM Student Days (Graduate School)

## Awards

CSC scholarship supported by China Scholarship Council (CSC)

Post prize of 2021 International Liver Congress 2021-EASL meeting

## Publications

Kanne J, Hussong M, Isensee J, Muñoz-López Á, Wolffgramm J, Heß F, Grimm C, Bessonov S, Meder L, **Wang J**, Reinhardt HC, Odenthal M, Hucho T, Büttner R, Summerer D, Schweiger MR. Pericentromeric Satellite III transcripts induce etoposide resistance. *Cell Death Dis.* 2021;12(6):530.

**Wang J**, Wang L, Schmiel M, Shen Y, Dalvi P, Yu X, Wang Z, Zhao Y, Büttner R, Odenthal M. The impact of histone modifier lysine-specific demethylase 1 (LSD1) in cell metabolism in hepatocellular carcinoma. (manuscript in preparation 2022)

Zhong H, **Wang J**, Zhu Y, Shen Y. Comprehensive Analysis of a Nine-Gene Signature Related to Tumor Microenvironment in Lung Adenocarcinoma. *Front Cell Dev Biol.* 2021;9:700607.

Gao J, **Wang J**, Gao N, Tian X, Zhou J, Fang Y, Zhang HF, Wen Q, Jia LJ, Zou D, Qiao HL. Prediction of cytochrome P450-mediated drug clearance in humans based on the measured activities of selected CYPs. *Biosci Rep.* 2017;37(6):BSR20171161.

Gao J, Wang Z, Wang GJ, Zhang HX, Gao N, **Wang J**, Wang CE, Chang Z, Fang Y, Zhang YF, Zhou J, Jin H, Qiao HL. Higher CYP2E1 Activity Correlates with Hepatocarcinogenesis Induced by Diethylnitrosamine. *J Pharmacol Exp Ther.* 2018;365(2):398-407.